ISSN 2683-9288

Science Reviews from the end of the world

Volume 1
Number 1
December 2019

Susana Fedrano - “El ala” (1991)

Science Reviews
from the end of the world

Science Reviews - from the end of the world **is a quaterly publication that aims at providing authoritative reviews on hot research topics developed mainly by scientists that carry out their work far away from the main centers of science. Its research reviews are short, concise, critical and easy-reading articles describing the state of the art on a chosen hot topic, with focus on the research carried out by the authors of the article. These articles are commissioned by invitation and are accessible not only to hardcore specialists, but also to a wider readership of researchers interested in learning about the state-of-the-art in the reviewed subject. The reviews cover all fields of science and are written exclusively in English. They are refereed by peers of international prestige and the evaluation process follows standard international procedures.**

Centro de Estudios sobre Ciencia, Desarrollo y Educación Superior
538 Pueyrredón Av. - 2° C – Second building
Buenos Aires, Argentina - C1032ABS
(54 11) 4963-7878/8811
sciencereviews@centroredes.org.ar
www.scirevfew.net

Vol. 1, No. 1
December 2019

ISSN 2683-9288

Our cover: *El ala* (1991), oil on canvas by Susana Fedrano. From the collection *Artistas plásticos con la ciencia.* Reproduced by permission from the Comisión Administradora Permanente de la Exposición de Arte Centro Atómico Constituyentes, Comisión Nacional de Energía Atómica.

Science Reviews
from the end of the world

Table of Contents

EDITORIAL

An editorial anomaly

Most of the science in the Latin-American region is funded with public money, and the institutions that provide the money have little or no record of the resulting published material. In a time when the open access initiative is gaining momentum and is advocated by financing institutions, the Argentine Association for the Progress of Science (AAPC) evaluated that launching a new publication was warranted, with distinctive features that make it an editorial anomaly:

1. Regional scientific journals mainly focus on the publication of research that, though relevant for the region, is not original enough to meet the standards of top journals. Our journal seeks to present highly relevant material, originated in the region but with global impact: authoritative, timely reviews of the fields of research by prestigious scientist that may constitute an important archive of the science carried out in the region.

2. All fields of science are included. We believe that well written reviews are of widespread interest, not restricted to specialists in a narrow discipline; however, topical issues are expected to appear alongside with other, more general issues.

3. Rather than focusing on the publication of marginal science – an unfortunate very widespread trend – our target authors are the most influential ones, those that currently publish in top journals from the learned societies or from the few large editorial houses. Thus, papers are received mainly by invitation and subjected to rigorous review.

4. The members of the Editorial Board are very prestigious scientists, currently from Argentina, with the possibility of enlarging it to include scientist from other countries in the region as well.

5. Open access is guaranteed; furthermore, the fast dissemination of the oncoming publications is achieved by personalized mailing lists.

The journal we now launch has become a reality in the form of a joint venture between AAPC and Centro Redes Foundation, a prestigious institution that is heavily involved in scientometric analyses for the region. Financing was provided by the Science, Technology and Productive Innovation Government Secretary.

The first issue collects four reviews on timely aspects of various fields of science and technology. I hope you enjoy them.

Miguel A. Blesa
Editor-in-Chief

IN THIS ISSUE

Science Reviews from the end of the world

Vol. 1, No. 1, December 2019 // pp. 6-18 /

The Malvinas (Falkland) Plateau derived from Africa? Constraints for its tectonic evolution

Victor A. Ramos[1*], Farid Chemale[2], Juan P. Lovecchio[3], and Maximiliano Naipauer[4]

[1] *Instituto de Estudios Andinos don Pablo Groeber (IDEAN), Universidad de Buenos Aires-Conicet, Argentina*
[2] *Programa de Pós-Graduação em Geologia, Universidade do Vale do Rio dos Sinos, Brazil*
[3] *YPF S.A., Exploration, Buenos Aires, Argentina*
[4] *Instituto de Geocronología y Geología Isotópica (INGEIS), Universidad de Buenos Aires-Conicet, Argentina*
** Corresponding author. Email: victoralbertoramos@gmail.com.*

Abstract

The latest studies on the tectonic evolution of the Malvinas (Falkland) Islands and their adjacent continental plateau further east are analyzed to assess a long controversy regarding the origin of these islands. Although new technologies and exploratory drillings have brought new data in recent times, the debate on the geological evolution of this area remains open. The two dominant hypotheses are analyzed by assessing the eventual collision between the islands and the South American continent, the presence of a large transcontinental fault such as Gastre, the potential 180º rotation of the Malvinas Islands, and the occurrence of a mega-decollement with opposite vergence. These hypotheses are contrasted with the processes that have occurred in Patagonia, especially those based on the new isotopic data on the Maurice Ewing Bank at the eastern end of the Malvinas Plateau, and the current knowledge of the adjacent Malvinas Basin. The new data highlights the inconsistencies of certain models that propose that these islands migrated from the eastern African coasts near Natal, to their current position and rotated 180º around a vertical axis. The new observations support the hypothesis that postulates that the islands have been part of the South American continent since before the Paleozoic.

Keywords:
Malvinas (Falkland) Plateau, rotation, paleomagnetic data, collision, microcontinent

Introduction

The tectonic evolution of the South Atlantic Ocean is heavily constrained by the adjustment and mismatch of several continental blocks associated with the fitting of South America and Africa as part of the supercontinent of Pangea. Several alternatives were presented based on different criteria in recent years, where the Malvinas (Falkland) Islands and their adjacent continental blocks play a significant role in the reconstructions. The finding of important hydrocarbon resources outboard the Outeniqua basin offshore South Africa, which is modifying the scenario of hydrocarbon resources in this country, further increases the need for a proper reconstruction and precise paleogeography of the South Atlantic Ocean to evaluate the South American conjugate continental margin.

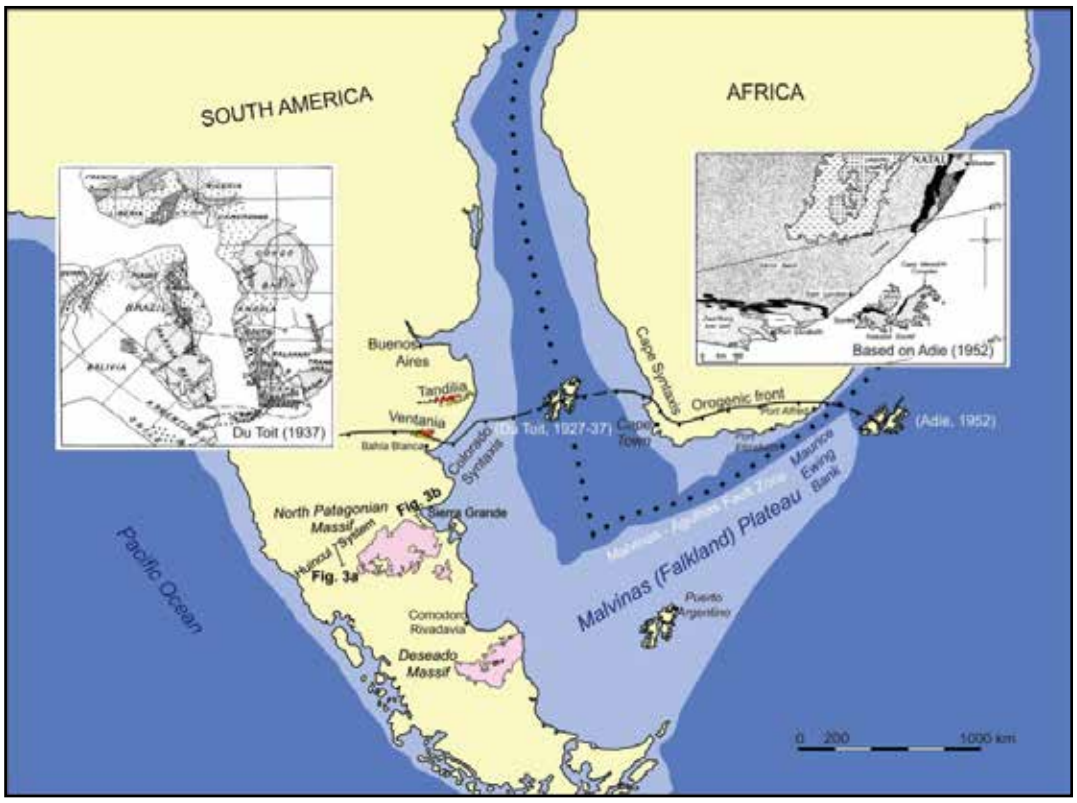

Figure 1. Two contrasting alternatives for the origin of the Malvinas (Falkland) Plateau (based on Ramos and others[1]). Note locations of figures 3a and 3b.

The aim of the present review is to assess the contrasting tectonic evolution proposed in the last two or three years based on old and new data obtained in the Malvinas (Falkland) Plateau. Most of the recent works can be divided into two different groups. One of these is based on a stable relationship between the South American continent and the different elements of the plateau since at least the Neoproterozoic. This option contrasts with the African-derived alternative that divides the plateau into two different blocks, which would have collided with South America in Jurassic-Cretaceous times.

Previous works

One of the first reconstructions of the paleogeography of the South Atlantic Ocean was advanced by Du Toit [2,3], who proposed a location of the Malvinas Islands between South America and Africa (Fig. 1). This South African geologist located the Malvinas Islands in the offshore continental platform between the Ventania System of Buenos Aires, and the Cape System of South Africa based on the geological correlation found by professor Keidel [4,5,6,]. This reconstruction took in consideration the stratigraphy of both systems and the shared late Paleozoic glacial deposits, and highlighted the coincidence in age and discontinuities of the common sedimentary sequences. Some years later, another South African geologist, Adie[7], who had worked in the Malvinas Islands, based on the southern vergence of the structures, located the islands "upside down", but in the eastern opposite side of South Africa (see Figure 1). This way, both the islands and the Cape System, which shares a common stratigraphy, present the same northern vergence.

This proposal was analyzed by Suero[8] and Borrello[9] who, based on the continuity of the late Paleozoic sedimentary basins of Patagonia, preferred the Present normal position of the islands attached to South America. The latter author disregarded Adie's proposal based on the common stratigraphic and paleontological characteristics between the Malvinas Islands and Patagonia.

Adie's hypothesis was almost forgotten for many years until the paleomagnetic work of Mitchell and others[10]. These authors published a high impact article in Nature, which deserved the journal cover, based on the paleolatitudes obtained from Mesozoic dolerite dyke swarms together with a 120º rotation in the paleopoles, that resurrected the "upside down" hypothesis. This was partially confirmed by some other paleomagnetic studies performed by Taylor and Shaw[11]. After these geophysical works, most of the British authors started to support that the Malvinas Islands were located in the offshore of South Africa, in front of the Natal province, in the late Paleozoic, and that after a subsequent rotation during

Jurassic times, prior to the opening of the South Atlantic, the islands departed from Africa to be transferred to South America (see Stone[12,13], and references therein).

Even though many authors have backed the hypothesis that the islands were in South Africa and later, in Jurassic times, were transferred to South America, this hypothesis has a series of drawbacks that require further evidence to be sustained. In order to evaluate the African-derived alternative for the islands, several premises required for this hypothesis should be analyzed.

1.- MALVINAS ISLANDS DERIVED FROM AFRICA

Collision of Malvinas Islands microplate with South America

As pointed out by Martin[14] in his editorial comments early on in Nature, 1986, the new paleomagnetic data, even though partially consistent with the "upside down" location in front of Natal, present new and more difficult problems. The main problems were for this author how this block rotated and moved from that position to its present setting. Several alternatives were suggested to explain this displacement.

Based on paleomagnetic data, Ben Avraham and others[15] proposed the existence of an independent block, the Lafonia microplate. This small block would have two advantages – first, it would facilitate a 120º rotation, and after this, it would make it easier to transport the islands to South America. However, there is no evidence of any suture between South America and the Malvinas Islands as recognized by Richards and others[16]. These authors, based on the study of the offshore seismic lines in the platform between the islands and the continent, disregarded the presence of a crustal suture.

The existence of an independent microplate to make the drift and collision to South America possible would also have the problem that it would require a subduction zone on its leading edge, which would have produced a volcanic arc and, after the collision, a suture. There is no evidence of either of these two things. This fact was soon realized by several authors, such as Ben Avraham et al.[15] who, in order to solve the lack of a suture, proposed that Patagonia was a terrane independent from South America that moved together with the Lafonia microplate after its rotation in Jurassic times.

Another drawback for the collision of the Lafonia microplate against South America is the rift preserved in the Malvinas Basin (see location in Fig. 5). New studies performed in this basin show two stages of rifting, one in the Late Triassic and another in Early-Middle Jurassic times (see Lovecchio and others[17]). Seismic sections across the rift (Fig. 6) show no deformation as expected if there had been a collision against a microplate (see discussion below).

The Gastre continental fault system

The proposal of Patagonia attached to the Malvinas Plateau, both together as an independent terrane, explains the lack of a suture and the nonexistence of a volcanic arc on the Lafonia microplate, but a continental scale fault system and a transform fault in the offshore would be required to displace this huge terrane from Africa to its present position.

The northern boundary of the Patagonia terrane as proposed by Ben Avraham et al.[15] was a large right-lateral transpressional shear zone, which bounded the North Patagonian massif to the north from the rest of Gondwana. However, this northern limit coincides with the proposed suture between Patagonia and Gondwana, which was formed by orthogonal contraction with almost no evidence of strike-slip motion[18,19] during the late Paleozoic. The development of the Ventania and Cape fold and thrust belts, as well as the Colorado, Garies, and Cape syntaxes[19,20], preclude the existence of such transform fault north of Patagonia in Jurassic times[1].

To avoid this problem, Marshall[21] proposed that the boundary was determined by the Gastre intracontinental fault system, suggested by Rapela and Pankhurst[22], which is located south of the North Patagonian Massif. However, that hypothesis requires a displacement larger than 500 km along that fault system produced between 190 Ma, age of emplacement of the older dyke swarms in the Malvinas Islands, and 170 Ma, a cooling episode of uplift based on fission track ages of these dikes[23]. This would require a displacement rate of more than 42 mm per year along such transcontinental fault. Several recent studies on the Gastre fault system, in the classic locality where it was defined by Coira and others[24], have proved that this fault is a ductile shear zone of Paleozoic age, with no evidence of Jurassic or younger offsets of that magnitude[25,26,27], among others.

If no displacement, such as required, ever occurred along the Gastre fault system, Patagonia and the Malvinas Islands could not have moved together as a single continental block as proposed by several authors[16,28,29,30,31], among many others.

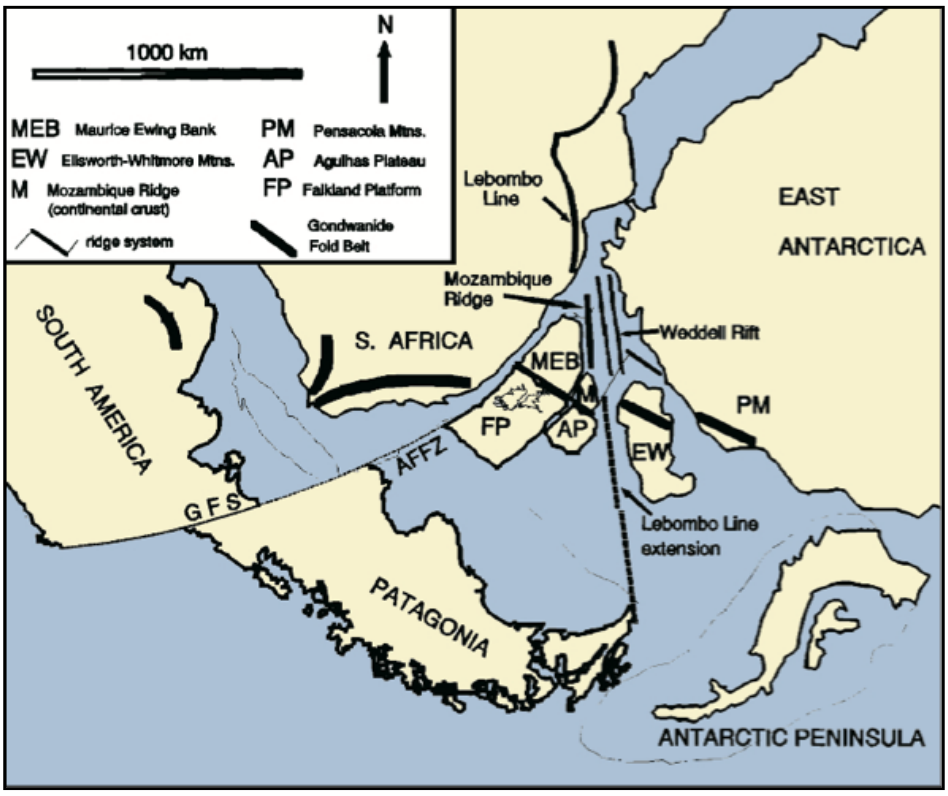

Figure 2. Proposed paleogeography based on the Gastre Fault System (G.P.S.) to accommodate the Malvinas Islands close to the Natal offshore (after Marshall[21]). See text for discussion.

The Jurassic rotation of the Malvinas Islands

Several alternatives have been proposed for a clock-wise rotation of the islands of at least 120º. The most feasible way this is possible would involve a rotation of the microplate associated to oceanic crust formation, as could be observed in the opening of the Bay of Biscay, between Spain and England[32]. One of the most popular alternatives for this model is the "double-saloon-door" rifting and seafloor spreading as proposed by Martin[29] and supported by Dalziel and others[30]. The main drawback is that there is no evidence of oceanic crust older than the early Cretaceous during the South Atlantic opening, where all the magnetic anomalies are parallel to the Agulhas-Malvinas transform without any evidence of rotation[33,34]. From the onshore perspective, as pointed out by Stone[13], the case for rotation of a microplate appears overwhelming, but offshore data do not support rotation and are compatible with a high degree of extension of a fixed Malvinas Plateau attached to South America[35,1].

Some other authors proposed a 120º-150º rotation during the break-up of Gondwana, previous to seafloor spreading without participation of oceanic crust but, as noticed by Stone[13], timing is crucial and most of the rotation of the microplate must have been pre-Cretaceous and probably mid-Jurassic. There is some consensus that rotation was a relatively rapid mid Jurassic event as envisaged by Curtis and Hyam[36] and Rapela and others[28]. Several mechanisms have been proposed for the rotation associated with the break-up of Gondwana[37,38,39,40]. However, there is neither seismic evidence of the microplate boundaries, nor indications of the extension and compression normally associated with block rotations[41]. No structures were identified nearby the predicted boundaries of the microplate to support the rotation on continental crust.

A recent study by Stanca and others[42] proposed crustal fragmentation and block rotation for the Malvinas Plateau, where the Malvinas Islands were a microcontinent; however, they state that the position of the plateau and the islands before the separation of Gondwana continues to be controversial. This work proposed a Malvinas Islands microplate, equivalent to the Lafonia microplate *sensu*[15,30], which underwent vertical-axis rotation during the break-up of Gondwana. As there is no deformation affecting the sedimentary basins offshore of the islands, rotation would have

had to occur prior to the older rift that took place in the southern sector of the North Malvinas basin. The oldest synrift deposits are not well dated in that basin, and a doubtful Upper (?) Jurassic age was assumed[42]. However, this WNW to NW-trending rift system, as seen in their Fig. 6, has the same trend as the Early Jurassic rift that crosscut the San Jorge and Cañadón Asfalto basins in Patagonia. The Malvinas rift, as well as its Patagonian equivalent, are linked to the 190-188 Ma old basaltic dike system parallel to the normal faults of the rift, located at the base of the synrift deposits. This WNW to NW-trending rift system crossing from Patagonia to the Malvinas Plateau was related to the opening of the Weddell Sea[1,43]. The rifting process started at about 190 Ma and ended with the first oceanic crust in that sea at about 160-155 Ma according to Ghidella and others[43]. The age of the synrift deposits across Patagonia is well dated and constrained to the Early to Middle Jurassic[44]. Some minor rotation occurred during the synextensional emplacement of the Chon Aike Magmatic Province[45,46] in the Early-Middle Jurassic. The observed rotational extension was recently interpreted by Lovecchio and others as produced by effect of a slab tear between Patagonia and Antarctica[47].

This fact is important because the rotation should have occurred and finished in the Early Jurassic. Furthermore, the paleomagnetic data found by Taylor and Shaw[11] and analyzed by Ramos and others[1] show the expected rotation in one site, while the other two sites have abnormal rotations, difficult to reconcile with a rigid-body vertical-axis rotation such as the one required for the Malvinas Islands microplate.

The mega-décollement controlling the Gondwanide Orogen

New detailed structural analyses performed north of the Malvinas Islands in the adjacent basin, combined with gravity and seismic data presented by Stanca et al.[42], enhanced the importance of the occurrence of a mega-décollement formed during the Gondwanide Orogeny. This décollement has been recognized underneath the Outeniqua Basin and South Africa[41,48], associated with north-verging thrusts. The décollement described in the Outeniqua Basin and underneath the Cape fold and thrust belt is dipping to the south, and it was reactivated as a detachment level during subsequent extension in Jurassic times. In the Malvinas plateau, this décollement is dipping to the north and reaches the same depth as in the Outeniqua Basin. The opposite polarity of this décollement at both sides of the Agulhas-Malvinas transfer zone is considered as a new evidence supporting the 180º rotation of the Malvinas Islands microplate[42].

However, if the structural characteristics of the Ventania fold and thrust belt in the province of Buenos Aires are considered, a series of new problems emerges. The seismic sections provided by Pángaro and Ramos[49] (their Figs. 8 and 12), Ramos et al.[19] (their Fig. 5), and Pángaro et al.[19], show withou shadow of a doubt the continuity of the Ventania fold and thrust belt in the adjacent offshore area and its eastern extension in the Cape belt of South Africa (see Paton et al.[20]). In those sections, what the authors considered to be the master shear is the equivalent to the mega-décollement of Stanca et al.[42]. Both structures have the same north-vergence, a similar depth of detachment and equivalent offsets. On top of that, recent studies in the Colorado offshore basin show three periods of extension, the oldest one being controlled by a postorogenic extensional collapse of the thrusts of the Ventania fold belt[17]. These extensionally reactivated Permian to Early Triassic thrusts were intersected by normal faults during Early Jurassic times, in a similar way as that described for the Outeniqua Basin and the Cape fold and thrust belt. It is evident that deformation kinematics north of the Gondwanide magmatic arc and north of the Agulhas-Malvinas transform were comparable.

On the other hand, there is evidence that deformation south of the magmatic arc has an opposite south-vergence, as described in the Sierra Grande area[50] close to the Atlantic margin. A similar conclusion with different approaches was arrived at by von Gosen[51] and López de Luchi and others[52]. Early Paleozoic quartzites are folded and thrusted with a south-southeast vergence (see Figure 3). Further inland, underneath the Mesozoic deposits of the Neuquén Basin, Mosquera et al.[53] recognized the Gondwanide deformation with south-vergent thrusts reactivated during latest Triassic-Early Jurassic extension[54,55,56].

The décollements that controlled the Permian thrusts and the subsequent Early Jurassic normal faults have a dominant south-vergence in the central and southern part of the Neuquén Basin as well as in the outcrops of Sierra Grande area near the Atlantic coast, very similar to the one described in the southern part of the North Malvinas Basin.

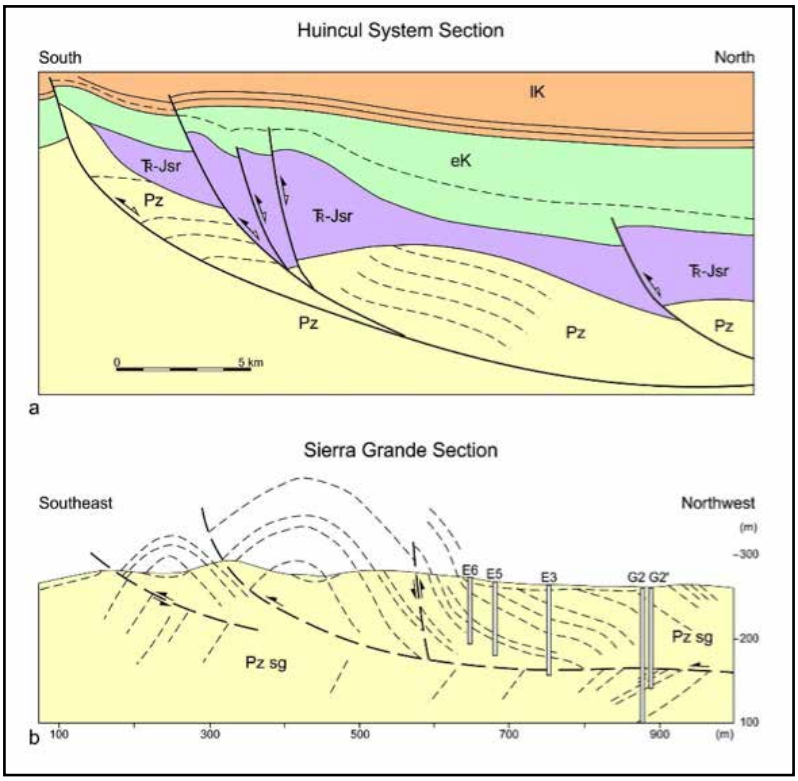

Figure 3. South verging fold and thrust belts developed in northern Patagonia; a) Basement folds with south-vergence in the Huincul System interpreted by Mosquera et al.[53] as Gondwanide thrusts extensionally reactivated during Late Triassic-Early Jurassic, and subsequent contraction in the southern Neuquén Basin. Pz: Paleozoic rocks, TRJsr: synrift deposits of Late Triassic-Early Jurassic age, eK and lK: Early and Late Cretaceous deposits; b) Silurian-Devonian quartzites with SE-vergence in the Sierra Grande mining district[50] . Pz sg: Sierra Grande Formation. Location of the sections indicated in Fig. 1.

One of the main drawbacks that the rigid model has according to Stanca et al.[42] is the lack of continuation of a south verging fold and thrust belt east and west of the islands. Available seismic information indicates that, at approximately 150 km west of the islands, the south vergence of the deformation is recognized by the steeper southern flanks of the folds (Figure 4), in comparison with gentler northern flanks[57].

Further to the west, the Mesozoic infill of the Malvinas Basin obliterates the structure of the underlying Paleozoic rocks, as well as the crystalline basement of the Dungeness Arch[1], also known as the Río Chico High[47]. There is some consensus that the Gondwanides has been formed by the collision of Patagonia and adjacent blocks as proposed by Ramos[18] and confirmed by Miller et al.[58] in South Africa.

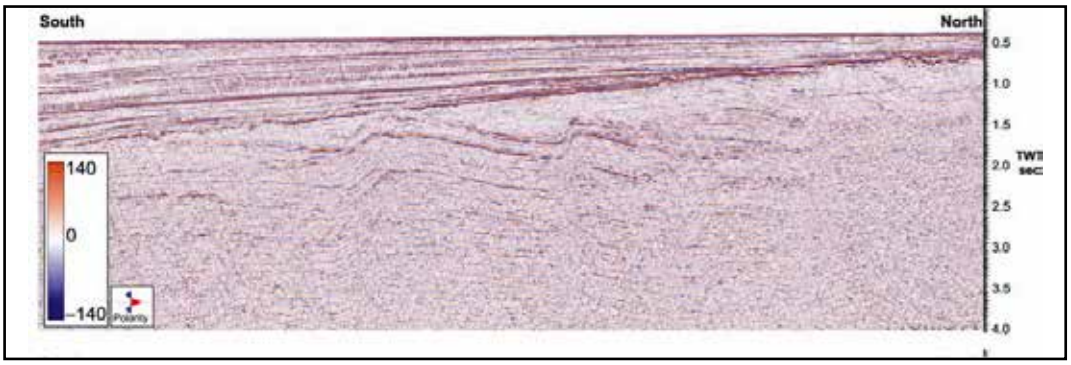

Figure 4. Seismic line southwest of the Malvinas Islands showing, beneath the Jurassic, an angular unconformity of the Gondwanide folds developed in Paleozoic rocks with a well-defined south vergence[57]. See location in Fig. 5.

West of the Malvinas Basin (Fig. 4), the early Paleozoic clastic platform is interrupted by the Devonian to Carboniferous magmatic arc that was identified by Ramos and Naipauer[59] (and cites therein). The magmatic arc is located along the western side of the Dungeness Arch (or Río Chico High) and continues to the north across the San Jorge Basin with a northwestern trend, to finally reach the northern Patagonian Andes[18]. The quartzitic platform can be recognized from the western off-shore of the Malvinas Islands, to the north in Cabo Blanco, in the basement of the Rawson Basin and in Sierra Grande (Fig. 5). In both extremes the southern vergence of the folds has been identified.

2.- MALVINAS ISLANDS FIXED TO PATAGONIA

The previous analyses have shown that there is no robust evidence to rotate the Lafonia (Falkland) microplate 120º, either surrounded by continental or oceanic crust. The paleomagnetic data is poor and not conclusive for a vertical-axis rotation; no suture or deformation has been recognized in the western contact with Patagonia, and if it is difficult to rotate the islands, it is almost impossible to rotate the entire Malvinas plateau. The occurrence of two sets of dolerite dykes in the Malvinas Islands, one WNW-trending of Jurassic age, and another one N-trending of Early Cretaceous age, was taken as an evidence of rotation of the islands[23,60]. However, this main stress rotation is seen in the entire Patagonia and in the adjacent offshore basins associated with the Jurassic WNW-trending opening of the Weddell Sea and the subsequent N-trending rifting of the South Atlantic in the Early Cretaceous[1,47].

Most of the similarities between the East Cape Supergroup and the Lafonia Supergroup, the so-called South African-Malvinas connection[42], is not taking into consideration the late Paleozoic glacial deposits of central Patagonia, and the exposed Paleozoic quartzites inland in eastern Patagonia (v.g. Sierra Grande and Cabo Blanco), as well as the deposits in the offshore adjacent basins (v.g. Rawson Basin). Besides these arguments[1,59], based on the new data obtained in the Malvinas Plateau, the “fixist alternative” will be analyzed.

New data on the Malvinas Basin

A recent update of the structural framework for the Malvinas Basin, together with two new U-Pb zircon ages for the synrift series[47] preclude a Lower to Middle Jurassic or younger collision between Patagonia and the Malvinas Islands (see Fig. 6). Recent works assume that the Weddell Sea Rift that separated the Ewing Bank from Gondwana was developed at ~164 Ma[62].

The new U-Pb dates are located within the synrift sequence. A volcanic breccia at the base of the sequence has an age of 215 Ma (on top of ROU horizon of Fig. 6), which indicates a Late Triassic age for this level[47]. Triassic deposits are also interpreted in the San Julián offshore rift basin by Figueiredo et al. (1996, see seismic line in Fig. 14), as well as in the El Tranquilo rift onshore Santa Cruz, where they are well known and dated[63,64].

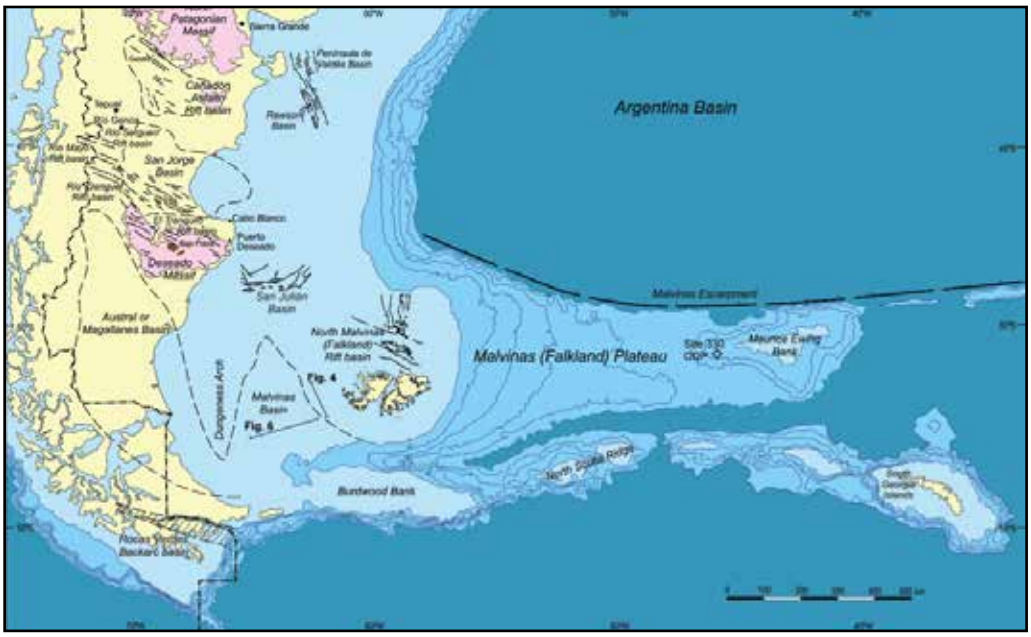

Figure 5. Main characteristics of the Malvinas (Falkland) Plateau and the adjacent Patagonia (modified from Ramos et al.[1] and Chemale et al.[61]. Note the location of the oceanic drill of ODP-330 in the Maurice Ewing Bank, and the location of figures 4 and 6, based on McCarthy et al.[57] and Lovecchio et al.[47].

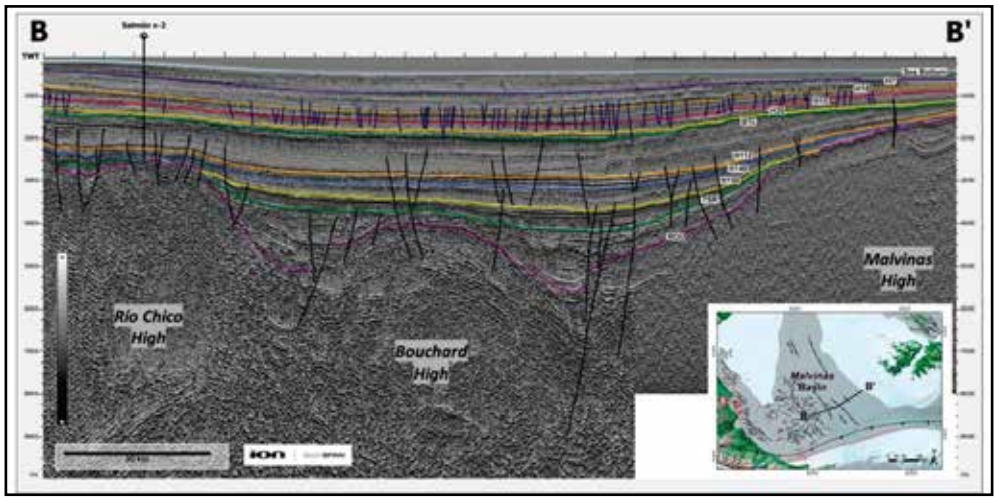

Figure 6. Seismic line across the Central Graben of the Malvinas Basin[47]. The rift sequence is encompassed between the ROU horizon (top pre-rift basement) and the TSR horizon (top synrift).

The second U-Pb date yielded 169.6 ± 2.1 Ma and corresponds to a tuff layer located near the top of the synrift sequence (TSR of Figure 6). This Middle Jurassic age constrains the age of the synrift deposits to Late Triassic- Middle Jurassic times, a similar time span recognized in the San Julián, El Tranquilo, and Cañadón Asfalto rift basins.

The period of time covered by the synrift deposit is the one that has been proposed for the collision of the Malvinas Islands; therefore, a compressive regime is unlikely in this time span.

New data on the Malvinas Plateau

The recent analyses of Site 330 of ODP presented by Chemale et al.[61] show that the basement of the Maurice Ewing Bank has similar ages to the Gran Malvina (Western) Island basement exposed in Cabo Belgrano (Cape Meredith). These metamorphic rocks have similar Mesoproterozoic U-Pb ages, between 1,200 and 1,030 Ma, and are intruded by pink leucogranites (without any deformation) of 1,006 ± 13 Ma in the Maurice Ewing Bank[62]. These ages closely correlate to the metamorphic dated rocks in Cape Meredith, as well as the associated similar pink granites of 1,003 ± 16 Ma (Thomas et al., 2000). These basement ages are similar to the detrital zircon ages[1] in the overlying Paleozoic quartzites in both islands, indicating a common basement. The occurrence of similar basement rocks with a common deformation history shows that the current location of the islands with respect to the Maurice Ewing Bank has not changed significantly and should have been even closer than in present times considering the amount of E-W extension recorded in the Malvinas Plateau.

Another important point is that the Jurassic fluvial sandstone over the Maurice Ewing Bank intersected at site 330 carries detrital zircons of Permian age. New geochronological work indicates an important peak at 266 Ma (Chemale et al., in prep.), which is difficult to reconcile with a position just east of South Africa[42,62] (and cites therein). Permian ages are common at these latitudes in the Darwin Cordillera, with a more prominent peak at c. 270 Ma[65]; this is well documented for the Patagonian Andes, with a large well-defined 260–300 Ma population likely derived from the Gondwanide belt formed during the Carboniferous–Permian assembly of Patagonia[66], bracketed by Suárez et al.[67] between 255-268 Ma, and even closer, in the South Georgia Island, at its previous position adjacent to eastern Tierra del Fuego Island, with a dominant younger peak at 275 Ma[68,69].

Both sets of data strongly suggest basement continuity between the Malvinas Islands and the Maurice Ewing Bank and their proximity with the Fuegian and Patagonian Andes.

Concluding Remarks

The previous reviews of Stone[12] and Ramos et al.[1] questioned the reliability of the existing paleomagnetic data, to support a 120º vertical axis rotation of the entire Malvinas Islands microplate. The fragmentation of the microplate in different blocks as proposed by Stanca et al.[42], on the other hand, is not supported by the existing paleomagnetic data.

The timing for the rifting of the southern part of the North Malvinas Basin could be partially constrained by the 188-190 Ma old dikes exposed in the Malvinas Islands. The correlation, based on the new data presented by Lovecchio et al.[47], with the adjacent rift of the Malvinas Basin is coherent not only between these two basins, but with the entire extensional trend of southern and central Patagonia (Fig. 5). It is well established that the timing and the direction of this extension was controlled by rifting prior to the opening of the Rocas Verdes Basin and the Weddell Sea, which ended with the first oceanic crust developed at 160-155 Ma[43,70] and references therein).

As discussed by Stanca et al.[42], the rotation of the islands, if it ever occurred, should be prior to the synrift deposits, since these sequences do not show any deformation. If a time span between Late Triassic and Early to Middle Jurassic is accepted for the rifting, rotation should be older than Late Triassic, when most of the Cape belt of South Africa was still under compression.

The several proposed collisions between the Lafonia (or Malvinas) microplate against Patagonia at different times during the Jurassic must be ruled out, since no deformation is observed in the Late Triassic-Early to Middle Jurassic sequences of the Malvinas Basin.

The detrital zircons of Permian age found in the sedimentary cover above the basement of the Maurice Ewing Bank are also indicative of the proximity to the Patagonian or Fuegian Andes, or to the Georgias Islands, in their location prior to the development of the Northern Scotia arc.

Based on these new observations, in addition to the detailed analyses by Stone[12] and Ramos and others[1], it is concluded that the Malvinas Islands and the Maurice Ewing Bank, as an integral part of the Malvinas Plateau, have been attached to Patagonia since Paleozoic times. There is compelling evidence that this land has been part of South America within Western Gondwana, at least since the Permian.

Acknowledgments

The authors are grateful to the critical review of Dr. Augusto Rapalini and the various suggestions received, which improved the understanding of the work. Additionally, the authors acknowledge numerous colleagues in the Institute for their discussions and exchanges on different aspects. This is contribution R 309 of the Instituto de Estudios Andinos Don Pablo Groeber.

References

[1] Ramos, V.A.; Cingolani, C.; Chemale Junior, F.; Naipauer, M.; Rapalini, A. The Malvinas (Falkland) Islands revisited: The tectonic evolution of southern Gondwana based on U-Pb and Lu-Hf detrital zircon isotopes in the Paleozoic cover. J. South Am. Earth Sci. 2017, 76: 320-345.

[2] Du Toit, A.L. A geological comparison of South America with South Africa. Publications Carnegie Institute, 1927, 381: 1-157.

[3] Du Toit, A.L. Our wandering continents. London, Oliver and Boyd, 1937.

[4] Keidel, J. Über das Alter, die Verbreitung und die gegenseitigen Beziehungen der verschiedenen tektonischen strukturen in den argentinischen Gebirgen. XII° Session du Congrés Géologique International, Compte Rendu pp. 671-687, Toronto, 1913.

[5] Keidel, J. La geología de las Sierras de la Provincia de Buenos Aires y sus relaciones con las montañas de Sudáfrica y Los Andes. Ministerio de Agricultura de La Nación, Sección Geología, Mineralogía y Minería, Anales, 1916, 11(3), p. 1-78.

[6] Keidel, J. Sobre la distribución de los depósitos glaciares del Pérmico conocidos en la Argentina y su significación para la estratigrafía de la serie del Gondwana y la paleogeografía del Hemisferio Austral. Academia Nacional de Ciencias, Boletín, 1921, 25, p. 239-368, Córdoba.

[7] Adie, R.J. The position of the Falkland Islands in a reconstruction of Gondwanaland. Geol. Mag., 1952, 89: 401-410.

[8] Suero, T. Paleogeografía del Paleozoico superior en la Patagonia (República Argentina). Rev. Asoc. Geol. Arg., 1961,16(1-2), p. 35-42.

[9] Borrello, A.V. Sobre la geología de las Islas Malvinas, Ediciones Cultura Argentina, Ministerio de Educación y Justicia, 70 pp., Buenos Aires, 1963.

[10] Mitchell, C.; Taylor, G.K.; Cox, K.G.; Shaw, J. Are the Falkland Islands a rotated microplate? Nature, 1986, 319, p. 131-134.

[11] Taylor, G.K.; Shaw, J. The Falkland Islands: new palaeomagnetic data and their origin as a displaced terrane from southern Africa. In Hillhouse, J.W. (ed.) Deep Structure and Past Kinematics of Accreted Terranes, AGU, Geophysical Monographs Series, 50, p. 59-72, Washington, D.C., 1989.

[12] Stone, P. Geological exploration of South Atlantic islands and its contributions to the continental drift debate of the early 20th century. Proceedings of the Geologists' Association, 2015, 126, p. 266–81.

[13] Stone, P. Geology reviewed for the Falkland Islands and their offshore sedimentary basins, South Atlantic Ocean. Earth and Environmental Science Transactions of the Royal Society of Edinburgh, 2016, 106, p. 115-143.

[14] Martin, A.K. Plate tectonics: Microplates in Antartica. Nature, 1986, 319: 100-101.

[15] Ben Avraham, Z.; Hartnady, C.J.H.; Malan, J.A. Early tectonic extension between the Agulhas Bank and the Falkland Plateau due to the rotation of the Lafonia microplate. Earth and Planet. Sc. Lett., 1993, 117, p. 43-58.

[16] Richards, P.C.; Gatliff, R.W.; Quinn, M.F.; Williamson, J.P.; Fannin, N.G.T. The geological evolution of the Falkland Islands continental shelf. In Storey, B.C., King, E.C., Livermore, R.A. (eds.) Weddell Sea Tectonics and Gondwana Breakup. Geol. Soc., Sp. Pub., 1996, 108, p.105-28.

[17] Lovecchio, J.P.; Rohais, S.; Joseph, P.; Bolatti, N.D.; Kress, P.R.; Gerster, R.; Ramos, V.A. Multistage rifting evolution of the Colorado basin (offshore Argentina): Evidence for extensional settings prior to the South Atlantic opening. Terra Nova 2018, 30, p. 359-368.

[18] Ramos, V.A. Patagonia: A Paleozoic continent adrift? J. South Am. Earth Sci., 2008, 26(3), p. 235-251.

[19] Pángaro, F.; Ramos, V.A.; Pazos, P.J. The Hesperides basin: a continental-scale upper Palaeozoic to Triassic basin in southern Gondwana. Basin Research, 2016, 28, p. 685–711.

[20] Paton, D.A.; Mortimer, E.J.; Hodgson, N.; Van Der Spuy, D. The missing piece of the South Atlantic jigsaw: when continental break-up ignores crustal heterogeneity. In Sabato Ceraldi, T., Hodgkinson, R.A., Backe, G. (eds.) Petroleum Geoscience of the West Africa Margin. Geol. Soc. (London) Sp. Pub., 2016, 438, p. 8.

[21] Marshall, J.E.A. The Falkland Islands: A key element in Gondwana paleogeography. Tectonics, 1994, 13, p. 499-514.

[22] Rapela C.W.; Pankhurst, R.J. The granites of northern Patagonia and the Gastre Fault System in relation to the break-up of Gondwana. In Storey, B.C., Alabaster, T., Pankhurst, R.J. (eds.) Magmatism and the Causes of Continental Break-up, Geol. Soc., Sp. Pub., 1992, 68, p. 209-220.

[23] Thomson, K.; Hegarty, K.A.; Marshallsea, S.J.; Green, P.F. Thermal and tectonic evolution of the Falkland Islands: implications for hydrocarbon exploration in the adjacent offshore region. Marine and Petroleum Geology, 2002, 19. p. 95–116.

[24] Coira, B.L.; Nullo, F.E.; Proserpio, C.; Ramos, V.A. Tectónica de basamento de la región occidental del Macizo Nordpatagónico, provincias de Río Negro y Chubut. Rev. Asoc. Geol. Arg., 1975, 30(4), p. 361- 383.

[25] Franzese, J.; Martino, R. Aspectos cinemáticos y tectónicos de la zona de cizalla de Gastre en la sierra de Calcatapul, provincia de Chubut, Argentina. In 10º Congreso Latinoamericano de Geología y 6º Congreso Nacional de Geología Económica, Actas 1998, 2, p. 3.

[26] Von Gosen, W.; Loske, W. Tectonic history of the Calcatapul Formation, Chubut Province, Argentina, and the "Gastre Fault System". Journal of South American Earth Sciences, 2004, 18, p. 73-88.

[27] Klinger, F.L.; Martinez, M.P.; Gimenez, M.E.; Ruiz, F. Profundidades al basamento en el bajo de Gastre, a partir de soluciones de señal analítica, Chubut. Argentina. Latinmag Letters, Special Issue, 2011, 1, p. 1-7, Tandil.

[28] Rapela, C.W.; Pankhurst, R.J.; Fanning, C.M.; Hervé, F. Pacific subduction coeval with the Karoo mantle plume: The Early Jurassic Subcordilleran Belt of northwestern Patagonia. In Vaughan, A.P.M., Leat, P.T., Pankhurst, R.J. (eds.)

Terrane Accretion Processes at the Pacific Margin of Gondwana. Geol. Soc., Sp. Pub., 2005, 246, p. 217-239.

[29] Martin, A.K. Gondwana breakup via double-saloon-door rifting and seafloor spreading in a backarc basin during subduction rollback. Tectonophysics, 2007, 445, p. 245–72.

[30] Dalziel, I.W.D.; Lawver, L.A.; Norton, I.O.; Gahagan, L.M. The Scotia Arc: Genesis, Evolution, Global Significance. Annual Review of Earth and Planetary Sciences, 2013, 41, p. 767–93.

[31] Andersen, T.; Elburg, M.; Cawthorn-Blazeby, A. U–Pb and Lu–Hf zircon data in young sediments reflect sedimentary recycling in eastern South Africa. J. Geol. Soc., 2016, 173, p. 337–351.

[32] Gong, Z.; Langereis, C.G.; Mullender, T.A.T. The rotation of Iberia during the Aptian and the opening of the Bay of Biscay. Earth and Planet. Sc. Lett., 2008, 273(1-2): 80-93.

[33] Franke, D.; Neben, S.; Schreckenberger, B.; Schulze, A.; Stiller, M.; Krawczyk, C. M. Crustal structure across the Colorado Basin, offshore Argentina. Geophysical Journal International, 2006, 165, p. 850–864.

[34] Torsvik, T.H.; Rousse, S.; Labails, C.; Smethurst, M.A. A new scheme for the opening of the South Atlantic Ocean and the dissection of an Aptian salt basin. Geophys. J. Int., 2009, 177, p. 1315–1333.

[35] Biddle, K.; Snavely III, P.D.; Uliana, M.A. Plateau de las Malvinas. In V.A. Ramos and M.A. Turic (eds.) Geología y Recursos Naturales de la Plataforma Continental Argentina. Asociación Geológica Argentina e Instituto Argentino del Petróleo, p. 225-252, Buenos Aires, 1996.

[36] Curtis, M.L.; Hyam, D.M. Late Palaeozoic to Mesozoic structural evolution of the Falkland Islands: a displaced segment of the Cape Fold Belt. J. Geol. Soc. of London, 1998, 155, p. 115–29.

[37] Storey, B.C.; Curtis, M.L.; Ferris, J.K.; Hunter, M.A.; Livermore, R.A. Reconstruction and break-out model for the Falkland Islands within Gondwana. J. Afr. Earth Sci., 1999, 29, p. 153–63.

[38] Storey, B.C.; Vaughan, A.P.M.; Riley, T.R. The links between large igneous provinces, continental break-up and environmental change: evidence reviewed from Antarctica. Earth and Environmental Science Transactions of the Royal Society of Edinburgh, 2013, 104, p. 17–30.

[39] Dalziel, I.W.D.; Lawver, L.A. The lithospheric setting of the West Antarctic ice sheet. In The West Antarctic Ice Sheet: Behavior and Environment, R.B. Alley, R.A. Bindschadler, Antarct. Res. Ser. 2001, 77, p. 29–44. Washington.

[40] Macdonald, D.; Gómez-Pérez, I.; Franzese, J.; Spalletti, L.; Lawver, L.; Gahagan, L.; Dalziel, I.; Thomas, C.; Trewin, N.; Hole, M.; Paton, D. Mesozoic break-up of SW Gondwana: implications for regional hydrocarbon potential of the southern South Atlantic. Mar. and Petrol. Geol., 2003, 20, p. 287-308.

[41] Tankard, A.; Welsink, H.; Aukes, P.; Newton, R.; Stettler, E. Geodynamic interpretation of the Cape and Karoo basins, South Africa. Phanerozoic Passive Margins, Cratonic Basins and Global Tectonic Maps, 2012, 23, p. 869-945.

[42] Stanca, R.M.; Paton, D.A.: Hodgson, D.M.; McCarthy, D.J.; Mortimer, E.J. A revised position for the rotated Falkland Islands microplate, J. Geol. Soc. (online), 2019, https://jgs.lyellcollection.org/content/jgs/early/2019/01/24/jgs2018-163.

[43] Ghidella, M.E.; Yañez, G.; LaBrecque, H.L. Revised tectonic implications for the magnetic anomalies of the Western Weddell Sea. Tectonophysics, 2002, 347(1-3), p. 65-86.

[44] Cúneo, R.; Ramezani, J.: Scasso, R.; Pol, D.; Escapa, I.; Zavattieri, A.M.; Bowring, S.A. High-precision U-Pb geochronology and a new chronostratigraphy for the Cañadón Asfalto Basin, Chubut, central Patagonia: implications for terrestrial faunal and floral evolution in Jurassic. Gondwana Research, 2013, 24, p. 1267-1275.

[45] Gust, D.A.; Biddle, K.T.; Phelps, D.W.; Uliana, M.A. Associated Middle to Late Jurassic Volcanism and Extension in Southern South America. Tectonophysics, 2013, 116, p. 223–253.

[46] Uliana, M.A.; Biddle, K.T.; Phelps, D.W.; Gust, D.A. Significado del vulcanismo y extensión mesojurasicos en el extremo meridional de Sudamérica. Rev. Asoc. Geol. Arg., 1985, 40, p. 231–253.

[47] Lovecchio, J.P.; Naipauer, M.; Lubin Cayo, E.; Rohais, S.; Giunta, D.; Flores, G.; Gerster, R.; Bolatti, N.D.; Joseph, P.; Valencia, V.; Ramos, V.A. Rifting evolution of the Malvinas basin, offshore Argentina: new constrains from zircon

U–Pb geochronology and seismic characterization. J. South Am. Earth Sci., 2019, 95, p. 102253.

[48] Hälbich, I. W (ed.). The Cape Fold Belt-Agulhas Bank Transect across the Gondwana Suture in southern Africa. American Geophysical Union Special Publication, AGU Press, 202, Washington. 1993.

[49] Pángaro, F.; Ramos, V.A. Paleozoic crustal blocks of onshore and offshore central Argentina: new pieces of the southwestern Gondwana collage and their role in the accretion of Patagonia and the evolution of Mesozoic south Atlantic sedimentary basins. Marine and Petroleum Geology, 2012, 37(1), p. 162-183.

[50] Ramos, V.A.; Cortés, J.M. Estructura e interpretación tectónica. In V. Ramos (ed.) Geología y recursos naturales de la Provincia de Río Negro, 9° Congreso Geológico Argentino (S.C. Bariloche), Relatorio, p. 317 - 346, Buenos Aires. 1984.

[51] Von Gosen, W. Thrust tectonics in the North Patagonian Massif (Argentina): Implications for a Patagonia plate. Tectonics, 2003, 22, 1, 1005, doi:10.1029/2001TC901039, 2003

[52] López de Luchi, M.G.; Rapalini, A.E.: Tomezzoli, R.N. Magnetic fabric and microstructures of Late Paleozoic granitoids from the North Patagonian Massif: Evidence of a collision between Patagonia and Gondwana? Tectonophysics, 2010, 494, p. 118–137.

[53] Mosquera, A.; Silvestro J.; Ramos, V.A.; Alarcón, M.; Zubiri, M. La estructura de la dorsal de Huincul. In Leanza, H. et al. (eds.) Geología y Recursos Naturales de la Provincia del Neuquén, 17° Congreso Geológico Argentino, Relatorio, 2011, p. 385-398, Neuquén.

[54] Silvestro, J.; Zubiri, M. Convergencia oblicua: modelo estructural alternativo para la dorsal neuquina (39ºS) – Neuquén. Rev. Asoc. Geol. Arg., 2008, 63(1), p. 49-64.

[55] Mosquera, A.; Ramos, V.A. Intraplate deformation in the Neuquén Basin. In S.M. Kay and V.A. Ramos (eds.) Evolution of an Andean margin: A tectonic and magmatic view from the Andes to the Neuquén Basin (35°–39°S latitude). Geol. Soc. Am., Sp. Paper, 2006, 407, p. 97-124.

[56] Mosquera, A. Mecánica de deformación en la cuenca neuquina, Neuquén. Facultad de Ciencias Exactas y Naturales, Universidad de Buenos Aires, Ph.D. Thesis (online), 2008, 264 pp., Buenos Aires.

[57] McCarthy, D.; Aldiss, D.; Arsenikos, S.; Stone, P.; Richards, P. Comment on "Geophysical evidence for a large impact structure on the Falkland (Malvinas) Plateau". Terra Nova, 2017, 29, p. 411–415.

[58] Miller, W.; de Wit, M.J.; Linol, B.; Armstrong, R. New Structural Data and U/Pb Dates from the Gamtoos Complex and Lowermost Cape Supergroup of the Eastern Cape Fold Belt, in Support of a Southward Paleo-Subduction Polarity. In de Wit, M.J., Linol, B. (eds.) Origin and Evolution of the Cape Mountains and Karoo Basin, Regional Geology Reviews, 2016, p. 35-44.

[59] Ramos, V.A.; Naipauer, M. Patagonia: Where does it come from? Journal of Iberian Geology 2014, 40(2), p. 367-379.

[60] Thomson, K. When did the Falklands rotate? Mar. Petrol. Geol., 1998, 15, p. 723-736.

[61] Chemale Jr., F.; Ramos, V.A.; Naipauer, M.; Girelli, T.J.; Vargas, M. Age of basement rocks from the Maurice Ewing Bank and the Falkland/Malvinas Plateau. Precambrian Research 2018, 314, p. 28-40.

[62] Hastie, W.W.; Watkeys, M.K.; Smith, A.M. Tectonic significance of the sedimentary and palaeocurrent record at the eastern edge of the Karoo Basin. Jour. Afric. Earth Sci., 2019, 158, p. 103-43.

[63] Homovc J.F.; Constantini, L. Hydrocarbon exploration potential within intraplate shear-related depocenters: Deseado and San Julián basins, southern Argentina. Am. Assoc. Pet. Geol. Bull., 2001, 85(10), p. 1795-1816.

[64] Jenchen, U. 2018. Petrography and geochemistry of the Triassic El Tranquilo Group, Deseado Massif, Patagonia, Argentina: implications for provenance and tectonic setting, J. South Am. Earth Sci. 88, p. 530–550.

[65] Hervé, F.; Fanning, C.M.; Pankhurst, R.J.; Mpodozis, C.; Klepeis, K.; Calderón, M.; Thomson, S.N. Detrital zircon SHRIMP U–Pb age study of the Cordillera Darwin Metamorphic Complex of Tierra del Fuego: sedimentary sources and implications for the evolution of the Pacific margin of Gondwana. J. Geol. Soc., 2010, 167, p. 555–568.

[66] Barbeu, D.L.; Olivero, E.B.; Swanson-Hysell, N.L.; Zahid, K.M.; Murray, K.E.; Gehrels, G.E. Detrital-zircon

geochronology of the eastern Magallanes foreland basin: Implications for Eocene kinematics of the northern Scotia Arc and Drake Passage. Earth and Planet. Sc. Lett., 2009, 284, p. 489-503.

[67] Suárez, R.; González, PG.; Ghiglione, M.C. A review on the tectonic evolution of the Paleozoic-Triassic basins from Patagonia: Record of protracted westward migration of the pre-Jurassic subduction zone. J. South Am. Earth Sci., 2019, 95, https://doi.org/10.1016/j.jsames.2019.102256

[68] Carter, A.; Curtis, M.; Schwanethal, J. Cenozoic tectonic history of the South Georgia microcontinent and potential as a barrier to Pacific-Atlantic through flow. Geology, 2014, 42(4), p. 299–302.

[69] Riley, T.A.; Carter, A.; Leat, P.T.; Burton-Johnson, A.; Bastias, J.; Spikings, R.A.; Tate, A.J.; Bristow, C.S. Geochronology and geochemistry of the northern Scotia Sea: A revised interpretation of the North and West Scotia ridge junction. Earth and Planet. Sc. Lett., 2019, 518, p. 136–147.

[70] Ghiglione, M. Orogenic Growth of the Fuegian Andes (52–56°) and Their Relation to Tectonics of the Scotia Arc. In Folguera et al. (eds.), Growth of the Southern Andes, Springer Earth System Sciences, 2016, p. 241-267.

Bios

Victor A. Ramos

Professor at the University of Buenos Aires and Researcher Emeritus of CONICET, Victor has studied the tectonic evolution of the Andes for more than 50 years, making numerous contributions to knowledge on this topic. He has also worked on the geological evolution of the Argentine continental shelf and the Malvinas plateau. He has directed more than 30 doctoral theses on these topics and is currently a researcher at Instituto de Estudios Andino don Pablo Groeber. Corresponding author. Email: victoralbertoramos@gmail.com.

Jaun Pablo Lovecchio

Juan Pablo Lovecchio works as Senior Exploration Geologist at YPF. He obtained a Geology degree from the National University of Córdoba in 2009, a M.Sc. in Petroleum Exploration from IFP-School (France) in 2011, and a PhD from the University of Buenos Aires and Sorbonne University (France) in 2018. He has more than ten years of experience working in frontier exploration across South America and Africa. For the last 5 years, he has been involved in the exploration of the main Argentinean offshore basins.

Farid Chemale

Farid Chemale Junior is an expert on tectonics working in South America, southern Africa and Antarctic. He earned a B.A. of Geology in 1978 from UNISINOS and a M.S of Geosciences in 1982 from UFGRS. He holds a degree in Nature Sciences from TU Clausthal, Ph.D. (1987). He is currently a Professor of Geology Graduate Program at UNISINOS and has previously served as member of the staff at the University of Brasilia, Ouro Preto and Rio Grande do Sul. He has written 196 research papers focused on tectonics, stratigraphy, geochemistry and isotope studies.

Maximiliano Naipauer

Maximiliano Naipauer is Doctor in Natural Sciences (2007) from University of La Plata. His main research topic is provenance analysis of sedimentary and metasedimentary rocks based on U-Pb ages in detrital zircons of the Neuquén Basin, Sierras Pampeanas and from Precordillera. He is Full Professor of Regional Geology at the University of La Plata, and head and researcher in the Institute of Geochronology and Isotopic Geology of the University of Buenos Aires - CONICET. He has a vast experience in Geochronology and has worked in different laboratories in Brazil and USA.

Science Reviews
from the end of the world

Vol. 1, No. 1, December 2019 // pp. 19-36 /

Scinderin, an actin severing and nucleating protein: molecular structure and possible roles in cell secretion, maturation, differentiation and cancer

José-María Trifaró

Emeritus Professor, Department of Cellular and Molecular Medicine, School of Medicine, University of Ottawa, Ottawa, Ontario, Canada.
Email: Jose-Maria.Trifaro@canada.ca

Abstract

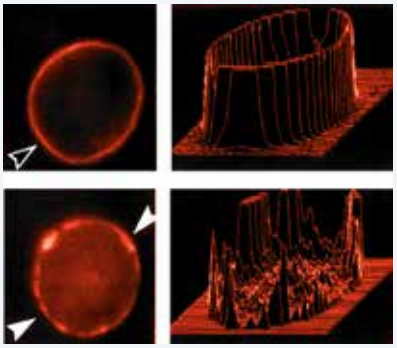

Scinderin is a filamentous actin-severing and capping protein. Segmental deletion and point-mutation studies have shown that this scinderin actin-severing activity resides in its NH2 terminal half, precisely in domains 1 and 2. The actin nucleating activity of scinderin is in its domain 5. Scinderin's F-actin severing activity plays a role in cell secretion. In secretory cells, scinderin is highly concentrated in the cell cortex, showing a distribution similar to that of filamentous actin. Two PIP2-binding sites have been described in scinderin domains 1 and 2. PIP2 inhibits the actin-severing activity of the protein. Several approaches [recombinant scinderin, antisence oligonucleotide, gene promoter activation, vector-mediated expression of scinderin active domains] were used to prove the role of scinderin in secretion. The promoter of SCIN, the scinderin gene, has been characterized and its responsive elements have been described. The activation of the SCIN promoter by two ligands of the aryl hydrocarbon receptor [AhR] transcription factor has been shown. This activation increased scinderin expression with a resulting increase in stimulation-induced cortical actin disassembly and exocytosis. A role for scinderin in the life cycle of megakaryocytes has also been demonstrated. Scinderin seems to be involved in the maturation, differentiation and apoptosis processes of these cells, releasing newly formed platelets. This completes the life cycle of a megakaryocyte. A role for scinderin in cancer is also emerging. The SCIN gene is silenced in megakaryocyte leukemia cells and its re-expression induces cell maturation, differentiation, apoptosis, as well as the release of platelet-like particles and anti-tumor effects. These are always accompanied by changes in cell morphology due to cytoskeleton re-arrangements. Scinderin over-expression is necessary to see anti–proliferation effects, which are always accompanied by maturation and differentiation. If there were methods to differentiate other types of tumor cells, a new area of treatment would be developed by inducing "cell maturation and/or differentiation".

Keywords:
Scinderin, actin, secretion, megakaryocyte, leukemia

1. Introduction

Cells contain actin filaments organized into a variety of structures, including a three-dimensional filament network in the cell cortex under the plasma membrane. This cortical actin network is very predominant in secretory cells [Orci et. al. 1972, Lee and Trifaró 1981, Trifaró 1983]. Actin networks are dynamic structures that go through cycles of filament

polymerization and de-polymerization as required for cell functions. In secretory cells, cortical actin seems to play a dual role – first, excluding secretory vesicles from releasing sites on the plasma membrane [Vitale et. al. 1991], and second, facilitating secretion through novo filament formation in the latest steps of exocytosis [Trifaró et. al. 2008]. Thus, cell stimulation brings about, in a calcium–dependent manner, a disassembly of the cortical actin filaments allowing the movement of vesicles towards release sites on the plasma membrane.

Cell actin dynamics is controlled through the action of capping and severing proteins. Capping proteins bind to either the pointed end [-] or barbed end [+] of actin filaments and thereby control G-actin unit exchange. Most capping proteins bind to the [+] end, and in this way limit filamentous actin growth. Capping proteins may also have a nucleating capacity under conditions favouring actin polymerization. Among this class of actin capping and severing proteins are fragmin, severin, gelsolin, scinderin and villin [Loppspeich et. al. 1988; Marcu et. al. 1994], which bind to actin in a calcium-dependent manner. Work from Trifaró's laboratory [Trifaró et. al. 1985; Bader et. al. 1986] first showed the presence of gelsolin-like proteins in a secretory cell, the chromaffin cell. One of these studies also showed the presence of a Ca^{2+}-dependent actin-binding protein that was immunologically different from gelsolin [Trifaró et. al. 1985]. The isolation and characterization of this protein was carried in our laboratory [Trifaró et. al. 1989; Rodríguez del Castillo et. al. 1990]. This work has shown that this protein was distinct from gelsolin, although gelsolin was also present in the cell [Bader *et al.* 1986; Trifaró et. al. 1989; Rodríguez Del Castillo et. al. 1990]. The name ***'scinderin'*** was given to this protein [a name derived from the Latin "scindere' meaning: 'to cut'], because of its actin filament severing properties [Trifaró et.al. 1989; Rodríguez Del Castillo et. al. 1990]. Subsequent work from our laboratory, demonstrated the presence of scinderin in platelets [Rodríguez Del Castillo et. al. 1992] as well as in other secretory tissues [Tchakarov 1990]. Cloning of scinderin cDNA [Accession number X78479, EMBL Data Library] and sequence analysis done in our laboratory [Marcu et. al. 1994] demonstrated that, similar to gelsolin, another actin severing protein, scinderin has 6 domains with 3 actin-binding sites [Marcu et. al. 1994; 1996; Zhang et. al. 1996].

This review describes the molecular structure and function of scinderin and its possible roles in the secretory process, cell maturation, differentiation and pathological conditions.

2. Molecular structure and function of scinderin

Scinderin is a protein with 715 amino acids that shares 63% and 53% homology, respectively, with gelsolin and villin [Marcu et al 1994], two other actin-capping and severing proteins [Lottspeich et. al. 1988, Marcu et. al. 1994]. Comparing the scinderin sequence with those of gelsolin and villin reveals that they share six internal short sequence motifs that are repeated [A, B. C; Figure 1]. Two other actin filament severing proteins, severin from the Distyostelium discoideum [Lottspeich et. al. 1988] and fragmin from Physarum polycecephalum [Ampe et. al. 1987], with half the molecular mass of scinderin, also have similarities with the end N-terminal half of scinderin. After aligning motifs A, B and C, gelsolin, villin and scinderin reveal six domains [D1-D6]. There are strong similarities between domains 1 and 4, 2 and 5, and 3 and 6 in gelsolin, villin and scinderin [Marcu et al 1994]. These, added to the fact that fragmin and severin have a better homology with the N-terminal half of scinderin, gelsolin and villin, would suggest that these three proteins have derived by gene duplication from an ancestral actin-filament severing protein which was similar to the N-terminal half of these molecules [Marcu et al 1994]. It has also been suggested that this family of actin filament-severing proteins may have evolved by tandem gene triplication with a predicted 14 kDa monomer unit of 120-130 amino acid residues [Way et. al. 1988]. This is approximately the size of domain or segment 1 in gelsolin.

Previous work from our laboratory has demonstrated that two actin molecules bind one scinderin molecule, and that this interaction is Ca^{2+}-dependent [Trifaró et. al. 1992]. Moreover, the two main fragments (40 and 38 kDa) obtained through limited proteolytic digestion interact with actin, also in a Ca^{2+}-dependent manner, yielding actin-fragment complexes of molar ratios 1:1 [Trifaró et. al. 1992]. These results suggest that each scinderin fragment contains an actin- and a Ca^{2+}-binding site. These results are in agreement with equilibrium dialysis studies [Rodríguez Del Castillo et. al. 1990] that demonstrated the presence of at least two Ca^{2+}-binding sites in scinderin (K_d 5.85 x 10^{-7} M, B_{max} 0.81 mol Ca^{2+}/mol protein and K_d 2.85 x 10^{-6}M, B_{max} 1.87 mol Ca^{2+}/mol protein). These two Ca^{2+} sites regulate activation with respect to severin in a single rate-limiting step [Lueck et. al. 2000]. The N-terminal half of scinderin [S1-S3] severs F-actin and sequesters G-actin in a Ca^{2+}-dependent process. In contrast, the N-terminal half of gelsolin (G1-G3) severs and sequesters actin in the absence of Ca^{2+}. Further comparison of scinderin sequences to those of gelsolin and villin showed the presence of two actin-binding site sequences in domains 1 and 2, respectively [Figures 1 and 2].

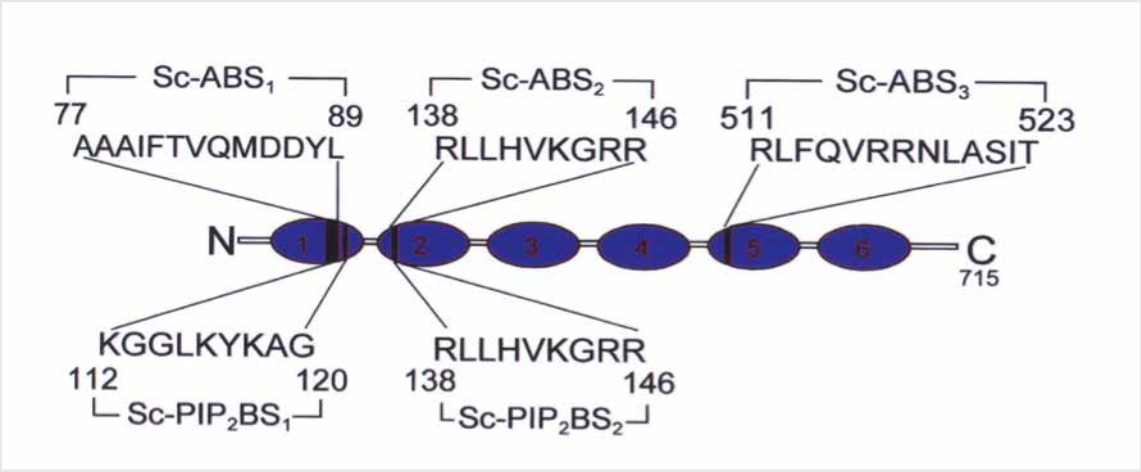

Figure 1. Diagram showing scinderin domains [S1-S6] and scinderin's three actin [$ScABS_{1,\ 2\ and\ 3}$] and two PIP_2 [$ScPIP_2BS_{1\ and\ 2}$]. The amino acid sequence and the number of the first and last amino acid in every construct is indicated. Every domain [S1 to S6] has 3 short sequence motifs – A, B and C – in common with gelsolin and villin, two other F-actin severing proteins.

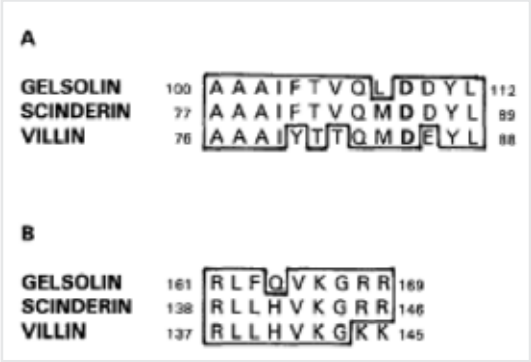

Figure 2. Comparison of amino acid sequences in two Scinderin regions with those sequences in known actin-binding domains of Gelsolin and Villin. Two stretches of amino acid sequences of scinderin from position 77-89 and from 138-146 show a high degree of homology with two (A and B) actin-binding domains previously described for human plasma gelsolin and chicken intestinal brush border villin. Aspartate 86 of scinderin corresponds to similar residues in position 109 and 85 of gelsolin and villin, respectively. Aspartate 109 has been shown to be one of Ca^{2+}-binding sites in gelsolin [McLaughlin et. al. 1993]. The numbers on either site indicate the position of amino acid residues.

The high homology between these two actin-binding sites in these proteins would suggest that the type of interaction described between gelsolin domains 1 and 2 and actin regarding the mechanism of filament severing [McLaughlin et. al. 1993] might be similar for scinderin and villin. Moreover, isoleucine residue 103 in gelsolin's first actin-binding site seems to be important for the interaction with subdomains 1 and 3 of actin [McLaughlin et. al. 1993]. Scinderin and villin have an isoleucine in the same position [residues 80 and 79 respectively; Figure 2 A] within their actin-binding site [Marcu et. al. 1994]. Comparison of the amino acid sequence of the first actin binding site in these proteins reveals that D86 in scinderin corresponds to D109 and D85 in gelsolin and villin, respectively [Figure 2A]. It has been suggested that one Ca^{2+} ion is intermolecularly bound between D109 in gelsolin and E167 in actin, with the rest of the coordination links coming from domain G1 in gelsolin [McLaughlin et. al. 1993].

A third actin-binding site for actin has also been described in domain S5 in scinderin [Marcu et. al. 1998]. This actin-binding site at the N-terminal of domain S5 [$Sc^{511-518}$] can bind and nucleate actin assembly. Moreover, $ScABP_3$, a peptide constructed with the sequence (RLFQVRRNLASIT), identical to $Sc^{511-523}$, blocked the binding of recombinant Sc5-6 to actin and its nucleating activity [Marcu et. al . 1998]. In addition, recombinant Sc5-6 and $Sc\text{-}ABP_3$ also prevent the actin-severing activity of full-length scinderin. This suggests that scinderin, in addition to binding actin on sites present in domains S1 and S2, must bind actin on a third site in domain S5 to sever and nucleate actin effectively [Marcu et. al. 1998]. The crystal structure of the C-terminus in scinderin has been published [Chumnarnsilpa et. al. 2009]. A comparative analysis [Chumnarnsilpa et. al. 2009] of x-ray data from actin-binding surfaces observed in domains G4-G6 in gelsolin suggested that scinderin in a similar conformation will also be able to interact with actin through Sc4 and Sc6, and that no interaction should occur with Sc5 as predicted and shown by Marcu et. al. [1998]. The suggestion on the absence of a binding- and nucleating-site for actin in Sc5 [Chumnarnsilpa et. al. 2009] is difficult to accept in view of the extensive published evidence on the location and function of this third actin-binding site of scinderin. The theory of the presence of an actin-binding site in Sc-5 came from experiments on actin nucleation, viscosity of actin gels, serotonin and catecholamine, and grow hormone release during over-expression in secretory cells of fragments Sc5, ScABP3 and ScL5-6 or ScL5; these last two fragments lacking the third actin binding site of scinderin [Marcu et. al. 1998; Trifaró et. al. 2000; Dumitrescu et. al. 2005].

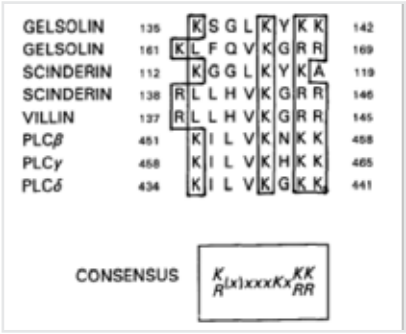

Figure 3. Comparison of amino acid sequences of two scinderin regions with those known PIP_2 binding sequences. Two stretches of amino acid sequences in scinderin show a high level of homology with villin's PIP_2 binding site, gelsolin's PIP_2 binding sites in domains 1 and 2 [Yu et. al. 1992], and the PIP_2 binding sequence in the conserved 'X box' of rat phospholipase C family [Rhee et. at. 1989]. The second scinderin sequence (138-145) is identical to villin sequence from position 134-145. The numbers on either side indicate the position of the amino acid residues.

Published work indicates that PIP_2 modulates the activity of many actin-regulatory proteins [Janmey et. al. 1987, Maekawa et. at. 1990, Isenberg 1991], including scinderin [Rodríguez Del Castillo et. al. 1992]. F-Sc1, a fusion protein obtained by the expression of scinderin's domain Sc1 in prokaryotes, binds PS and PIP_2 in a Ca^{2+}-dependent manner [Marcu et. al. 1994]. Previous work also carried out by our laboratory has demonstrated that native scinderin has the ability to interact with these two phospholipids [Del Castillo et. al. 1992]. Comparison of amino acid sequences showed the presence in scinderin of sequences that are highly homologous to those known to bind PIP_2 in gelsolin [Figure 3]. These amino acid sequences are in both scinderin and gelsolin, in the C-terminal of the S1/G1 domain, and in the N-terminal of the S2/G2 domain [Fig 2]. As shown in Figure 3, villin has only one PIP_2 binding site. Interestingly, this sequence is also found in several phospholipase C isozymes [Rhee et. al. 1989, Yu et. al, 1992] where it is known as the 'X Box' [Rhee et. al. 1989]. Scinderin shows a difference in the consensus sequence in one of PIP_2 binding motifs – there is an alanine instead of a lysine in position 119 [Figure 3]. Consequently, it appears that the replacement of the KK motif by a KA one would impair the ability of scinderin to interact with PIP_2. However, published evidence on site-directed mutagenesis of gelsolin has shown that a gelsolin mutant with a single lysine [K] in the 'X Box' substituted by alanine [A] does not show any decrease in either PIP_2 binding or its ability to modulate the severing activity [Yu et. al. 1992]. As with gelsolin, the second PIP_2-binding site of scinderin overlaps with the second actin-binding site. This would explain, at least in part, the inhibitory effect of PIP_2 on gelsolin and scinderin F-actin severing activities [Zhang et. al. 1996]. The binding of PS to scinderin S1 domain [Rodríguez Del Castillo et. al. 1992; Marcu et. al. 1994] is a property not described for gelsolin [Janmey et. al. 1987]. The amino acid sequence responsible for the binding of PS is still unknown. However,

we have proposed earlier that plasma membrane PS might provide a binding site for scinderin on the inner surface of the membrane [Rodríguez Del Castillo et. al. 1992]. This hypothesis is based on the following facts: a) that scinderin binding to PS liposomes in the presence of other cytosolic proteins is higher at pH 6 and 10^{-8} M Ca^{2+}, a condition similar to that found in resting cells [Rodríguez Del Castillo et. al. 1992; Marcu et al 1994] and b) under resting conditions in secretory cells (i.e. chromaffin cell), scinderin cortical cell distribution does not depend on its binding to actin [Vitale et. al. 1991; Marcu et. al. 1994].

SCIN, the scinderin gene, is located in chromosome 7 [Cytogenic location7p21.3, Accession number AB067492: GenBank; Nagase et. al. 2001]. It has been shown that SCIN is conserved in chimpanzee, Rhesus monkey, dog, cow, mouse, rat, chicken, zebrafish and frog. The SCIN promoter has also been described and characterized in our laboratory [Trifaró et. al. 2008]. The promoter shows the presence of several Ap_2 and four dioxin responsive element [DRE] motifs at -14, -31, -185 and -217 upstream of the scinderin initiation site ATG. DREs are recognition sites for the transcription factor aryl hydrocarbon receptor [AhR], and its presence in a secretory cell (i.e., chromaffin cell) has been demonstrated [Trifaró et al, 2008]. The activation of scinderin's promoter in vitro by two AhR ligands; 2, 3, 7, 8-tetrachlorodibenzo-p-dioxin [TCDD], and all trans-retinoic acid [ATRA] with the consequent increase in scinderin transcription and over-expression was also demonstrated. Treatment of chromaffin cell cultures for 48 hr. with either 10 nM TCDD or 10 µM ATRA resulted in high levels of scinderin expression and potentiation of cell depolarization-induced F-actin disassembly and catecholamine release [Trifaró et. al. 2008].

3. Scinderin in the secretory process

The F-actin severing activity of scinderin seems to play a role in cell secretion [Vitale et. al. 1995; Zhang et. al. 1996; Marcu et. al. 1996]. Scinderin is present in secretory cells, including chromaffin cells [Rodríguez del Castillo et. al. 1990] and platelets [Rodríguez Del Castillo et. al. 1992]. In chromaffin cells, scinderin is highly concentrated in the cortex [Vitale et. al. 1991], showing a distribution similar to that of filamentous actin [Vitale et. al. 1991]. Immunocytochemical experiments have shown that cell stimulation simultaneously induces cortical F-actin disassembly and redistribution of subplasmalemmal scinderin [Vitale et. al. 1991]. Stimulation removal allows cells to recover actin and scinderin cortical localization, as demonstrated by immunocytochemistry [Vitale et al 1991]. However, cortical scinderin distribution is recovered before cortical actin distribution, suggesting that scinderin is bound to structures other than cortical actin at the subplasmalemmal zone of the cell [Vitale et. al. 1991], as indicated above. Consequently, cortical F-actin acts as a barrier to the free movement of secretory vesicles to release sites (Figure 4), and only during cell stimulation-induced Ca^{2+} entry, cortical F-actin is disassembled through a Ca^{2+} dependent activation of scinderin (Vitale et. al. 1991). This would allow the movement of secretory vesicles (Figure 4) towards release sites on the plasma membrane [Vitale et. al. 1991; Trifaró et. al. 1992, Vitale et. al. 1995]. Areas of actin disassembly correspond to plasma membrane areas of vesicle exocytosis as the experiments with dopamine β-hydroxylase antibodies have demonstrated [Trifaró et. al. 1993]. Ultrastructural [Tchakarov 1998] and path clamp experiments [Vitale et. al. 1995] have confirmed this hypothesis. Secretory vesicles are in different cellular pools (Reserve pool: Pool A; Readily-releasable: Pool B, Immediately-releasable: Pool C), where vesicles are in various states of release ability. The transit of vesicles between compartments is not random, but an event controlled and regulated by Ca^{2+}, the cortical actin network and their regulatory proteins [Trifaró 1997]. Myosin V seems to be the molecular motor involved in the transport of secretory vesicles from the reserve pool to the release-ready vesicle pool [Rosé et. al. 2003].

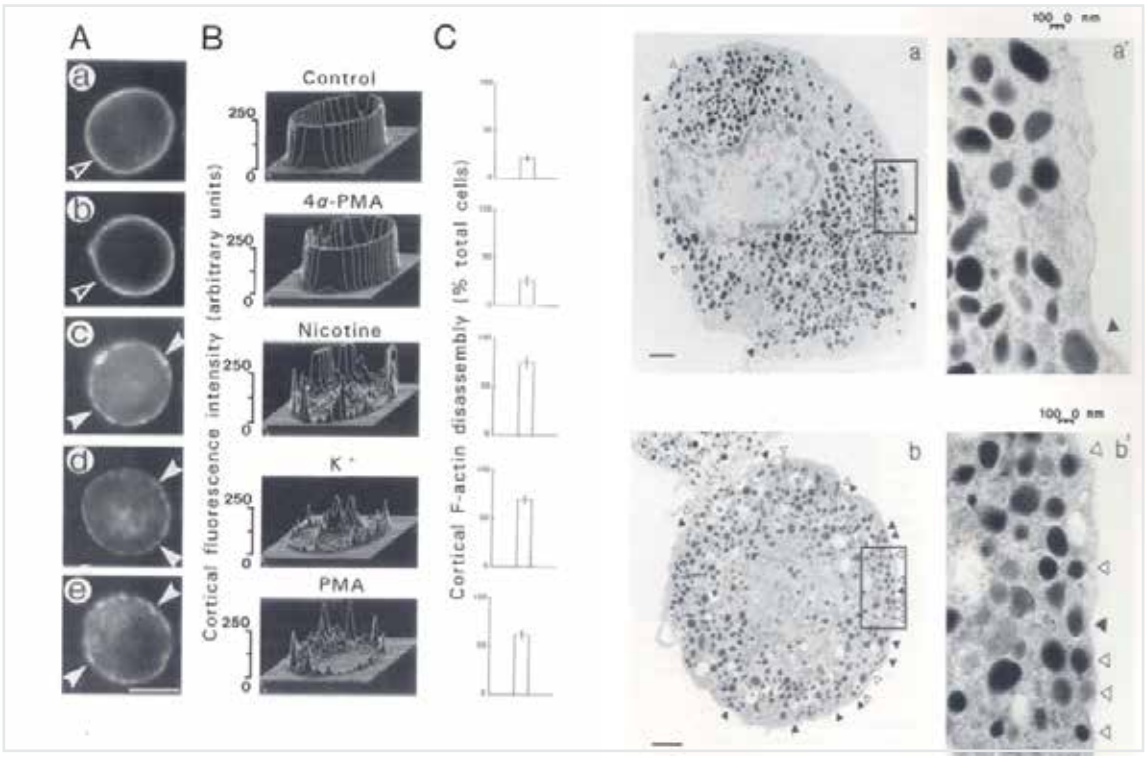

Figure 4. A) Fluorescence microscopy and B) video-enhanced image analysis of F-actin fluorescence profiles (rhodamine-phalloidin staining) in chromaffin cells under controlled or stimulated conditions. (C) shows the effects of different treatments on the percentage of cells displaying cortical F-actin disassembly. Control cells in (A) and (B) show a contiguous and bright fluorescent cortical ring (open arrowheads). 4α-PMA is an inactive isomer of PMA. Stimulation with nicotine, high K+ and PMA caused the disruption of the cortical fluorescent ring (actin disassembly). Some fluorescent patches are shown by closed arrowheads. B) Three-dimensional image analysis of cells shown in (A). In stimulated cells [c, d and f], the cortical fluorescence patterns show irregularities such as valleys and peaks. The peaks correspond to the fluorescent patches of cells shown in (A). The four panels on the right show electron micrographs of isolated adrenal chromaffin cells, control in upper panels and stimulated in lower panels. (A) shows a control cell with a cortical zone of 150nm, practically devoid of secretory vesicles. In this exclusion zone, only few secretory vesicles (about 200 vesicles per cell) are located close (0-50 nm) to the plasma membrane (closed arrowhead). (A') shows a large magnification of the area within the box in (A). Most secretory vesicles in control cells are situated at about 150 nm from the plasma membrane and separated from the plasma membrane by cortical F-actin. B) stimulated cells show an increased number of secretory vesicles in the 0-50 nm area (open arrowheads). These are areas of cortical F-actin disassembly and exocytosis. This can be seen at higher magnification in (B'). Magnification: 234x (A); 10,773x (B); 51,072x (A' and B'). Bar: 1µm.

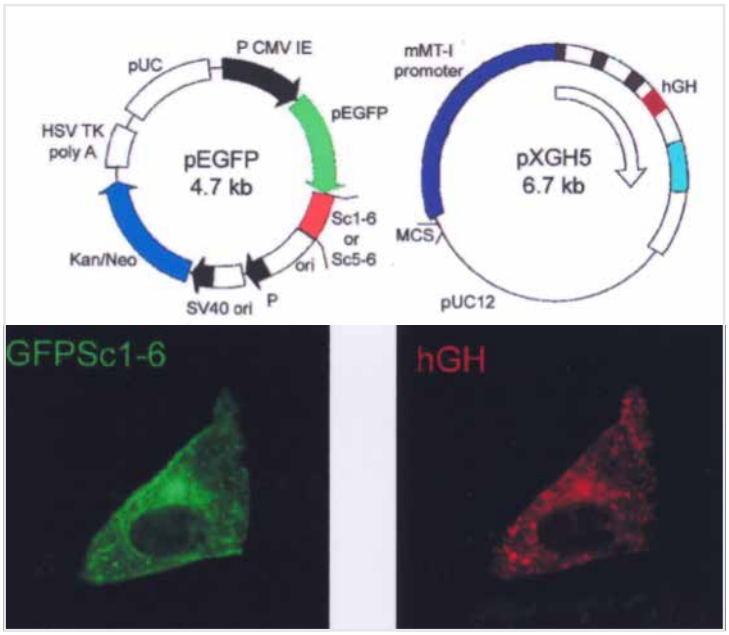

Figure 5. Co-expression of green fluorescent protein [GFP]-fused Scinderin [Sc] and human growth hormone [hGH] gene in chromaffin cells. A diagram of the components of the two vectors used in co-transfection is shown at the top of the figure. Co-transfected cells were fixed, permeabilized and stained for hGH using a polyclonal antibody against hGH. The immunocytochemistry panel shows a co-transfected cell stained for hGH and, at the same time, expressing GFPSc1-6. In these experiments, co-transfected chromaffin cells synthesized hGH and stored it in chromaffin vesicles (dopamine B-hydrolase positive vesicles). Several Sc constructs [Sc1-2, Sc5-6, Sc5, ScL5, $ScABS_2$] were also prepared and co-transfected with the hGH carrying vector. See Figures 6 and 7 and Dumitrescu et. al. [2005].

Four approaches followed in our laboratory have demonstrated a role of scinderin in secretion:

1) Ca^{2+}-induced F-actin disassembly and exocytosis from permeabilized chromaffin cells and platelets was increased by recombinant scinderin [Zhang et. al. 1996; Marcu et. al. 1996]. No effects were observed when recombinant scinderin was devoid of actin-binding sites 1 and 2 (truncated Sc). Recombinant scinderin-evoked increases in exocytosis of catecholamines and serotonin in permeabilized chromaffin cells and platelets, respectively, were inhibited by exogenous G-actin, by two peptides with sequences corresponding to the two scinderin actin-binding sites ($ScABS_1$ and $ScABS_2$), and by PIP_2, an inhibitor of scinderin activity [Zhang et. al. 1996; Marcu et. al. 1996]. These results were confirmed in mouse pancreatic β-cells, where three peptides with sequences corresponding to each of three actin-binding sites of scinderin inhibited insulin stimulated secretion as measured by patch clam [Trine et. al. 2000].

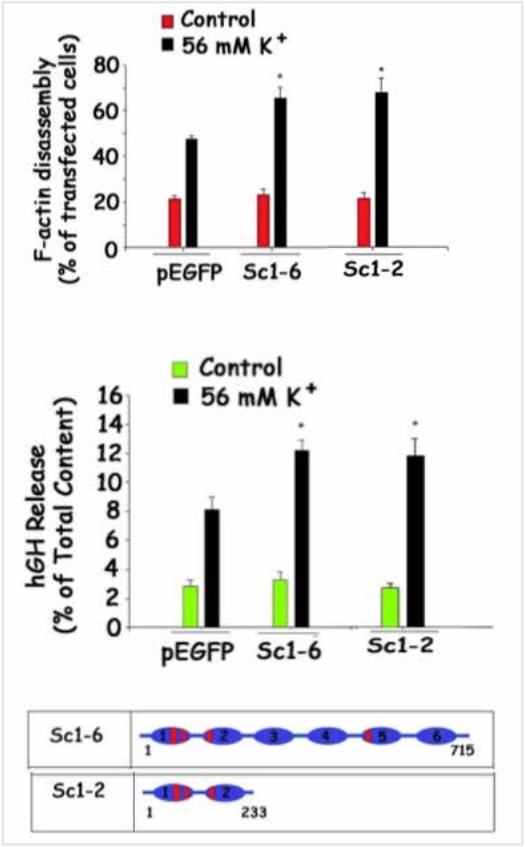

Figure 6. Effects of over-expression of scinderin [S1-6] and a construct [Sc1-2] with F-actin severing activity on cortical F-actin disassembly and human growth hormone [hGH] release from chromaffin cells upon high K^+-induced cell depolarization. A schematic representation of constructs is shown at the bottom of the figure. A potentiation of both cortical actin disassembly and hGH release is observed in cells over-expressing Sc 1-6 and Sc1-2. Control cells were co-transfected with vector [pEGPP] alone [Dumitrescu et. al. 2005].

2) Oligonucleotide targeting the scinderin gene SCIN decreased the expression of scinderin and depolarization and/or Ca^{2+}-evoked F-actin disassembly and exocytosis, either in intact or permeabilized secretory cells (Figure 8A) [Lejen et. al. 2001].

3) The promoter region of SCIN has, as indicated above, dioxin-responsive element [DRE] sequences and binding sites for the transcription factor aryl hydrocarbon receptor (AhR), a receptor shown to be present in chromaffin cells. Ten nM TCCD (2,3,7,8-tetra-chlorodibenzo-p-dioxin) or 10 µM ATRA (all *trans*-retinoic acid), both ligands for the AhR, increased scinderin expression and potentiated stimulation induced F-actin disassembly and exocytosis (Figure 8B) [Lejen et. al. 2003; Trifaró et. al. 2008].

4) Similar potentiation of F-actin disassembly and exocytosis was observed with vector-mediated expression of full length scinderin or its active domains S1-Sc2 (Figure 6) [Dumitrescu et. al. 2005]. On the other hand, vector-mediated expression of scinderin domains S5-6, S5 or $ScABS_3$ (a peptide with the amino acid sequence of actin-binding site 3), all with actin nucleating activity, decreased F-actin disassembly and exocytosis (Figure 7) [Dumitrescu et. al. 2005]. All these effects were probably due to an increase or decrease in the number of chromaffin vesicles at release sites (see also Figure 4). Additional experiments suggest that scinderin acts as a molecular switch during the secretory cycle; thus inducing F-actin disassembly when intracellular Ca^{2+} increases and, later in the cycle, when Ca^{2+} has returned to normal levels, promoting actin nucleation (through the third actin-binding site in domain S5) and polymerization with restoration of cortical actin networks [Dumitrescu et. al. 2005].

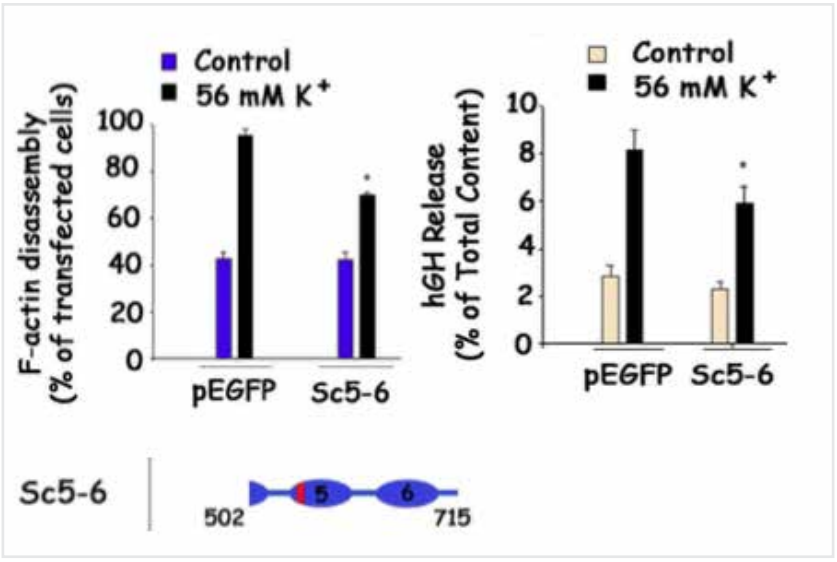

Figure 7. Effects of over-expression a [Sc5-6] construct with actin-nucleating activity on cortical actin and human growth hormone [hGH] release from chromaffin cells upon high K^+-induced cell depolarization. A schematic representation of the Sc construct is shown at the bottom of the figure. Both cortical actin disassembly and hGH release were significantly decreased in cells co-transfected with Sc5-6. Similar results were obtained with other constructs [Sc5, $ScABS_2$] with actin-nucleating activity. ScL5, a construct without a scinderin nucleation site, did not show an inhibitory effect on cortical actin disassembly and hGH release [Dumitrescu et. al. 2005].

There is also a second cellular mechanism that controls actin networks in secretory cells involving protein kinase C activation and induction of a myristoylated alanine-rich C kinase substrate (MARKS) phosphorylation [Elzagallaai et. al. 2000, 2001, Rosé et. al. 2001]. MARKS cross-links actin filaments and stabilizes actin networks. Its phosphorylation by protein kinase C activation eliminates the cross-linking of actin filaments with the consequent actin filament disassembly [Rosé et. al. 2001]. Contrary to receptor activation of Ca^{2+} entry through plasma membrane Ca^{2+} channels, a requirement for scinderin activation, MARKS-dependent actin filament disassembly is mainly observed when Ca^{2+} is released from the endoplasmic reticulum [Zhang et. al. 1995, Trifaró et. al. 2000]. This is observed when cells are stimulated by histamine [Zhang et. al. 1995].

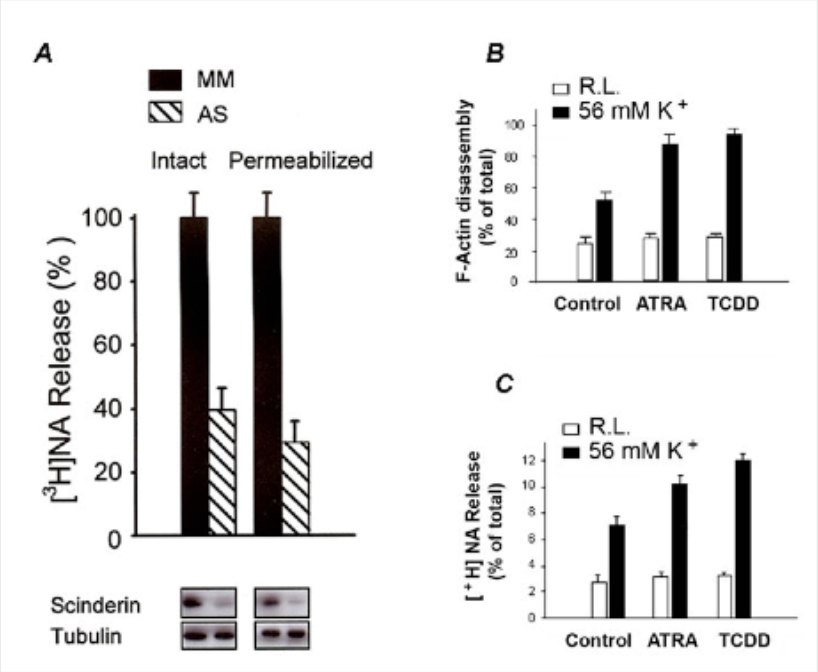

Figure 8. A) Intact or permeabilized chromaffin cells were stimulated for 60 sec. with 56 mM K^+ or 20 :M Ca^{2+} respectively. Cell cultures were previously incubated for 72 hr. with either scinderin antisense oligodeoxynucleotide (AS) or its oligodeoxynucleotide mismatch (MM, control). At the bottom, Western blots of samples from the cultures showing decreased scinderin expression in the AS-treated cells. Similar effects were observed with cortical F-actin disassembly. B) and C) Scinderin gene promoter stimulation: Cell cultures were treated with 10 µM ATRA or 10 nM TCCC for 48 hr. and then, stimulated by high K^+. A potentiation of B) F-actin disassembly and C) [^{3}H]-noradrenaline output was observed [Trifaró et. al. 2008].

4. Scinderin in cell maturation and differentiation

Acute megakaryoblastic leukemia (M7) is a recognized disorder characterized by rapid proliferation of atypical megakaryocytes and their precursor cells. This disease is often associated with myelofibrosis. Cell lines have been established with cells from patients with this disease [Ogura et. al. 1985] and these cells have shown some degree of differentiation with phorbol ester (PMA) treatment. Megakaryopoiesis is a complex process that involves the proliferation of committed precursor cells and their differentiation with nuclear polyploidization, leading to platelet formation [Leven and Yee 1987]. This process is thought to be regulated by a lineage-specific humoral factor called thrombopoietin. After differentiation, the fate of megakaryocytes is apoptosis, with cell fragmentation resulting in cytoplasmic areas released as newly formed platelets [Zauli et. al. 1997].

Cells from patients with this disorder and cell lines established from this type of leukemia showed the presence of gelsolin but the absence of scinderin expression (Figure 9A) [Zunino et. al. 2001]. These two actin filament-severing proteins are present in normal megakaryocytes and platelets [Rodríguez Del Castillo et. al. 1991]. Vector-mediated expression of scinderin in the megakaryoblastic cell line MEG-01 induced a decrease in both F-actin (Figure 9B) and gelsolin. This was accompanied by increased Rac2 expression and by activation of the PAK/MEKK.SEK/JNK/*c-jun, c-fos* transduction pathway [Zunino et al 2001]. An increase in Rac might be the result of the decreased expression of gelsolin observed in these cells, because it has been demonstrated that there is a reciprocal correlation between gelsolin and Rac expressions [Azuma et. al. 1998]. Indeed, in experiments with MEG-01 cells, a good reciprocal correlation between the levels of these 2 proteins was also observed [Zunino et. al. 2001]. In gelsolin-null mice, Rac is overexpressed and the re-expression of gelsolin in these animals restores normal levels of Rac [Azuma et. al. 1998]. The Raf/MEK/ERK pathway was also activated in these cells. There was evidence that an earlier activation of the Raf-MEK-ERK pathway increased expression of platelet antigen CD41a between days 4 and 8 in cell culture.

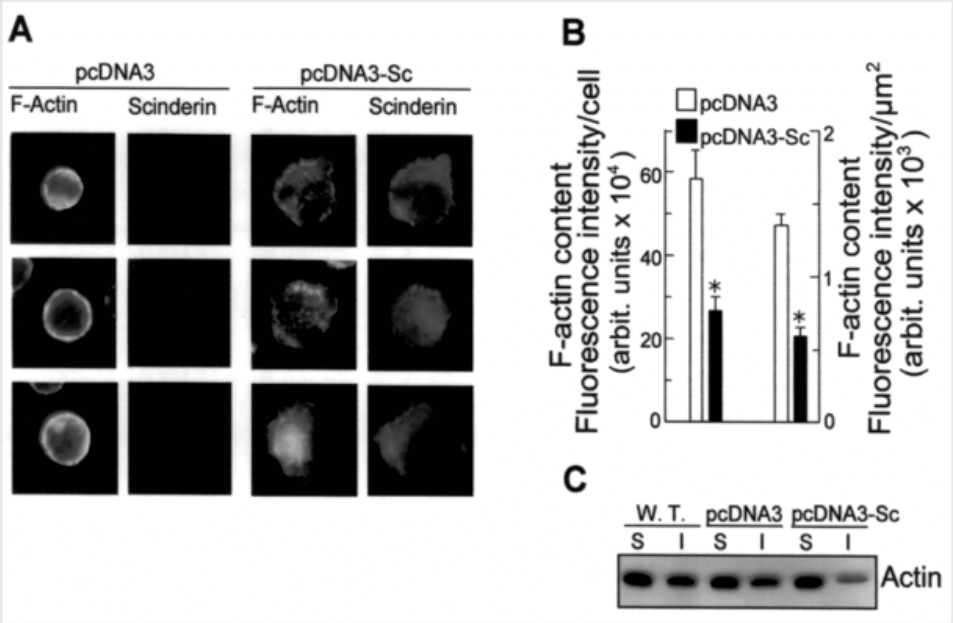

Figure 9. Effect of scinderin expression and filamentous actin content in MEG-01 cells. A) Fluorescence microscope images of cells stained with scinderin (Sc) antibodies and rhodamine phalloidin (a probe for F-actin) after transfection either with vector pcDNA3 (2 left panels) or with Sc cDNA carrying vector pcDNA3-Sc (2 right panels). B) Image analysis data of the fluorescent cells described in panel A. C) Western blot analysis carried out with actin antibody of wild type (WT) cells and transfected cells. S: supernatants and sediments of Triton-100 insoluble extracts (I). Twelve preparations of pcDNA3-transfected cells were analyzed, and 18 preparations from 3 different clones (6 from each clone) were measured for pcDNA3-Sc–transfected cells (*$P < .001$) [Zunino et. al. 2001].

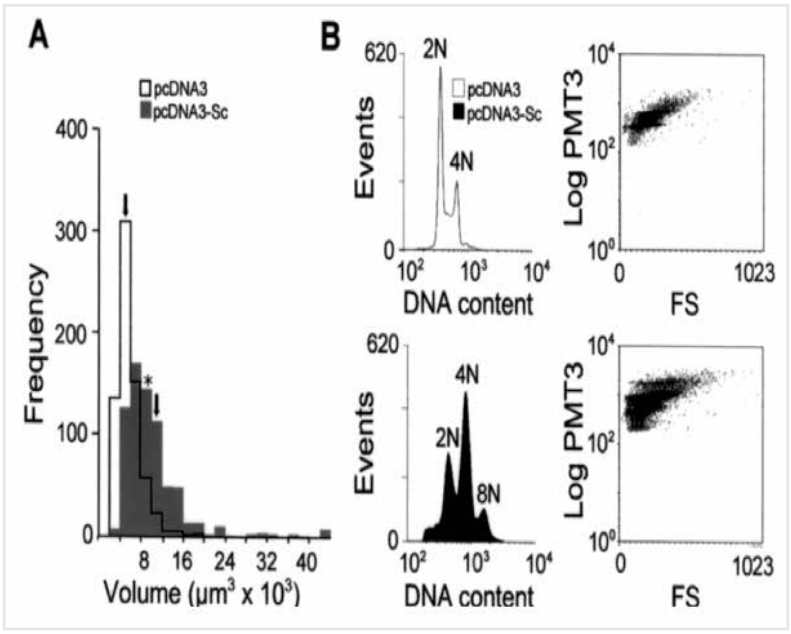

Figure 10. Effect of scinderin expression on MEG-01 volume and nucleus number. Cells transfected with either pcDNA3 or pcDNA3-Sc were cultured for 8 days after removal of the antibiotic G 418. A) and B) Cells were then fixed and stained with Wright-Giemsa, and (A) volumes of pcDNA3 (n = 484) and pcDNA3-Sc (n = 600) transfected cells were measured (*$P < .001$). B) Comparison of gated DNA distribution of 35 000 cells transfected with pcDNA3 and the same number of cells transfected with pcDNA3-Sc (clone Sc I-E). Similar results were obtained with 5 other Sc expressing clones [Zunino et. al. 2001].

Transduction pathway activation was followed by cell volume increase (Figure 10A) differentiation (Figure 11), polyploidization (Figure 10B), maturation (Figure 11), and apoptosis with release of platelet-like particles. Particles expressed surface CD41a antigen (glycoprotein IIb/IIIa or fibrinogen receptor), had dense bodies, high-affinity serotonin transport, and circular array of microtubules [Zunino et. al. 2001]. Treatment of particles with thrombin, and similar to normal platelets, induced serotonin release and aggregation that was blocked by CD41a antibodies. PAC-1 antibodies also blocked aggregation [Zunino et. al. 2001].

Similar to chromaffin cells, and as discussed above, stimulation of the MEG-01 transcription factor AhR by two of its ligands (dioxin and ATRA, see above) induced expression of scinderin, polyploidization and expression of antigen CD41a (Figure 12); all manifestations of maturation and differentiation. Exposure of cells to PD98059, a blocker of MEK, inhibited all: antigen CD41a expression, increases in cell volume, and number of protoplasmic extensions [Zunino et. al. 2001]. Therefore, it seems that the restitution of scinderin expression in human megakaryoblastic leukemia cells activates specific transduction pathways leading to cell differentiation and maturation.

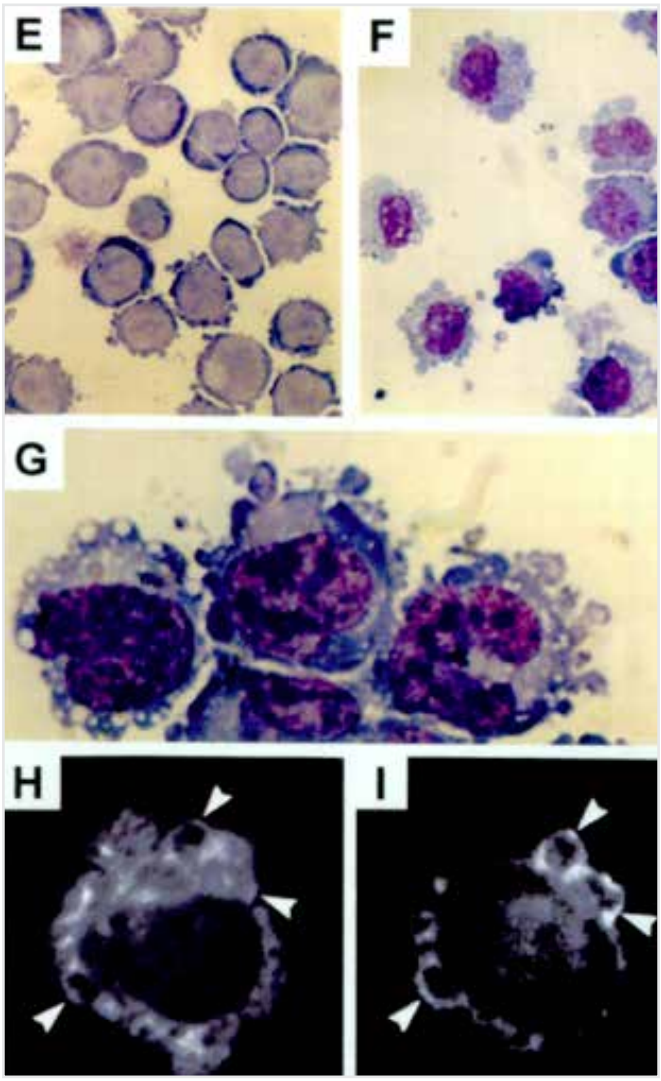

Figure 11. Cells, cultured for 12 days, were also fixed and stained with Wright-Giemsa (E-G) or rhodamine phalloidin, a probe for F-actin (I), or they were immunostained with a Sc antibody (H). Cells transfected with pcDNA3 (E) showed a large single nucleus surrounded by a thin layer of cytoplasm (×**400**). F) Cells expressing Sc (pcDNA3-Sc) were much larger and were multinucleated or had multi-lobulated nuclei, abundant cytoplasm, and numerous cytoplasmic extensions (×**40**). G) Same cells at a large magnification (×**1000**). Distribution of Sc (H) and filamentous actin (I) in a double-stained cell (×**1200**). There was some degree of correlation between the distribution of the 2 markers, especially in the cytoplasmic extensions (arrowheads).

Furthermore, it has also been demonstrated that scinderin is up-regulated during chondrocyte maturation, and the observed increased expression of Indian hedgehog (Ihh) and collagen type X is indicative of chondrocyte differentiation [Nurminsky et. al. 2007]. As with MEG-01 cells, the MEK-ERK pathway was activated and its inhibition blocked chrondrocyte differentiation [Nurminsky et. al. 2007].

5. Scinderin in cancer

As discussed above, the expression of the scinderin gene in MEG-01 cells induces their maturation and differentiation. Moreover, cell proliferation and cell ability to form tumors in nude mice were also inhibited by the expression of scinderin [Zunino et. al. 2001]. An important observation in this study was the fact that cells expressing scinderin either did not form tumors in nude mice or that the small tumors observed in two of nine cases have histologic characteristics different from those large, solid, and vascularized tumors observed in mice injected with cells previously transfected with vectors alone (Figure 13). The two small tumors produced by pcDNA3-Sc–transfected cells showed cells in apoptosis surrounded by large numbers of platelet-like particles, a situation similar to that observed *in vitro*. Therefore, it seems that the restitution of scinderin expression in human megakaryoblastic leukemia cells activates specific transduction pathways leading not only to cell differentiation and maturation, but also to the inhibition of proliferation and tumor formation (Figure 13). Whether these cells had acquired all characteristics of normal cells, including lack of tumorigenesis, remains to be determined.

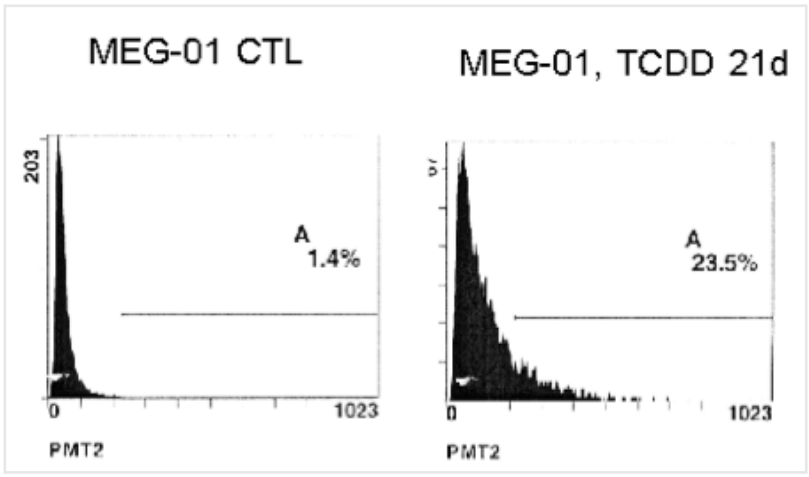

Figure 12. Flow cytometry showing an Increase of CD41a (glycoprotein IIb/IIIa or fibrinogen receptor) expression in MEG-01 cells by stimulation of scinderin promoter with a TCDD 21-day treatment. An Increase expression of 15.4 times was observed. Activation of the Raf/MEK/ERK was involved in this increased CD41a expression [Zunino et. al. 2001].

Scinderin expression was absent from human megakaryoblastic leukemia cells as well as from cell lines derived from these malignant cells [Zunino et. al. 2001]. On the other hand, scinderin is also well expressed in other types of malignant cells [Abouzahr et. al. 2006, Miura et. al. 2012, Hasmim et. al. 2012, Wang et. al. 2014].

In the prostate carcinoma cell line PC3, the knock down of the SCIN gene by a lentivirus-mediated RNAi technique inhibited the proliferation and colony formation ability of these cells. Moreover, a cell cycle analysis showed that decreased SCIN expression lead to GO/G1 cell cycle arrest through the regulation of cell cycle genes, such as p21Waf1/Cip1, cyclin-dependent kinase inhibitor 2A (CDKN2A, p16ln4A) and cyclin A2 [Wang et. al. 2014]. These results allowed the authors to conclude that SCIN plays an important role in the proliferation of prostate cancer cells and that inhibition of SCIN expression may be a potential therapeutic method in this cancer type.

Similarly, a non-small-cell lung carcinoma cell line rendered resistant to T cell lysis (CTL) showed over-expression of actin-related genes EFNA1 and SCIN. These cells resistant to $CD8^+$ cytolytic T lymphocytes also displayed strong morphological changes and alterations of the actin cytoskeleton [Abouzahr et. al. 2006]. Silencing of these genes using

RNA interference resulted in a restoration of normal cell morphology and a significant attenuation of variant resistance to CTL killing. Consequently, a shift in cytoskeletal organization may allow cancer cells to promote their resistance to T cell lysis.

Cisplatin is a most effective antitumor agent available against bladder cancer. It promotes apoptosis of bladder cancer cells. Unfortunately, bladder cancer cells develop a resistance to cisplatin with time. During cell resistance to the drug, cancer cells show overexpression of several proteins [Miura et. al. 2012]. Scinderin was one the most highly over-expressed (4 fold up-regulation) proteins in this cisplatin-resistance cell line (HT1376-CisR). SCIN mRNA knockdown significantly reduced cell proliferation with increased mitochondrial mediated apoptosis. Immunoprecipitation studies revealed mitochondrial voltage dependent anion channels (VDACs) to be bound to scinderin. SCIN silencing by siRNS transfection showed apoptosis in HT1376-CisR cells cultured with cisplatin. The results of this study suggested that

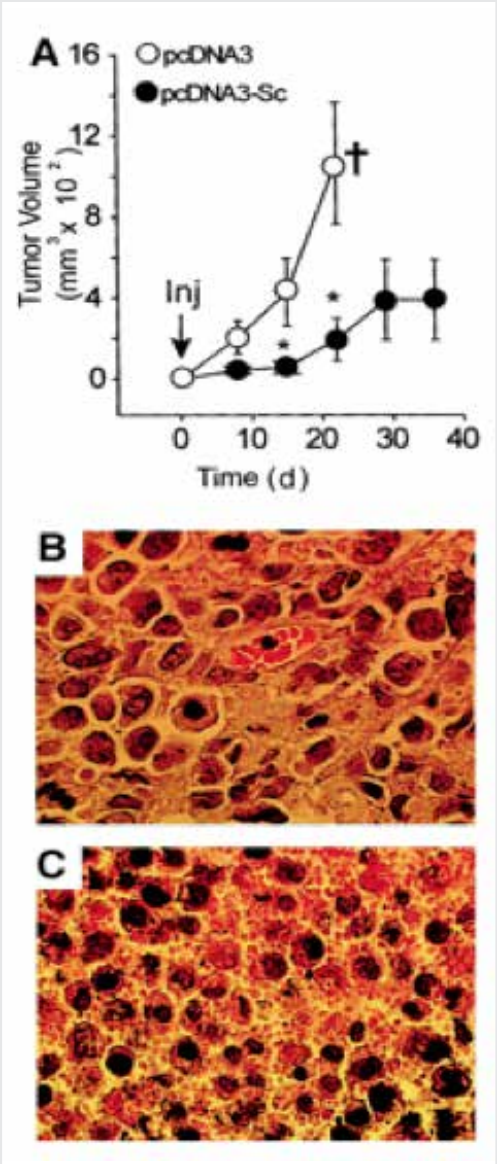

Figure 13. Expression of scinderin inhibits tumor growth in nude mice. Balb/c nude mice were injected with cells cultured for 14 days after transfection with either vector (pcDNA3) alone or with the same vector carrying a full-length insert of Scinderin cDNA (pcDNA3-Sc). A) Tumor volumes after subcutaneous injection (Inj) with 10^7 cells in 100 **µL** saline for each condition. Open and closed circles represent mean ± SEM from 2 groups of 9 mice each (*P<.05). †All pcDNA3-transfected mice were killed at 3 weeks after injection in accordance with institutional animal care policies. B) Hematoxylin-eosin staining of a section from a large tumor produced by pcDNA3-transfected cells. The histology of 8 remaining tumors in this group was similar, and so was that of tumors formed by wild-type cells. C) Similar staining of a section from 1 of the 2 small tumors produced by pcDNA3-Sc-transfected cells showing apoptotic nuclei surrounded by numerous platelet-like particles. The second small tumor in this group had a similar histology [Zunino et. al. 2001].

scinderin is somehow involved in cancer cell resistance to cisplatin through an interaction with the mitochondria VDAC [Miura et. al. 2012].

It has also been found that high levels of scinderin expression in gastric cell tumors was correlated with poor overall survival of patients. Silencing of the SCIN gene effectively suppressed the migratory and invasive capabilities of human gastric cancer cells *in vitro* and tumorigenicity and metastasis *in vivo*. In this case, the formation of filopodia and the expression of Cdc42, a filopodia regulator, are inhibited [Liu et. al. 2016]. However, additional studies have shown that, although ephrin-A1 and scinderin are highly expressed in head and neck cancers, this overexpression is not sufficient criteria for prognosis in cancer patients. [Hasmim et. al. 2013].

It is very rewarding for us to see how the discovery and early studies on scinderin done in our laboratory have triggered research on possible roles of this protein in cancer.

6. General inferences

Scinderin is a protein that belongs to the family of gelsolin and villin, which are filamentous actin-severing and capping proteins. Like gelsolin and villin, the scinderin actin-severing activity resides in its NH_2-terminal half [Marcu et. al. 1994], precisely in domains 1 and 2 [Marcu et. al. 1994; 1996, Zhang et. al. 1996]. The actin-nucleating activity of scinderin is in domain 5 of the protein [Marcu et. al. 1998]. The F-actin severing activity of scinderin seems to play a role in cell secretion. In secretory cells, scinderin is highly concentrated in the cell cortex [Vitale et. al. 1991], showing a distribution similar to that of filamentous actin [Vitale et. al. 1991]. Cortical F-actin acts as a barrier to the free movement of secretory vesicles to release sites and, only during the cell stimulation induced Ca^{2+} entry, cortical F-actin is disassembled [Vitale et. al. 1991] through the activation of scinderin [Vitale et. al. 1991]. This would allow the movement of secretory vesicles to release sites on the plasma membrane [Vitale et. al. 1991, Trifaró et. al. 1992]. Moreover, two PIP_2-binding sites have been described for scinderin and, as in gelsolin, they are present in domains 1 and 2. PIP_2 inhibits the actin-severing activity of scinderin [Zhang et. al. 1996]. Several experimental approaches have been used to demonstrate the role of scinderin in the secretory process, and these have been discussed above. Therefore, it seems that during the secretory cycle, scinderin acts as a molecular switch, first removing the cortical F-actin barrier (F-actin severing) allowing movement of secretory vesicles to release sites (release-ready vesicle pool) on the plasma membrane and, later in the cycle, by inducing G-actin assembly (G-actin nucleation) and reconstitution of cortical F-actin networks [Dumitrescu et. al. 2005]. The position of the switch (disassembly↔assembly) would be controlled by the concentration of the intracellular Ca^{2+}, which increases during depolarization and decreases by sequestration into mitochondria and ER during repolarization. The promoter of SCIN, the scinderin gene, has been characterized and its important responsive elements described. An activation of the SCIN promoter by two ligands of the transcription factor aryl hydrocarbon receptor [AhR] has been demonstrated. This activation increased scinderin expression with a consequent potentiation of stimulation-induced cortical actin disassembly and exocytosis.

A role for scinderin in the life cycle of megakaryocytes has been suggested [Zunino et. al. 2002]. Scinderin seems to be involved in the maturation, differentiation and apoptosis of these cells, with release of newly formed platelets. Moreover, the stimulation of SCIN promoter by transcription factor AhR ligands also induced over-expression of scinderin accompanied by cell differentiation and maturation. A similar role for scinderin in the differentiation and maturation of chondrocytes has been described.

A role for scinderin in cancer is also emerging, although more substantial research is needed in this area to elucidate scinderin's function in this pathological condition. It has been suggested that scinderin is over-expressed in tumor cells showing resistance to cisplatin and $CD8^+$ T lymphocyte-mediated cell lysis, and that silencing the SCIN gene restores sensitivity to $CD8^+$ T cell lysis and cisplatin. On the other hand, the SCIN gene is silenced in megakaryocyte leukemia cells and a vector-mediated expression of scinderin induces cell maturation, differentiation, apoptosis and anti-tumor effects. This is always accompanied by changes in cell morphology due to cytoskeleton re-arrangements. Silencing the SCIN gene has anti-proliferation effects in some cancer cells (*i.e.*, bladder, lung, prostate), whereas in others, over-expression (i.e. megakaryoblastic leukemia) is necessary to see anti-proliferation effects [Zunino et. al. 2001]. In this case, it may be due to the fact that the over-expression of scinderin either by vectors carrying the gene or by the stimulation of the gene promoter, a condition that induces maturation and differentiation of the megakaryoblatic cells and this "differentiated" cells, enter the normal life cycle of a megakaryocyte, which ended in apoptosis, cell fragmentation with liberation of

platelets [Zunino et. al. 2002]. If, as in this case, it would be possible to differentiate other type of tumor cells, a new area of treatment would be developed by inducing "cell maturation and/or differentiation".

7. References

[1] Ampe C. and Vandekerchove J. [1987]. The F-actin capping proteins of Physarum polycephalum: cap42 (a) is very similar if not identical to fragmin and is structurally and functionally very homologous to gelsolin; cap42(b) is Physarum actin. EMBO J. 6: 4149-4157.

[2] Azuma T., Witke W., Stossel T. Hatwig J. and Kwiatowsky D. [1998]. Gelsolin is a downstream effector of Rac for fibroblast motility. EMBO 17: 1362-1370.

[3] Bader M. F., Trifaró J. M., Langley O. K., Thierse D. and Aunis D. [1986]. Secretory cell actin-binding proteins: Identification of a gelsolin-like protein in chromaffin cells. J. Cell Biol. 102:636-646.

[4] Chumnarnsilpa S., Lee W. L., Nag S., Kannan B., Larsson M., Burtnick L. D., and Robert C. Robinson R. C. [2009]. The crystal structure of the C-terminus of adseverin reveals the actin-binding interface. PNAS 106: 13719-13724.

[5] Dumitrescu T., Rose S.D., Lejen, T., Marcu, M. G. and Trifaró J. M. [2005]. Expression of various domains in chromaffin cells indicates that this protein acts as a molecular switch in the control of actin filament dynamics and exocytosis. J. Neurochem. 92: 780-789.

[6] Elzagallaai A., Rosé S. D., Brandan N.C. and Trifaró J.M. [2001]. Myristoylated alanine-rich C kinase substrate phosphorylation is involved in thrombin-induced serotonin release from platelets. Brit. J. Haematol. 112:593-602.

[7] Elzagallaai A., Rosé S. D. and Trifaró J.M. [2001]. Protein secretion induce by phorbol esters stimulation is mediated through phosphorylation of MARCKS. A MARCKS-derived peptide blocks MARCKS phosphorylation and serotonin release without affecting pleckstrin phosphorylation. Blood 95: 894-902.

[8] Hasmim M., Baduoal C., Vielh P., Drush F., Marty V., Laplanche De Oliveira Diniz M. A., Roussel H., De Guillebon E., Oudard S., Hans S., Tartour E. and Chouaib S. [2013]. Expression of EPHRIN-A1, Scinderin and MHC class I molecules in head and neck cancers and relationship with the prognostic value of intratumoral $CD8^+$ T cells. BMC Cancer 13: 592-604.

[9] Isenberg G. [1991]. Actin-binding proteins-lipid interactions. J. Muscle Res. Cell Motil. 12: 136-144.

[10] Janmey P. A. and Stossell T.P. [1987]. Modulation of gelsolin function by phosphatidylinositol 4,5-biphosphate. Nature 325: 78-80.

[11] Lee R. W. H. and Trifaró J.M. [1981]. Characterization of anti-actin antibodies and their use in immunocytochemical studies on the localization of actin in adrenal chromaffin cells in culture. Neuroscience, 6: 2087-2108.

[12] Lejen, T., Skolnik, K., Rosé S.D., Marcu M.G., Elzagallaai A. and Trifaró J. M. [2001]. An antisence oligodeoxinucleotide targeted to the scinderin gene decreased scinderin levels and inhibited depolarization induced cortical F-actin disassembly and exocytosis. J. Neurochem. 76: 768-777.

[13] Leven R. M., Yee M. K. [1987]. Megakaryocyte morphogenesis stimulated in vitro by whole and partially fractionated thrombocytopenic plasma: a model system for the study of platelet formation. Blood 69: 1046-1052.

[14] Liu J. J., Liu J. Y., Chen J., Wu Y. X., Yan P., Ji C. D. J., Wang Y. X., Xiang D. F., Zhang X., Zhang P., Cui Y. H., Wang J. M., Bian X. W. and Qian F. [2016]. Scinderin promotes the invasion and metastasis of gastric cancer cells and predicts the outcome of patients. Cancer Letters, 376:110–117.

[15] Lueck A., Yin H. L., David J. Kwiatkowski D. and Allen P. G. [2000]. Calcium regulation of gelsolin and adseverin: A natural test of the helix latch hypothesis. Biochem. 39:5274-5279.

[16] Lottspeich A. E., Schleicher M. and Noegel A. [1988]. Severin, gelsolin and villin share homologous sequence in regions presumed to contain F-actin severing domains. J. Biol. Chem. 263:722-728

[17] Maekawa S, and Sakai H. [1990]. Inhibition of actin regulatory activity of the 74-kDa protein from the adrenal medulla (Adseverin) by some phospholipids. J. Biol. Chem. 265:10940-10942

[18] Marcu M.G., Rodríguez Del Castillo A., Vitale M. L., and Trifaró J. M. [1994]. Molecular cloning and functional expression of chromaffin cell scinderin indicates that it belongs to the family of Ca2+-dependent F-actin severing proteins. Molec. Cell. Biochem. 141:153-165.

[19] Marcu, M.G., Zhang L., Nau-Staudt K. and Trifaró J. M., [1996]. Recombinant scinderin, an F-actin severing protein, increases calcium-induced release of serotonin from permeabilized platelets, an effect blocked by two scinderin derived actin-binding peptides and phosphatidylinositol 4,5-bisphosphate. Blood, 87: 20-24.

[20] Marcu, M.G., Zhang L., Elzagallaai A. and Trifaró J. M. [1998]. Localization by segmental deletion analysis and functional characterization of a third binding site in domain 5 of scinderin. J. Biol. Chem. 273: 3661-3668.

[21] McLaughlin P. G., Gooch J. T., Mannherz H. G. and Weed A. G. [1993]. Structure of gelsolin segment 1-actin complex and the mechanism of filament severing. Nature 364: 685-692.

[22] Miura N., Takemori N., Kikugawa T., Tanji N., Higashiyama S. and Yokoyama M. [2012]. Adseverin; A novel cisplatin-resistant marker in the human bladder cancer cell line HT1376 identified by quantitative proteomic analysis. Molec. Oncol. 6: 311-322.

[23] Nagase T., Kikuno R. and Ohara O. [2001]. Prediction of the coding sequences of unidentified human genes. XXI. The complete sequences of 60 new cDNA clones from brain which code for large proteins. DNA Res. 8: 179-187

[24] Nurminsky D., Magee C., Faverman L. and Nurminskaya M. [2007]. Regulation of chondrocyte differentiation by actin-severing protein adseverin. Develop. Biol. 302: 427-437.

[25] Ogura M., Morishima Y. and Ohno R. [1985]. Establishment of a novel human megakaryoblastic leukemia cell line, MEG-01, with positive Philadelphia chromosome. Blood 86: 1384-1392.

[26] Orci L., Gabbay K. H. and Malaisse W. J. [1972]. Pancreatic beta-cell web: its possible role in insulin secretion. Science 175: 1128-1130.

[27] Rhee S. G., Such P. G., Ryu S. H. and Sang Y. L. [1989]. Studies of inositol Phospholipid-specific Phospholipase C. Science 244: 546-550

[28] Rodríguez Del Castillo A., Lemaire S., Tchakarov L., Jeyapragasan M., Doucet J. P., Vitale M. L., and Trifaró J. M. [1990]. Chromaffin cell scinderin: a novel calcium-dependent actin filament severing protein. EMBO J. 9: 43-52.

[29] Rodríguez Del Castillo A., Vitale M. L. and Trifaró J. M. [1992]. Ca^{2+} and pH determine the interaction of chromaffin cell scinderin with phosphatidylserine and phosphatidylinositol 4,5-biphosphate and its cellular distribution during nicotinic-receptor stimulation and protein kinase C activation. J. Cell Biol. 119: 797-810.

[30] Rodríguez Del Castillo, Vitale M. L., Tchakarov L. and Trifaró J. M. [1992]. Human platelets contain scinderin, a Ca^{2+}-dependent actin filament-severing protein. Thrombosis & Haemostasis 67: 248-251.

[31] Rosé S.D., Lejen T., Zhang L. and Trifaró J. M. [2001]. Chromaffin cell F-actin disassembly and potentiation of catecholamine release in response to protein kinase C activation by phorbol esters is mediated through myristoylated alanine-rich C kinase substrate phosphorylation. J. Biol. Chem. 276: 36757-36763.

[32] Rosé S. D., Lejen T., Casaletti L., Larson R. E., Dumitrescu P. T. and Trifaró J. M. [2003]. Myosins II and V in chromaffin cells: myosin V is a chromaffin vesicle molecular motor involved in secretion. J. Neurochem. 85: 287-298.

[33] Tchakarov, L., Vitale M. L., Jeyapragasan M., Rodríguez Del Castillo M. and Trifaró J.M. [1990]. Expression of scinderin, an actin filament-severing protein, in different tissues. FEBS Lett. 268: 209-212.

[34] Tchakarov, L., Zhang L., Rosé S. D., Tang R. and Trifaró J. M. [1998]. Light and electron microscope study of changes in the organization of cortical actin cytoskeleton during chromaffin cell secretion. J. Histochem. Cytochem. 46: 193-203.

[35] Thrine Z. B., Hoy M. and Gromada J. [2000]. Scinderin-derived actin-binding peptides inhibit Ca^{2+}- and GTP ϒS-dependent exocytosis in mouse pancreatic β-cells. Europ. J. Pharmacol. 403: 221-224.

[36] Trifaró J. M. [1983]. International Symposium on Contractile Proteins in Muscle and Non-muscle Systems and Their Morpho-physio-pathology: Cytoskeleton Organization and Adrenal Chromaffin Cell Function, Sassari, Italy.

[37] Trifaró J. M., Tchakarov L., Rodríguez Del Castillo A., Lemaire S., Jeyapragasan M. and Doucet J. P. [[1989]. Adrenal medullary scinderin, a novel calcium-dependent actin filament-severing protein. XXIX Ann. Meet. Soc. Cell Bio., San Diego, USA, J. Cell Biol. 109: 274a.

[38] Trifaró J., Rodríguez Del Castillo A. and Vitale M. L. [1992]. Dynamic changes in chromaffin cell cytoskeleton as prelude to exocytosis. Mol. Neurobiol. 6:339-358.

[39] Trifaró J., Vitale M. L. and Rodríguez Del Castillo A. [1993]. Scinderin and chromaffin cell actin network dynamics during neurotransmitter release. J. Physiol. (Paris) 87: 89-106.

[40] Trifaró, J. M., Glavinovic M. and Rosé S. D. [1997]. Secretory vesicle pools and rate and kinetics of single vesicle exocytosis in neurosecretory cells. J. Neurochem. Res. 22: 831-841.

[41] Trifaró J. M., Rosé S. D., Lejen T. and Marcu M. G. [2000]. Scinderin, a Ca2+- dependent actin filament severing protein that controls cortical actin network dynamics during secretion. Neurochem. Res. 25:133-144.

[42] Trifaró J. M., Rosé S. D., Lejen T. and Elzagallaai A. [2000]. Two pathways control chromaffin cell cortical F-actin dynamics during exocytosis. Biochemie 82:339-352.

[43] Trifaró, J. M, Gasman, S. and Gutierrez L. M. [2008]. Cytoskeletal control of vesicle transport and exocytosis in chromaffin cells, Acta Physiol. 192: 165-172.

[44] Vitale M. L., Rodríguez Del Castillo A., Tchakarov L. and Trifaró J. M. [1991]. Cortical filamentous actin disassembly and scinderin redistribution during chromaffin cell stimulation precede exocytosis, a phenomenon not exhibited by gelsolin. J. Cell Biol. 113: 1057-1067.

[45] Vitale M. L., Seward E. P. and Trifaró J. M [1995]. Chromaffin cell cortical actin network dynamics control the size of the release-ready vesicle pool and the initial rate of exocytosis. Neuron 14: 353-363.

[46] Wang D., Sun S.Q., Yu Y. H., Wu W. Z., Yang S. L. and Tan J. M. [2014]. Suppression of SCIN inhibits human prostate cancer cell proliferation and induces G0/G1 phase arrest, Int. J. Oncol. 44: 161–166.

[47] Way M. and Weeds A. [1988]. Nucleotide sequence of pig plasma gelsolin. Comparison of protein sequence with human gelsolin and other actin-severing proteins shows strong homologies and evidence for large internal repeats. J. Mol. Biol. 203: 1127-1133.

[48] Yu F. X., Sun H. Q., Janmey P. A. and Yin H. L. [1992]. Identification of a polyphosphoinositide-binding sequence in an actin monomer-binding domain of gelsolin. J. Biol. Chem. 267: 14616-14621.

[49] Zauli G., Vitale M. and Falcieri E. [1997]. In vitro senescence and apoptotic cell death in human megakaryocytes. Blood 90: 2234-2243.

[50] Zhang, L., Rodríguez Del Castillo A. and Trifaró J.M. [1995]. Histamine-evoked chromaffin cell scinderin redistribution, cortical F-actin disassembly and secretion: In absence of cortical F-actin disassembly, an increase in intracellular Ca^{2+} fails to trigger exocytosis. J. Neurochem. 65: 1297-1308.

[51] Zhang L., Marcu M. G., Nau-Staud K., and Trifaró J. M. [1966]. Recombinant scinderin enhances exocytosis, an effect blocked by two scinderin-derived actin-binding peptides and PIP_2. Neuron 17: 287-296.

[512] Zunino R., Li Q., Rosé S. D., Romero-Benítez M. M. I., Lejen T., Brandan N. C. and Trifaró J. M. [2001]. Expression of scinderin in megakaryoblastic leukemia cells induces differentiation, maturation with release of platelet-like particles and inhibits proliferation and tumorigenesis. Blood 98: 2210-2219.

Bio

Jose-Maria Trifaro

Jose-Maria Trifaro was born in Argentina and graduated in Medicine in 1961 from the University of Buenos Aires. He started his biomedical research carrier at the Institute of Physiology at the same University. He continued his research at Tulane University [New Orleans] and at the Albert Einstein College of Medicine (New York) as a Fellow of the Rockefeller Foundation. He later moved to McGill University (Montreal) as an Assistant Professor of Pharmacology in the Faculty of Medicine. In 1973 he became an Associate Professor and five years later a Full Professor of Pharmacology. In 1986 he moved to the University of Ottawa as Chairman of the Department of Pharmacology in the Faculty of Medicine. In 1997 he was appointed as Professor of Cellular and Molecular Medicine. He is at the present time an Emeritus Professor of Medicine at the same Institution. His main area of research is on the cellular and molecular mechanisms involved in hormone and neurotransmitter secretion and in particular, on the role of the cytoskeleton and its regulatory proteins in these processes. One of these cytoskeleton regulatory proteins is Scinderin. This protein was discovered and its gene cloned in Dr. Trifaro's laboratory. Research on this protein has also opened a new area of research in his laboratory on the role of this protein in leukemia. Other laboratories in the world are presently investigating the possible role of this protein in other types of cancer. Dr. Trifaro's research has been performed mainly under the support of grants from the Canadian Institute of Health Research. He has been invited to present his work at international conferences and symposia and work from his lab has been described and discussed in more than 250 publications. He has also served on the editorial board of several biomedical journals. Email: Jose-Maria.Trifaro@canada.ca.

Science Reviews
from the end of the world

Vol. 1, No. 1, December 2019 // pp. 37-53 /

Artificial Pancreas: the Argentine experience

P. Colmegna[1], F. Garelli[2], E. Fushimi[2], M. Moscoso-Vásquez[3], N. Rosales[2], D. García-Violini[3], H. De Battista[2], and R. S. Sánchez-Peña[3*]

[1] *Center for Diabetes Technology, University of Virginia, USA and CONICET, Argentina*
[2] *LEICI, Facultad de Ingeniería, UNLP, Buenos Aires, and CONICET, Argentina*
[3] *Instituto Tecnológico de Buenos Aires and CONICET, Argentina*
[*] *Corresponding author. Email: rsanchez@itba.edu.ar.*

Abstract

The objective of this work is to present a brief review on the international Artificial Pancreas project. In addition, the local project that led to the first Latin American clinical trials with an Artificial Pancreas will be described. These trials were performed in Buenos Aires during 2016 and 2017. The last trial used an algorithm developed in Argentina and defined as the ARG (Automatic Regulation of Glucose). This procedure and its in silico and clinical results will also be presented in this paper.

Keywords:

Diabetes type 1, closed-loop control, Artificial pancreas

1. Introduction

Type 1 Diabetes Mellitus (T1DM) is a disease characterized by the inability to produce insulin, due to the destruction of the pancreatic β-cells. Insulin deficiency generates chronic hyperglycemia that can be related to several health complications, like the acceleration of Atherosclerosis [1]. In order to regulate their glucose levels, patients have to be continuously measuring their glycemia, and calculating how much insulin they need, making T1DM an extremely demanding disease. On the other hand, Insulin Intensive Treatment (IIT) is also associated with an increase risk of hypoglycemia [2].

An Artificial Pancreas (AP) is a system that automatically modulates patient's insulin infusion rate in order to maintain his/her blood glucose within safe limits. Although intravenous AP is possible [3], both measurement and infusion are, in general, performed subcutaneously via a Continuous Glucose Monitoring (CGM) sensor, and a Continuous Subcutaneous Insulin Infusion (CSII) pump, respectively. This represents a minimally invasive AP scheme that allows ambulatory use, but unfortunately, makes the control problem much harder. Amongst other difficulties, lag-times and errors in glucose measurement and insulin action, nonlinearities, large dynamic uncertainties and technical difficulties (sensor dropouts and insulin set failure) have to be coped with (see [4] and [5] for a complete review of the challenges in the development of an AP system). It is worth remarking that even rapid-acting insulin introduces a significant delay that affects the performance of a glucose controller [5]. Actually, this is the main limitation for AP systems, considering that according to pharmacodynamics profiles the peak of insulin action occurs about 70 min after infusion [6].

The AP development has been accelerated by the use of elaborated simulators, such as the UVa/Padova metabolic simulator which was accepted by the US Food and Drug Administration (FDA) in lieu of animal trials ([7, 8]. Recently, clinical trials were performed in different countries of the EU, USA, Israel and Australia [9–12]. The great majority of the control algorithms that have been clinically tested are based on Proportional-Integral-Derivative (PID), Model Predictive Control (MPC) or fuzzy logic controllers. Generally, they are hybrid (semi-automatic) control loops, where the controller action is complemented with premeal insulin boluses in both the single-hormone [13–17] and the dual-hormone [18, 19] AP. Although the injection of an open-loop bolus based on the carbohydrate intake facilitates the reduction of postprandial glucose values [20], inaccurate carbohydrate counting is frequent [21]. In [19] meal announcement is not required, but it is suggested in order to trigger a meal-priming bolus based on a meal size classification akin to the proposal of [22, 23].

Studies involving fully closed-loop AP systems can be found in [24, 25] and more recently in [26–29]. Despite

promising results, there is still a strong compromise between the aggressiveness of the control action and the postprandial glucose excursion. This compromise exists even when meals can be anticipated based on a probabilistic approach like the one presented in [30]. If the controller is not aggressive enough to a meal perturbation, then prolonged hyperglycemia may occur [20, 26]. On the other hand, if the controller is too aggressive, there is a higher risk of insulin overdosing, and consequently, postprandial hypoglycemia [28]. The latter is partially because the effect of the meal on the CGM signal is not immediate, and therefore, the insulin response generated by the controller to cope with the meal is delayed several minutes. It should also be considered that in the standard open-loop basal-bolus treatment, a unique insulin bolus is applied at meal times. Instead, in a feedback control scheme, multiple insulin boluses are generated in response to the change in the CGM signal. Furthermore, because the counter-regulatory response in people with T1DM is often compromised, the response of an AP control algorithm should be less aggressive than the β-cell's secretory response [5]. As a consequence, fully closed-loop systems have an increased risk of initial hyperglycemia and late hypoglycemia during meals in comparison with semi-automated hybrid strategies. In [29], this problem is reduced, because the insulin bolus to cover the meal is not generated by the multivariable adaptive controller *per se*, but by an additional module that infuses an insulin bolus when a meal is detected. A very recent set of articles in this area can be found in [31].

In this paper, relatively unexplored control techniques in the field are proposed to address the glucose control paradigm, and take a step forward towards a fully automatic control loop. In particular, a couple of Linear Quadratic Gaussian (LQG) controllers are employed as main feedback controllers in combination with a sliding-mode safety layer to include Insulin on Board (IOB) constraints. Both LQG controllers are arranged into a switched structure to cope with the trade-off between prandial and fasting periods by triggering the controller into an *aggressive* mode during meals. The combination of the switched LQG controller with the safety mechanism allows compensating for delays associated with subcutaneous insulin infusion. When the *aggressive* mode is triggered, an insulin spike is generated. This mimics the first-phase insulin secretion of the β-cell response [5]. On the other hand, the purpose of the safety layer is to reduce the insulin infusion commanded by the switched LQG controller when a predefined IOB limit is going to be violated. This latter characteristic can be associated with the suppression of the β-cell in proportion to plasma insulin levels [5]. In this way, an initial "under-damped" insulin response can be generated to compensate for insulin delays, without increasing the risk of postprandial hypoglycemia. It is worth remarking that here it is the first time the safety layer is employed to adapt a closed-loop control without premeal insulin boluses.

The proposed control structure also intends to simplify both controller tuning and implementation. This facilitated its *in vivo* validation in a clinical trial, where it was tested on five T1DM adults during 36 hours without carbohydrate counting. This was the second phase of the first AP clinical trial campaign in Latin America. In the first phase a hybrid controller was tested in the same site and by the same team [32].

2. From The Conventional Therapy to Fully Automatic Control

As it was previously mentioned, patients with T1DM are insulin dependent. This means that, according to the conventional therapy, they should monitor their glucose concentration levels and administer insulin injections every day for the rest of their lives. This makes T1DM a highly demanding disease for both the patients and their families. For example, the patient not only has to maintain a basal insulin delivery to stabilize fasting glucose levels, but also has to count the amount of carbohydrates present in every meal before eating in order to calculate how much insulin is necessary to counteract its effect. Sadly, this calculation is far from being exact in real life, which is why the patient is constantly exposed to hyperglycemia (in the case of an underestimation of carbohydrates) and hypoglycemia events (in the case of overestimation of carbohydrates). Also, there exists a risk of hypo and hyperglycemia due to the effects of stress, physical activity and other multiple situations related to every day life that end up having an impact on the glycemic levels of the patient, and therefore, in his/her quality of life. This is why automatic regulation of glycemia in T1DM is a issue that dates to the beginnings of the 1960's. At first, the intravenous route was considered for both insulin infusion and glucose monitoring. Afterwards, alternative routes were analyzed, but the biggest breakthrough was in the 1990's with the appearance of the continuous glucose monitor (CGM). This allowed to go from having a few measurements a day to having them every 5 minutes or less through a minimally invasive procedure. Fig. 1 shows a diagram of this monitoring system. Its main disadvantage is that there exists a delay between what is being measured in the interstitial space and the actual plasma glucose levels.

Regarding insulin infusion, the first continuous subcutaneous insulin infusion (CSII) pumps emerged in the mid 1970's. Even though the implantable pumps in the peritoneal cavity represent a more suitable alternative from the physiological point of view, the subcutaneous pumps, as they are less expensive and invasive, prevailed alongside CGMs as the main elements for an AP. Nevertheless, what is known in the scientific community as an AP needs to have, apart from the CGM and the CSII pump, an element to close the loop. This element is the control algorithm that is in charge of calculating the adequate amount of insulin to be infused according to the CGM readings (see Fig. 2). Calculating the adequate insulin dose is not an easy task. Some of the biggest challenges that the control algorithm must face are:

- The subcutaneous route introduces a delay between the CGM measurements and the actual plasma glucose levels. Additionally, the measurements usually have significant error, which is why CGMs require daily calibrations.

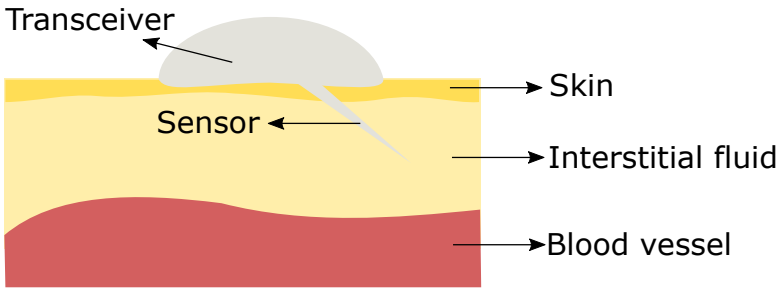

Figure 1. Continuous glucose measurement in the interstitial space.

- Like subcutaneous measurements, there exists a delay of several minutes associated to the absorption of the insulin that is infused at a subcutaneous level. In fact, the peak in the insulin action occurs approximately 1 hour after it has been infused, and its effect prevails for several hours. This means that the decision that is made every instant regarding how much insulin to administer, has prolonged consequences in time. An associated effect is the accumulation of active insulin, or what is known as *Insulin On Board* (IOB). In consequence, not taking into account past infusions might lead to insulin-induced hypoglycemia due to insulin stacking.
- The response to the same insulin dose varies from patient to patient (inter-patient variability).
- The same patient might respond differently to the same dose of insulin in different occasions (intra-patient variability).

A fundamental aspect to increase the celerity in the AP development was the progress of computational models of the insulin-glucose dynamics. Generally, the design of a control algorithm is based on a mathematical model of the system to be controlled. This is why numerous simulation models describing T1DM have been reported. These models have allowed not only to rapidly progress in the design of different controllers, but also to perform *in silico* tests previous to *in vivo* trials with humans.

3. ARG algorithm

The closed-loop glycemic regulation system with the ARG algorithm for a given #j subject is illustrated in Fig. 3. It can be seen in the figure that the algorithm has two main components:

- a switched Linear Quadratic Gaussian (LQG) regulator; and
- a safety layer called SAFE (*Safety Auxiliary Feedback Element*)

In a first instance and with an introductory purpose, the interaction between these two components will be discussed. Subsequently, each element will be explained with detail.

As it is usual in a closed-loop system, there is a reference signal r, which in this particular case is the desired glucose concentration at fasting state. The difference between the desired glucose concentration and the one measured by the CGM is defined as the error signal e, which is the input to the ARG algorithm. A control signal $u_{\mathscr{C}}$ is generated by the algorithm,

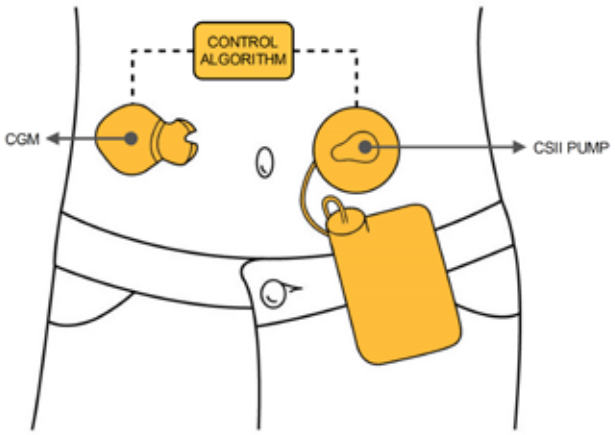

Figure 2. AP diagram.

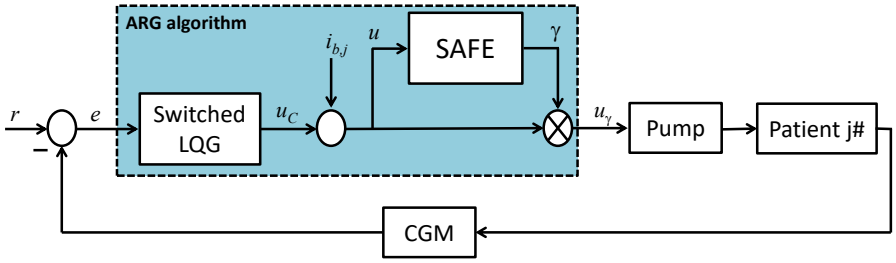

Figure 3. Closed-loop system with the ARG algorithm, where $i_{b,j}$ is the patient-specific basal rate, and r is the reference glucose concentration.

which corresponds to the switched LQG output. Since there is not integral action in order to avoid insulin stacking, the basal infusion of the patient $i_{b,j}$ is added to the $u_{\mathscr{C}}$, thus generating the signal u. If the SAFE block is not present, the signal u would command the patient's insulin pump. However, the presence of the SAFE layer, where u is its input and γ is the output, modulates the proposed infusion by the switched LQG controller in order to avoid an insulin overdose. In this way, the control action that commands the insulin pump is u_γ, consisting in the infusion proposed by the switched LQG regulator multiplied by the output of the SAFE block γ.

For a more detailed description of the algorithm, the reader is referred to [33].

3.1 Switched LQG regulator

The switched LQG regulator is constituted by two LQG regulators: on one hand, by default $\mathscr{K}_1$ makes smooth corrections on the basal insulin infusion; and on the other $\mathscr{K}_2$ is conceived for fast and aggressive corrections. The commutation to the $\mathscr{K}_2$ controller occurs at meal time and it can be both manual or automatic. If the commutation is produced manually, the patient must announce the meal time by means of a button, for example. If it is in an automatic manner, there must be a detection mechanism that allows inferring that the patient has eaten, for example, by means of the CGM signal. The problem that arises with this mechanism is the strong compromise between a fast detection and an immunity to the large CGM noise, which is of great importance in postprandial glycemic control. Because of this reason, the authors have chosen a manual commutation for the first clinical trials, although obtaining good *in-silico* results of the automatic mechanism [34–37].

It should be noted that, although the patient must announce the moment of the meal, he does not have to count the amount of carbohydrates that is about to ingest, translating thus in a lower burden in their daily tasks. Once the meal has been announced, the algorithm does not commute immediately to the aggressive controller $\mathscr{K}_2$, but switches to a listening mode in which the CGM signal trend is processed. When a sustained rise of the measurements is detected, the commutation to $\mathscr{K}_2$ is produced with the purpose of generating a control action similar to the standard insulin bolus treatment. The commutation from $\mathscr{K}_2$ back to $\mathscr{K}_1$ is produced in an automatic manner after 1 hour of operation of the aggressive controller, but other strategies involving the SAFE layer could be exploited.

A fundamental element when designing controllers are the control oriented models. On one side, models for simulation, as in the case of the UVA/Padova simulator, are developed in order to offer a response as real as possible, but are often complex, nonlinear and high order. On the other side, control theory generally applies simpler models in order to obtain low-order controllers and numerically better conditioned problems. To this end, assumptions over the simulation models are done, thus obtaining control-relevant low-order models for controller design. The drawback that adds to the obtaining of control oriented models in T1DM is that, what is commonly known as the plant in control engineering, are people in the case of T1DM. Thus, the usual identification methods applied to other types of systems, such as an engine, can not be extrapolated here for obvious reasons. That is why usually in this area, mean models are proposed as a first approach for describing insulin-glucose dynamics. Nevertheless, as mentioned above, there is a huge inter-patient variability which makes impossible the task of designing a single controller for all patients. Then, how can control-oriented models be adjusted? The model can be customized, in most cases, from the patient's clinical data, such as weight, Total Daily Insulin (TDI), the insulin to carbohydrate ratio (CR), among others. That is to say, that the control-oriented models are tuned taking into account the parameters that the patients use daily for their own glucose control.

The ARG algorithm switched LQG regulator is based on a Linear Time Invariant (LTI) version of the Linear Parameter Varying (LPV) control-oriented model previously developed by two of the authors in [37, 38]. Without going into greater detail, in [37] a low-order LTI model is proposed, similar to the one in [39], where the input corresponds to the subcutaneous

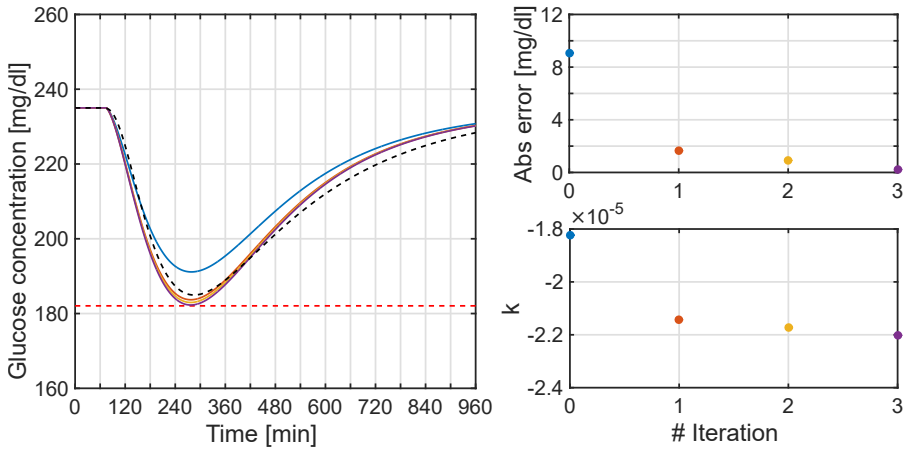

Figure 4. Parameter k adjustment process for an adult from the UVa/Padova simulator database.**Left:** Glucose excursion before 1 U of insulin for the average LPV model (light-blue solid-line) and nonlinear model (black dashed-line); minimum reachable glucose concentration given by the 1800 rule (red dashed-line). **Upper-right:** Absolut error between the obtained and the desired glucose drop. **Lower-right:** Evolution of the parameter k.

insulin infusion (in pmol/min) and the output is the glucose concentration deviation (in mg/dl):

$$G(s) = k\frac{s+z}{(s+p_1)(s+p_2)(s+p_3)}\mathrm{e}^{-15s}. \tag{1}$$

Afterwards, a time varying behavior of the insulin-glucose system is described through the construction of an LPV average model, by making the parameter p_1 vary with respect to glucose concentration g and keeping the rest parameters fixed as follows: $z = 0.1501$, $p_2 = 0.0138$ and $p_3 = 0.0143$. The gain parameter k is also time invariant, but is adjusted for each particular patient, exploding the insulin sensitivity factor of the standard therapy, known as the 1800 rule (may vary between authors). Given a patient $\#j$, the gain is computed as $1800/\mathrm{TDI}_j$, where TDI_j the total daily insulin of the patient, and represents the glucose drop in mg/dl before an infusion of 1 U of rapid acting insulin. Since insulin sensitivity depends on the glucose concentration, among other factors, the 1800 rule is verified in average starting from an initial glucose concentration of 235 mg/dl [37]. Therefore, the adjustment process for obtaining the customized value of k, namely k_j, is that when the model is excited with 1 U of insulin at 235 mg/dl, the result matches the 1800 rule. The larger the glucose drop, the more sensitive the patient is to insulin, thus, greater is the absolute value of k_j. An illustrative example of the iterative process for obtaining the parameter k_j is depicted in Fig. 4 (this could also be done analytically). This process consists in adjusting the value of k_j by means of a Proportional-Integral (PI) discrete controller until the relative error between the glucose drop by the LPV model and the 1800 rule be less than a small enough value. In summary, a low-order average LPV model is proposed first, which is then personalized through a parameter easily accessible and known by the patient. This LPV model has a better fit with the UVa/Padova simulator in terms of the RMSE and also with the ν-gap metric. The latter indicates a potentially better closed-loop performance when designing a controller based on this LPV model.

Although previously designed LPV controllers had successful results, the original idea behind the ARG algorithm was that it would have to have the lowest possible computational cost, in view of its verification in clinical trials. That is why LQG regulators were selected in order to allow adjusting the aggressiveness in an easy and intuitive way. Hence, for each patient $\#j$ two LQG regulators are designed: $\mathscr{K}_{i,j}$ with $i \in \mathscr{I} = \{1,2\}$, based in the following model:

$$G_j(s) = k_j\frac{s+z}{(s+p_1^*)(s+p_2)(s+p_3)}\mathrm{e}^{-15s}, \tag{2}$$

which is the LTI version of the custom LPV model with $p_1^* = p_1(120)$. In this case, p_1 is set for a concentration of 120 mg/dl, which is the average basal glucose concentration determined in the UVa/Padova simulator.

Since the CGM sensor does not send measures continuously, but every 5 min, the continuous model $G_j(s)$ is discretized by means of a zero-order hold, being expressed by the following realization:

$$\begin{aligned} x(k+1) &= A_j x(k) + B_j u_\Delta(k) \\ y_\Delta(k) &= C_j x(k) \end{aligned} \tag{3}$$

with $u_\Delta(k) = u(k) - i_{b,j}$, and $y_\Delta(k) = y(k) - 120$ mg/dl. Given this realization, a state feedback control is proposed

$$u_\Delta(k) = -K_{i,j}x(k) \tag{4}$$

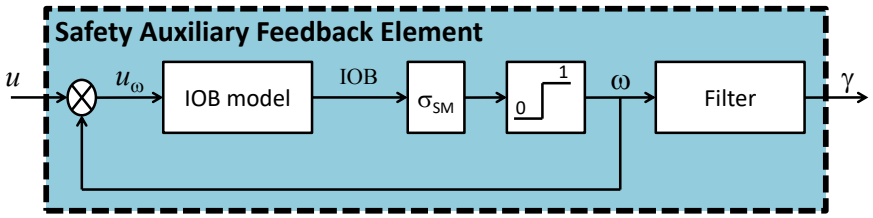

Figure 5. SAFE layer block diagram.

which minimizes the following functional cost

$$J_i(u_\Delta, y_\Delta) = \sum_{k=0}^{\infty} \left(R_i u_\Delta^2 + Q y_\Delta^2\right) \tag{5}$$

where $R_1 = 1$, $R_2 = 0.5$, and $Q = 5 \times 10^3$. The parameter R_2 is defined smaller than R_1 in order to $\mathscr{K}_{2,j}(z)$ be more aggressive than $\mathscr{K}_{1,j}(z)$. In addition, the states are estimated with a Kalman filter in the form of:

$$\hat{x}(k+1|k) = A_j \hat{x}(k|k-1) + B_j u_\Delta(k) + L_{i,j}[y_\Delta(k) - C_j \hat{x}(k|k-1)] \tag{6}$$

where $L_{i,j}$ is obtained assuming that the process noise $w(k)$ and the measurement noise $v(k)$ correspond to white noise, satisfying

$$E[w(k)w(k)^T] = W_i, \quad E[v(k)v(k)^T] = V_i \tag{7}$$

with $W_1 = V_1 = W_2 = 3$, and $V_2 = 45 \times 10^{-4}$. Here, V_2 is defined smaller than V_1 in order to $\mathscr{K}_{2,j}(z)$ have a faster response than $\mathscr{K}_{1,j}(z)$.

Both controllers $\mathscr{K}_{1,j}(z)$ and $\mathscr{K}_{2,j}(z)$ have an observer structure with state feedback and constitute the switched controller. The stability of this switching can be proved using the results detailed in [40]. The details of this result are beyond the scope of this paper, but the basic idea is to express the switched controller in such a way that it can arbitrarily switch between both LQG controllers without the need to reset the states and in a very simple way (only a part is switched from the C matrix of the controller).

3.2 SAFE layer

The SAFE layer, detailed in Fig. 5, is based on the sliding mode reference conditioning technique, developed by one of the authors in his PhD. Thesis [41]. This technique, designed in general for control of constrained systems, was first applied in the T1DM problem in [42], and then successfully tested on clinical trials in Spain. Its main objective is to modulate the gain of the controller to prevent Insulin On Board (IOB) from stacking by imposing a constraint $\overline{\text{IOB}}_j(t)$, thus reducing the risk of hypoglycemia in late postprandial periods.

The original SAFE layer was simplified with the objective of programming it in the hardware provided for the tests. The core element of any sliding mode control is the switching logic, which in this case is:

$$w(t) = \begin{cases} 1 & \text{if } \sigma_{\text{SM}}(t) > 0 \\ 0 & \text{else} \end{cases} \tag{8}$$

with $\sigma_{\text{SM}}(t)$ being the sliding function, defined simply as the difference between the actual IOB level and the imposed limit

$$\sigma_{\text{SM}}(t) = \overline{\text{IOB}}_j(t) - \text{IOB}(t). \tag{9}$$

The limit $\overline{\text{IOB}}_j(t)$ is considered piecewise constant a-priori, as it is explained later.

Because IOB cannot be measured in real time, it must be estimated. To this effect, the model presented in [43] is considered, which has the advantage that it can be customized based on a single clinical parameter:

$$\begin{aligned} \dot{I}_{sc1}(t) &= -K_{\text{DIA}} I_{sc1}(t) + u_w(t) \\ \dot{I}_{sc2}(t) &= K_{\text{DIA}} \left[I_{sc1}(t) - I_{sc2}(t)\right] \\ \text{IOB}(t) &= I_{sc1}(t) + I_{sc2}(t). \end{aligned} \tag{10}$$

where I_{sc1} and I_{sc2} are, respectively, the amount of nonmonomeric and monomeric insulin in the subcutaneous space, u_w is the exogenous insulin infusion rate in [pmol/min/kg], and K_{DIA} [min^{-1}] is a constant that can be tuned in order

to replicate each patient's duration of insulin action (DIA) [44]. It should be noted that DIA is a clinical parameter adjusted in actual insulin pumps. As a starting point, an average DIA of 5 hours was selected, leading to a K_{DIA} fixed at $16.3 \times 10^{-3}[\text{min}^{-1}]$ [45].

When the $\overline{\text{IOB}}_j(t)$ limit is reached by the IOB estimation, a sliding regime is established over the surface $\sigma_{\text{SM}}(t) = 0$. During this mode, from (8), the signal $w(t)$ switched at high frequency between 0 and 1, in order to fulfill the imposed restriction and force the system (10) to remain within the invariant set

$$\Sigma = \{x(t) \,|\, \sigma_{\text{SM}}(t) \geq 0\} \tag{11}$$

where $x(t) \in \mathbb{R}^2$ are the states of (10). The switching signal $w(t)$ is smoothed by a first order filter (or averaged between infusion intervals), given place to $\gamma(t)$, which is the factor that modulates the signal commanding the pump.
Observation: It is easy to prove that the derivative of the switching function $\sigma_{\text{SM}}(t)$ depends on the control action $u_w(t)$, and therefore of the discontinuous action $w(t)$, which is a necessary condition for establishing the sliding mode, known as transversality condition.

Like the main controller, the SAFE layer is implemented in a discrete way, obtained from (10) as:

$$\begin{aligned} x(k+1) &= \begin{bmatrix} 1 - K_{\text{DIA}} T_r & 0 \\ K_{\text{DIA}} T_r & 1 - K_{\text{DIA}} T_r \end{bmatrix} x(k) + \begin{bmatrix} 1 \\ 0 \end{bmatrix} u_w(k) \\ \text{IOB}(k) &= \begin{bmatrix} 1 & 1 \end{bmatrix} x(k) \end{aligned} \tag{12}$$

with $T_r = 0.1$ being min the sample time. It should be noticed that T_r is smaller than $T_s = 5$ min since the SAFE algorithm is programmed entirely in software, thus, the switching frequency is only limited by the speed of the pump microprocessor.

While there may be different criteria to define the IOB limit, from the conducted clinical test it was defined from a classification of the meal size, as follows:

- Small meal < 35 gCHO. $\overline{\text{IOB}}_{\text{s},j}(t) = \text{IOB}_{\text{ss},j}(t) + 40$ gCHO$/\text{CR}_j(t)$.
- Medium meal $[35, 65)$ gCHO. $\overline{\text{IOB}}_{\text{m},j}(t) = \text{IOB}_{\text{ss},j}(t) + 55$ gCHO$/\text{CR}_j(t)$.
- Large meal ≥ 65 gCHO. $\overline{\text{IOB}}_{\text{l},j}(t) = \text{IOB}_{\text{ss},j}(t) + 70$ gCHO$/\text{CR}_j(t)$.

where $\text{IOB}_{\text{ss},j}(t)$ is the steady state value of the model (12) corresponding to the basal insulin rate of each patient $i_{b,j}(t)$, and XX gCHO$/\text{CR}_j(t)$ is the insulin bolus corresponding to xx grams of carbohydrates (gCHO) by using the $\text{CR}_j(t)$ factor of each patient at the meal time. When the system is not at a prandial period, the IOB limit is fixed as $\overline{\text{IOB}}_{\text{s},j}(t)$, corresponding to a small meal. In this manner, the controller has an extra a degree of freedom in order to make adjustments to the basal infusion when necessary.

4. Simulations

All the *in-silico* experiments were carried out with the UVa/Padova Simulator, considering:

- a Dexom G4 Share® CGM;
- a generic CSII pump with a quantization of 0.1U, and a maximum bolus of 25U (these characteristics are analogous to Roche Accu-Check Combo® pump);
- a glucose reference of 120 mg/dl; and
- meal announcement.

Fig. 6 shows how the ARG algorithm works. It can be observed that the controller $\mathscr{K}_1$ is in charge of the insulin infusion most of the time, while the controller $\mathscr{K}_2$ only works during the meals. Once the controller $\mathscr{K}_2$ is selected, larger insulin boluses are delivered in order to avoid postprandial hyperglycemia. These boluses are modulated by the SAFE layer through the signal γ in order to avoid the violation of the imposed constraint on the IOB. This way, excessive insulin stacking is avoided and the risk of hypoglycemia is reduced. From this analysis it can be seen that while the aggressive controller ($\mathscr{K}_2$) diminishes hyperglycemia, the SAFE protection avoids hypoglycemia. Both systems work together in such a way to maintain the patient glycemia in the desirable $[70, 180]$ mg/dl or acceptable $[70, 250]$ mg/dl range.

It is also important to note that, as may be seen in figure 6, the peak in the insulin infusion happens after the meal intake, opposed to the traditional therapy where the meal bolus is delivered minutes before eating. This delay is due to the feedback strategy. Here, the effect of the meal is not detected by the CGM until several minutes after the intake. This results in an inevitable increase in the levels of glycemia, that is later compensated by the aggressive LQG controller. Other control strategies have a hybrid structure, in which the patient administers a meal bolus and the controller is in charge of

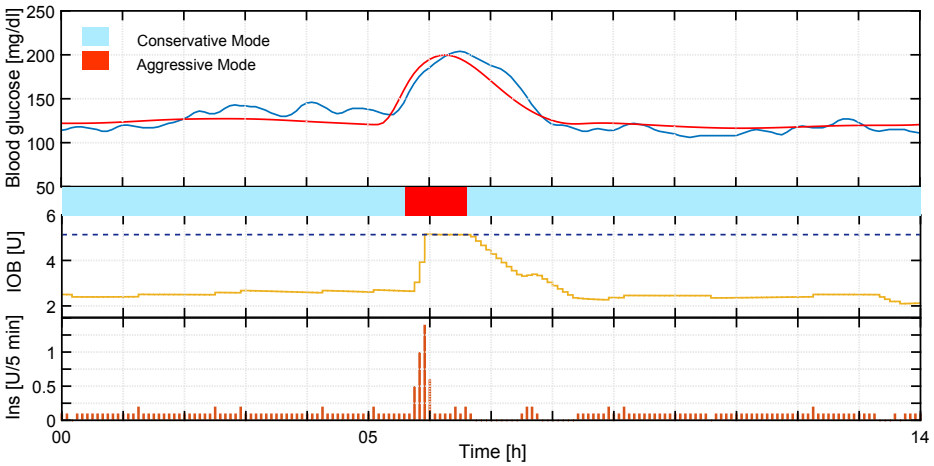

Figure 6. Example of the closed-loop response obtained when facing a 50gCHO meal of an *in silico* patient of the UVa/Padova Simulator. The meal intake happens 5 hours after the beginning of the simulation.

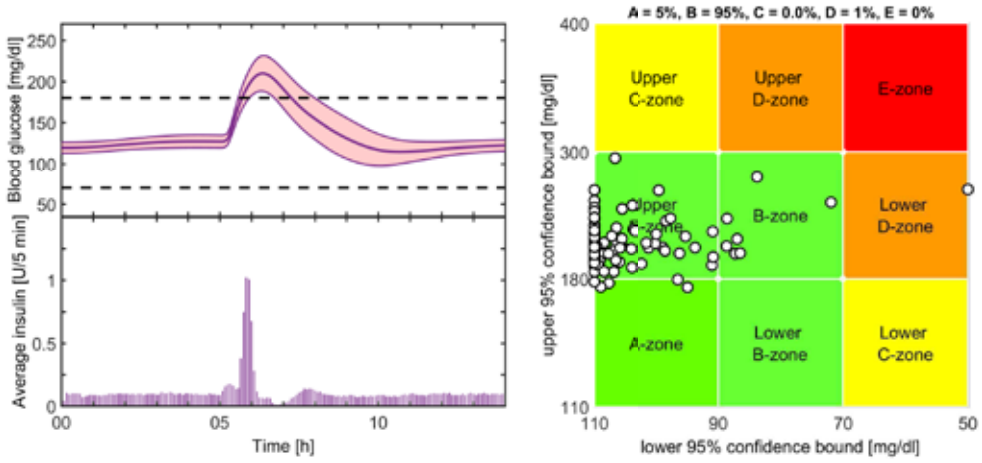

Figure 7. Mean closed-loop response for all the available adults in the UVa/Padova Simulator when facing a 50gCHO meal. **Upper left:** The solid line indicates the mean glucose and the shaded area is ± 1 standard deviation. The dashed lines indicate the boundaries of the desirable range.**Bottom left:** Mean insulin infusion **Right:** CVGA plot.

regulating the basal delivery. This way, postprandial peaks could be reduced as the bolus would be infused at an earlier time than with the proposed strategy. Nonetheless, the patient would be responsible of carbohydrate counting, which is rarely exact in daily life and also imposes a task that goes against his/her quality of life.

Figure 7 shows the mean closed-loop response for all the available adults in the full version of the UVa/Padova Simulator, along with the Control Variability Grid Analysis (CVGA) plot. The different regions of the CVGA represent glycemic control as follows:

- **A-zone:** Accurate control.
- **Lower/Upper B-zones:** Benign deviations into hypo/hyperglycemia.
- **B-zone:** Benign control deviations.
- **Upper/Lower C-zone:** Over-correction of hypo/hyperglycemia.
- **Lower/Upper D-zone:** Failure to deal with hypo/hyperglycemia.
- **E-zone:** Erroneous control.

As it was previously mentioned, due to the greater autonomy the patients have, the upper B-zone has a larger density of points. Fortunately, this does not imply a greater risk to the patients health. Figure 7 also shows that there is one patient that fell into the lower D-zone (failure to deal with hypoglycemia). On one hand, it must be considered that not every *in silico* patient has parameters that make sense physiologically, given that the data base was generated for statistical ends.

Table 1. Mean closed-loop results with the ARG algorithm, analyzing separately the entire simulation time (C) and the postprandial period (PP).

		50 g meal	25 g meal	75 g meal	Two 50 g meals
Mean glucose [mg/dl]	**C**	132	126	141	139
	PP	160	135	188	155
% time in [70 180] mg/dl	**C**	91.8	99.1	84.8	86.2
	PP	68.5	96.5	46.3	73.4
% time > 250 mg/dl	**C**	0.2	0.0	2.2	0.3
	PP	0.8	0.0	9.7	0.6
% time > 180 mg/dl	**C**	8.1	0.7	15.1	13.6
	PP	31.4	2.9	53.7	26.5
% time < 70 mg/dl	**C**	0.1	0.3	0.1	0.2
	PP	0.1	0.5	0.0	0.1
LBGI		0.1	0.1	0.0	0.1
HBGI		1.7	0.8	3.2	2.7

On the other hand, the proposed strategy allows facing these kind of singular cases where the controller action was either too conservative or too aggressive. To illustrate this, Fig. 8 shows how a slight adjustment in the IOB constraint for this particular patient allows avoiding postprandial hypoglycemia and solves this problem.

Figure 9 displays the results obtained when facing different amounts or consecutive carbohydrates. This figure shows the performance of the algorithm in these situations without considering the meal size (i.e. always using the IOB constraint defined for medium meals). Table 1 displays the meal results for all the considered cases. This table analyzes the glycemic levels obtained in both the entire simulation time and in the postprandial period (defined as 5 hours after meal intake). The risk of hypo and hyperglycemia indexes are also included. The scale for these indexes are defined according to [46]:

- **Risk of hypoglycemia:** LBGI $\leq$ 2.5 (low); 2.5 $<$ LBGI $\leq$ 5 (moderate); LBGI $>$ 5 (high).
- **Risk of hyperglycemia:** HBGI $\leq$ 4.5 (low); 4.5 $<$ HBGI $\leq$ 9 (moderate); HBGI $>$ 9 (high).

It can be observed that the ARG algorithm allows achieving minimal risk of hypo and hyperglycemia. Even though the results are satisfactory, they can be further improved with the addition of a meal classifier to help establish a more adequate IOB constraint. For example, when an IOB constraint for small meals (<35 gCHO) is considered for the simulations with the 25gCHO meal, the mean time in hypoglycemia is reduced form 0.5% to 0.2%, maintaining a mean time of 96.5% in the desirable range in the postprandial period. On the other hand, when an IOB constraint for large meals (>65 mg/dl) is considered with the 75gCHO meal, the mean time in the desirable range increases from 46.3% to 52.5% in the postprandial period, with a minimal increase in the mean time in hypoglycemia from 0 to 0.1%.

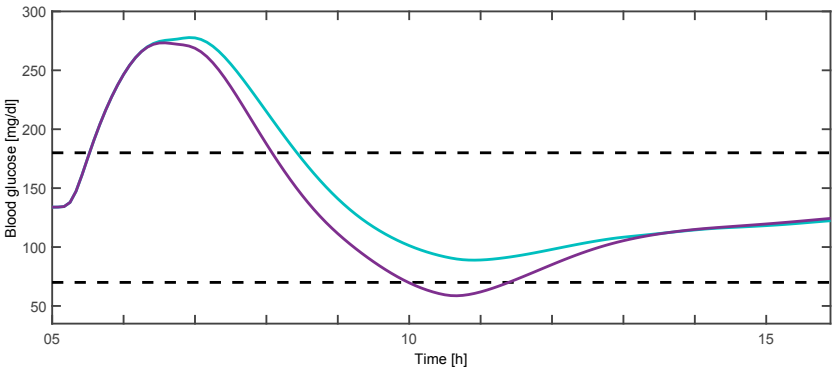

Figure 8. Closed-loop response for adult #090 of the UVa/Padova Simulator with a standard IOB constraint (purple) and with an IOB constraint 30% lower than the standard (blue). The dashed lines indicate the boundaries of the desirable range.

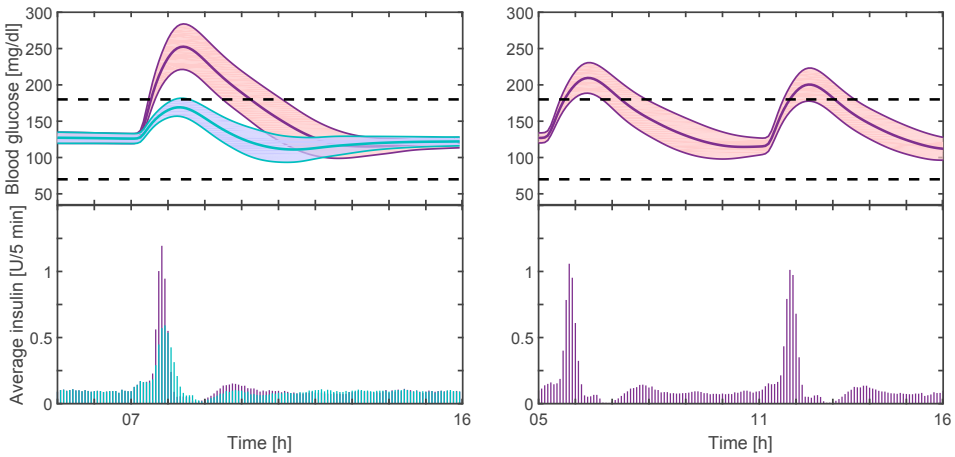

Figure 9. Mean closed-loop response for all the available adults in the UVa/Padova Simulator when facing one meal of 25gCHO (blue-left), 75 gCHO (purple-left) and two meals of 50 gCHO (right). **Upper boxes:** The solid line indicates the mean glucose and the shaded area is ± 1 standard deviation. The dashed lines indicate the boundaries of the desirable range. **Lower boxes:** Mean insulin infusion.

5. Clinical trials

The first clinical trials with an AP in Latin America were carried out in two stages at the Hospital Italiano de Buenos Aires (HIBA). The first one in November 2016 with the algorithm of the University of Virginia that had been tested internationally in several occasions. The second trial was in June 2017 with the Automatic Regulation of Glucose (ARG) algorithm, fully developed in Argentina, a collaboration between researchers from the Instituto Tecnológico de Buenos Aires (ITBA), the Universidad Nacional de Quilmes (UNQ) and the Universidad Nacional de La Plata (UNLP). Both stages had the same numbers of patients (5), the same hardware, and followed the same clinical protocol. However, the main difference between both trials is that in the latter, the patients did not have to count CHO nor apply an insulin bolus. Here we will focus on this second clinical trial.

The selection of the 5 patients with T1DM that participated in the trials was made according to the clinical protocol, particularly the inclusion and exclusion criteria as indicated in NCT02994277 (www.clinicaltrials.gov).

5.1 Hardware and software

For the implementation of the AP the following devices were used in each patient:

- CGM Dexcom G4 Share®;
- Accu-Check Combo® insulin pump from Roche; and
- a NEXUS-5 smartphone based on Android containing the Diabetes Assistant (DiAs) from the University of Virginia (UVa) [47].

The Diabetes Assistant (DiAs) is a software that includes several mobile applications and allows every 5 minutes the communication between the control algorithm, the CGM sensor (through Android Bluetooth Low Energy) and the insulin pump (through standard Bluetooth). Due to FDA regulations, to be accepted as a Class III medical device, the phone, navigator, Android Market, games, etc., were removed. The system also includes the SQLite database for the asynchronous data management for requests from the user.

The DiAs is a modular system where the control algorithm is contained. The ARG algorithm was programmed in the DiAs using Object-oriented programming on the Eclipse IDE for Java Developers version: Kepler Service Release 2, with the plugin Android Development Tools (ADT).

5.2 Clinical procedures

Patients were called to attend the HIBA nine days before the trial. That day, the protocol was explained in detail, the Informed Consent was signed, the inclusion/exclusion criteria were revised and a blood extraction was made for laboratory *screening*. These results, as well as a supervised glycaemic control were reviewed two days before the trial. That same day, the insulin pump and the CGM were connected to each patient, with a brief training in the use of both devices. The communication among these devices with the smartphone was verified and the systems remained in open loop (without the algorithm active in the smartphone) in order for the patients to perform their usual controls. They also had to perform

eight daily capilar glycaemia measurements until the day of the trial, for comparison purposes. During these days, patients were allowed to carry on with their daily routines and to continue with their usual treatment. Meals were not restricted and patients were asked to record their daily food intakes.

The trial started at 1700 hs on day 0 and ended the morning of day 2. The loop was closed by activating the control algorithm in the smartphone and all patients had 5 meals during the 36 hs tests: two dinners, one lunch, one breakfast and one afternoon snack (see details below) with a continuous monitoring of their glycaemia and injected insulin values from the medical and researcher staff room. During these 36 hs, the ARG algorithm regulated the patients glycaemia using only CGM information and the meal announcement with CHO classification. Patients were allowed to walk freely around the hospital. If an hypoglycemia event occurred, rescue CHO were provided by the medical staff. If a patient presented glycemic values over 300 mg/dl for more than two hours, a manual bolus was injected following medical indications.

The menu coordinated by the nutritionist was as follows:

- **Breakfast and afternoon snack**

Meal	**Quantity** (g)	**CHO** (g)
Tea, coffee or mate	C/N	-
Wholegrain bread or 5 water crackers	50 (2 units)	20
Diet jam	8 (1 jar)	8
Spread cheese	20	-
Total		28

- **Dinner**

Meal	**Quantity** (g)	**CHO** (g)
Wheat pasta with natural filetto sauce	50 (raw)	40
Lean meat	100	-
Fressh fruit	1 unit	15
Total		55

- **Lunch**

Meal	**Quantity** (g)	**CHO** (g)
Smashed potatoes with water (285 cc)	200 (2 units)	40
Lean meat	100	-
Fresh fruit	1 unit	15
Total		55

5.3 Results

Next, a brief description of the results is presented. For the Open Loop (OL) analysis is considered a time interval from 7 p.m. on day -2 up to 7 a.m. on day 0. In the case of the Closed Loop (CL) period, the time interval is considered from 7 p.m. on day 0 up to 7 a.m. on day 2. The insulin pump of one of the patients had an occlusion during the first night in CL, therefore, these hours were not considered in the analysis. The OL is used as a reference of their habitual glucose management and it should be noted that the patients did not follow the same diet during OL and CL. On table 2 it can be seen the statistical data obtained from the 36 hours of CL trial and the comparison with those obtained in OL. As can be observed, there is a significant improvement in the patient's glucose regulation when using the ARG algorithm. The null hypothesis at a level of significance of 5% ($\rho = 0.05$), defined as the difference between the results obtained in OL and CL have zero mean, can be rejected in the percentage of time in euglycemic range [70, 180] mg/dl, being statistically significant ($\rho = 0.0356$).

Since it is the first clinical trial of the ARG algorithm, the 3 initial meals were used to make the necessary adjustments to the IOB maximum limit. For this reason, if the analysis of the results is concentrated in the last 15 hours of CL and it is

Table 2. Comparison of the statistical data obtained from 36 hs in OL *vs* CL, considering a confidence interval of 95%.

	OL		CL	
	Mean	**CI 95 %**	**Mean**	**CI 95%**
% time [70, 250] mg/dl	82.9	[67.3, 98.6]	88.6	[82.4, 94.7]
% time [70, 180] mg/dl	59.1	[41.9, 76.2]	74.7	[68.1, 81.4]
% time $<$ 70 mg/dl	7.6	[2.9, 12.4]	5.8	[1.6, 10.0]
% time $<$ 50 mg/dl	1.7	[0.3, 3.1]	0.8	[0.2, 3.5]
LBGI	2.8	[1.8 3.7]	2.3	[1.4, 3.1]
HBGI	7.2	[3.4, 11.0]	4.9	[2.9, 6.9]

compared with the 15 hours of OL that involve the same period of the day, an even more significant control improvement is noticed, as it is shown in Table 3. A two-sampled t-test was carried out to determine if the results obtained in OL and CL are different at a level of significance of 5% ($\rho = 0.05$). In this way, the null hypothesis was defined as "the difference between the results obtained in OL and CL has zero mean". For this trial, the null hypothesis can be rejected for the percentage time in euglycemic range [70, 180] mg/dl ($\rho = 0.0142$), in $<$ 70 mg/dl ($\rho = 0.049$), LBGI index (p = 0.0383) and HBGI index ($\rho = 0.0469$), these being statistically significant.

Table 3. Comparison of the statistical data obtained from first 15 hs in OL and the last 15 hs in CL, considering a confidence interval of 95%.

	OL		CL	
	Mean	**CI 95 %**	**Mean**	**CI 95%**
% time [70, 250] mg/dl	73.5	[49.8, 97.2]	94.7	[83.8, 98.4]
% time [70, 180] mg/dl	49.8	[24.5, 75.1]	82.6	[69.9, 95.2]
% time $<$ 70 mg/dl	13.6	[4.4, 22.7]	4.1	[0.8, 18.0]
% time $<$ 50 mg/dl	5.4	[1.6, 16.4]	0.2	[0.0, 3.5]
LBGI	4.2	[2.1 6.2]	1.8	[0.3, 3.3]
HBGI	8.7	[2.9, 14.5]	2.8	[0.1, 5.5]

It is important to remark that taking into account the night period (from 23 p.m. until 7 a.m.) the ARG algorithm presents a notorious improvement in comparison with the OL treatment. In Fig. 10 it is highlighted the comparison of the glucose excursion obtained during the second night in OL and in CL (time lapse without meals). In Table 4 the statistical data is presented regarding this period. Again, an improvement in percentage of time in euglycemia ($\rho = 0.0351$) and HBGI index ($\rho = 0.0309$) was obtained.

Table 4. Comparison of the statistical data obtained from the last nights in OL *vs* CL, considering a confidence interval of 95%

	OL		CL	
	Mean	**CI 95 %**	**Mean**	**CI 95%**
% time [70, 250] mg/dl	78.1	[29.1, 96.9]	95	[66.9, 99.4]
% time [70, 180] mg/dl	50.3	[23.2, 77.4]	87.7	[76.5, 99.0]
% time $<$ 70 mg/dl	3.6	[0.3, 29.5]	5	[0.6, 33.1]
% time $<$ 50 mg/dl	0	[0.0, 0.0]	0	[0.0, 0.0]
LBGI	2.0	[0.6, 3.4]	1.5	[0.4, 4.1]
HBGI	9.8	[2.8, 16.8]	1.9	[0.4, 5.7]

6. Conclusions

In this paper a brief review of the artificial pancreas project in Argentina was presented alongside with a novel control strategy for glycemic regulation: the ARG algorithm. It consists of a two-degree-of-freedom control structure that includes a switched LQG inner controller together with an outer sliding mode safety loop, the Safety Auxiliary Feedback Element (SAFE) mechanism, for IOB constraints. The switched LQG control strategy is a simplified version of the one in [35]. The switched nature of the inner controller enables different tunings for dealing with prandial and fasting periods and can be extended to other situations, e.g., physical activity. New and more complex scenarios could be potentially

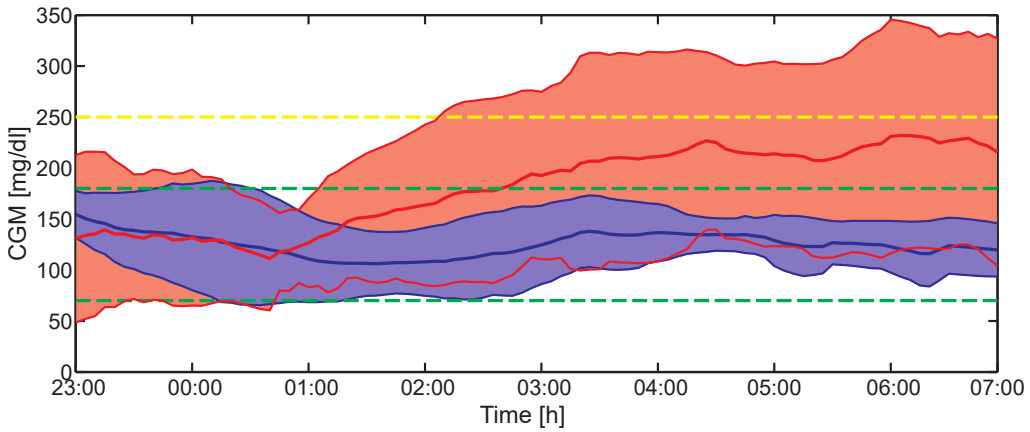

Figure 10. Mean glycemic excursion of all 5 patients in OL (red) and in CL (blue) during night time. The solid line indicates mean and the grey area ± 1 standard deviation.

addressed by redesigning the switching policy and/or the IOB constraints. The SAFE layer quickly adapts the controller gain to automatically obtain insulin spikes like the open-loop boluses. Promising results were obtained both *in silico* and later *in vivo* during the first clinical trials in Latin America.

Acknowledgements

Access to the complete version of the University of Virginia/Padova metabolic simulator was provided by an agreement with Prof. C. Cobelli (University of Padova) and Prof. B. P. Kovatchev (University of Virginia) for research purposes. The authors would like to acknowledge Dr. Daniel Cherñavvsky for his very generous collaboration. We would also like to thank the physicians of the Hospital Italiano Ventura Simonovich, Paula Scibona, Cintia Rodriguez, Javier Giunta and Valeria Beruto coordinated by Dr. Luis Grosembacher and Dr. Waldo Belloso without whom this clinical trial could not have been possible. Additionally, we express our gratitude to the nutritionist Marianela Stasi who worked with us in the elaboration of the menu used. Finally, we want to highlight the collaboration with Dexcom, the generous donation by Roche and the funding of the Cellex (Spain) and Nuria (Argentina) Foundations.

References

[1] A. Chait and K. E. Bornfeldt. Diabetes and atherosclerosis: Is there a role for hyperglycemia? *J. Lipid Res.*, 50:S335–S339, Apr. 2009.

[2] The Diabetes Control and Complications Trial Research Group. Hypoglycemia in the diabetes control and complications trial. *Diabetes*, 46(2):271–286, 1997.

[3] E. Renard. Insulin delivery route for the artificial pancreas: Subcutaneous, intraperitoneal, or intravenous? Pros and cons. *J. Diabetes Sci. Technol.*, 2(4):735–738, July 2008.

[4] B. W. Bequette. Challenges and recent progress in the development of a closed-loop artificial pancreas. *Annu. Rev. Control*, 36(2):255–266, Dec 2012.

[5] G. M. Steil, A. E. Panteleon, and K. Rebrin. Closed-loop insulin delivery-the path to physiological glucose control. *Adv. Drug Deliv. Rev.*, 56(2):125–144, Feb 2004.

[6] J Walsh, R. Roberts, and L. Heinemann. Confusion regarding duration of insulin action: A potential source for major insulin dose errors by bolus calculators. *J. Diabetes Sci. Technol.*, 8(1):170–178, Jan 2014.

[7] B. P. Kovatchev, M. Breton, C. Dalla-Man, and C. Cobelli. In silico model and computer simulation environment approximating the human glucose/insulin utilization. *Food and Drug Administration Master File MAF 1521*, 2008.

[8] B. P. Kovatchev, M. Breton, C. Dalla Man, and C. Cobelli. In silico preclinical trials: A proof of concept in closed-loop control of type 1 diabetes. *J. Diabetes Sci. Technol.*, 3(1):44–55, Jan. 2009.

[9] R. Hovorka, D. Elleri, H. Thabit, J. Allen, L. Leelarathna, R. El-Khairi, K. Kumareswaran, K. Caldwell, P. Calhoun, C. Kollman, H. Murphy, C. Acerini, M. Wilinska, M. Nodale, and D. Dunger. Overnight closed-loop insulin delivery in young people with type 1 diabetes: A free-living, randomized clinical trial. *Diabetes Care*, 37(5):1204–1211, 2014.

[10] R. Gondhalekar, E. Dassau, and F. J. Doyle III. Periodic zone-MPC with asymmetric costs for outpatient-ready safety of an artificial pancreas to treat type 1 diabetes. *Automatica*, 71(9):237–246, Sept. 2016.

[11] Moshe Phillip, Tadej Battelino, Eran Atlas, Olga Kordonouri, Natasa Bratina, Shahar Miller, Torben Biester, Magdalena Stefanija, Ido Muller, Revital Nimri, and Thomas Danne. Nocturnal glucose control with an artificial pancreas at a diabetes camp. *N. Engl. J. Med.*, 368(9):824–833, Feb. 2013.

[12] Martin de Bock, Anirban Roy, Matthew Cooper, Julie Dart, Carolyn Berthold, Adam Retterath, Kate Freeman, Benyamin Grosman, Natalie Kurtz, Fran Kaufman, Timothy Jones, and Elizabeth Davis. Feasibility of outpatient 24-hour closed-loop insulin delivery. *Diabetes Care*, 38(11):e186–e187, Nov. 2015.

[13] T.T. Ly, A Roy, B Grosman, J Shin, A Campbell, S Monirabbasi, B Liang, R von Eyben, S Shanmugham, P Clinton, and B. A. Buckingham. Day and night closed-loop control using the integrated Medtronic hybrid closed-loop system in type 1 diabetes at diabetes camp. *Diabetes Care*, 38(7):1205–1211, Jul 2015.

[14] L. Bally, H. Thabit, H. Kojzar, J. K. Mader, J. Qerimi-Hyseni, S. Hartnell, M. Tauschmann, J. M. Allen, M. E. Wilinska, T. R. Pieber, M. L. Evans, and R. Hovorka. Day-and-night glycaemic control with closed-loop insulin delivery versus conventional insulin pump therapy in free-living adults with well controlled type 1 diabetes: An open-label, randomised, crossover study. *Lancet Diabetes Endocrinol.*, 5(4):261–270, Apr 2017.

[15] Boris P. Kovatchev, Peiyao Cheng, Stacey M. Anderson, Jordan E. Pinsker, Federico Boscari, Bruce A. Buckingham, Francis J. Doyle III, Korey K. Hood, Sue A. Brown, Marc D. Breton, Daniel Chernavvsky, Wendy C. Bevier, Paige K. Bradley, Daniela Bruttomesso, Simone Del Favero, Roberta Calore, Claudio Cobelli, Angelo Avogaro, Trang T. Ly, Satya Shanmugham, Eyal Dassau, Craig Kollman, John W. Lum, and Roy W. Beck. Feasibility of long-term closed-loop control: A multicenter 6-month trial of 24/7 automated insulin delivery. *Diabetes Technol. Ther.*, 19(1):18–24, Jan 2017.

[16] G. P. Forlenza, S. Deshpande, T. T. Ly, D. P. Howsmon, F. Cameron, N. Baysal, E. Mauritzen, T. Marcal, L. Towers, B. W. Bequette, L. M. Huyett, J. E. Pinsker, R. Gondhalekar, F. J. Doyle III, D. M. Maahs, B. A. Buckingham, and E. Dassau. Application of zone model predictive control artificial pancreas during extended use of infusion set and sensor: A randomized crossover-controlled home-use trial. *Diabetes Care*, 40(8):1096–1102, Aug 2017.

[17] Mirko Messori, Jort Kropff, Simone Del Favero, Jerome Place, Roberto Visentin, Roberta Calore, Chiara Toffanin, Federico Di Palma, Giordano Lanzola, Anne Farret, Federico Boscari, Silvia Galasso, Angelo Avogaro, Patrick Keith-Hynes, Boris P. Kovatchev, Daniela Bruttomesso, Lalo Magni, J Hans DeVries, Eric Renard, Claudio Cobelli, and for the AP@home consortium. Individually adaptive artificial pancreas in subjects with type 1 diabetes: A one-month proof-of-concept trial in free-living conditions. *Diabetes Technol. Ther.*, 19(10):560–571, Oct 2017.

[18] A Haidar, V Messier, L Legault, M Ladouceur, and R. Rabasa-Lhoret. Outpatient 60-hour day-and-night glucose control with dual-hormone artificial pancreas, single-hormone artificial pancreas, or sensor-augmented pump therapy in adults with type 1 diabetes: An open-label, randomised, crossover, controlled trial. *Diabetes Obes. Metab.*, 19(5):713–720, May 2017.

[19] F. H. El-Khatib, C Balliro, M. A. Hillard, K. L. Magyar, L Ekhlaspour, M Sinha, D Mondesir, A Esmaeili, C Hartigan, M. J. Thompson, S Malkani, J. P. Lock, D. M. Harlan, P. Clinton, E Frank, D. M. Wilson, D DeSalvo, L Norlander, T Ly, B. A. Buckingham, J Diner, M Dezube, L. A. Young, A Goley, M. S. Kirkman, J. B. Buse, H. Zheng, R. R. Selagamsetty, E. R. Damiano, and S. J. Russell. Home use of a bihormonal bionic pancreas versus insulin pump therapy in adults with type 1 diabetes: A multicentre randomised crossover trial. *Lancet*, 389(10067):369–380, Jan 2017.

[20] Stuart A. Weinzimer, Garry M. Steil, Karena L. Swan, Jim Dziura, Natalie Kurtz, and William V. Tamborlane. Fully automated closed-loop insulin delivery versus semiautomated hybrid control in pediatric patients with type 1 diabetes using an artificial pancreas. *Diabetes Care*, 31(5):934–939, May 2008.

[21] A. S. Brazeau, H Mircescu, K Desjardins, C Leroux, I Strychar, J. M. Ekoé, and R. Rabasa-Lhoret. Carbohydrate counting accuracy and blood glucose variability in adults with type 1 diabetes. *Diabetes Res. Clin. Pract.*, 99(1):19–23, Jan 2013.

[22] V Gingras, R Rabasa-Lhoret, V Messier, M Ladouceur, L Legault, and A. Haidar. Efficacy of dual-hormone artificial pancreas to alleviate the carbohydrate-counting burden of type 1 diabetes: A randomized crossover trial. *Diabetes Metab.*, 42(1):47–54, Feb 2016.

[23] V Gingras, A Haidar, V Messier, L Legault, M Ladouceur, and R Rabasa-Lhoret. A simplified semiquantitative meal bolus strategy combined with single- and dual-hormone closed-loop delivery in patients with type 1 diabetes: A pilot study. *Diabetes Technol. Ther.*, 18(8):464–471, Aug 2016.

[24] G. M. Steil, K Rebrin, C Darwin, F Hariri, and M. F. Saad. Feasibility of automating insulin delivery for the treatment of type 1 diabetes. *Diabetes*, 55(12):3344–3350, Dec 2006.

[25] E. Dassau, H. Zisser, R. Harvey, M. Percival, B. Grosman, W. Bevier, E. Atlas, S. Miller, R. Nimri, L. Jovanovič, and F. J. Doyle III. Clinical evaluation of a personalized artificial pancreas. *Diabetes Care*, 36(4):801–809, Apr. 2013.

[26] M Reddy, P Herrero, M. E. Sharkawy, P. Pesl, N Jugnee, D Pavitt, I. F. Godsland, G Alberti, C Toumazou, D. G. Johnston, P Georgiou, and N. S. Oliver. Metabolic control with the bio-inspired artificial pancreas in adults with type 1 diabetes: A 24-hour randomized controlled crossover study. *J. Diabetes Sci. Technol.*, 10(2):405–413, Nov 2015.

[27] H Blauw, A. C. van Bon, R Koops, J. H. DeVries, and on behalf of the PCDIAB consortium. Performance and safety of an integrated bihormonal artificial pancreas for fully automated glucose control at home. *Diabetes Obes. Metab.*, 18(7):671–677, Jul 2016.

[28] F. M. Cameron, T. T. Ly, B. A. Buckingham, D. M. Maahs, G. P. Forlenza, C. J. Levy, D Lam, P Clinton, L. H. Messer, E Westfall, C Levister, Y. Y. Xie, N. Baysal, D Howsmon, S. D. Patek, and B. W. Bequette. Closed-loop control without meal announcement in type 1 diabetes. *Diabetes Technol. Ther.*, 19(9):527–532, Sep 2017.

[29] K. Turksoy, I. Hajizadeh, S. Samadi, J. Feng, M. Sevil, M. Park, L. Quinn, E. Littlejohn, and A. Cinar. Real-time insulin bolusing for unannounced meals with artificial pancreas. *Control Eng. Pract.*, 59(Supplement C):159–164, Feb 2017.

[30] F. M. Cameron, G. Niemeyer, and B. W. Bequette. Extended multiple model prediction with application to blood glucose regulation. *J. Process Contr.*, 22(8):1422–1432, Sep 2012.

[31] Ali Cinar. Special issue on artificial pancreas systems. *IEEE Control Systems Magazine*, 38(1), Feb. 2018.

[32] R. S. Sánchez-Peña, P. Colmegna, L. Grosembacher, M. Breton, H. De Battista, F. Garelli, W. Belloso, E. Campos-Náñez, V. Simonovich, V. Beruto, P. Scibona, and D. Cherñavvsky. Artificial Pancreas: First clinical trials in Argentina. In *20th IFAC World Congress*, pages 7997–8002, Toulouse, France, 2017.

[33] P.Colmegna, F. Garelli, H. De Battista, and Ricardo Sánchez-Peña. Automatic regulatory control in type 1 diabetes without carbohydrate counting. *Control Engineering Practice*, 74:22–32, 2018.

[34] P. Colmegna, R. S. Sánchez-Peña, R. Gondhalekar, E. Dassau, and F. J. Doyle III. Reducing risks in type 1 diabetes using $\mathscr{H}_\infty$ control. *IEEE Trans. Biomed. Eng.*, 61(12):2939–2947, Dec. 2014.

[35] P. Colmegna, R. S. Sánchez-Peña, R. Gondhalekar, E. Dassau, and F.J. Doyle III. Switched LPV glucose control in type 1 diabetes. *IEEE Trans. Biomed. Eng.*, 63(6):1192–1200, June 2016.

[36] P. Colmegna, R. S. Sánchez-Peña, R. Gondhalekar, E. Dassau, and F. J. Doyle III. Reducing glucose variability due to meals and postprandial exercise in T1DM using switched LPV control: In silico studies. *J. Diabetes Sci. Technol.*, 10(3):744–753, May 2016.

[37] P. Colmegna, R. Sánchez-Peña, and R. Gondhalekar. Linear parameter-varying model to design control laws for an artificial pancreas. *Biomed. Signal Process Control*, 40:204–213, Feb. 2018.

[38] P. Colmegna, R. Sánchez-Peña, and R. Gondhalekar. Control-oriented linear parameter-varying model for glucose control in type 1 diabetes. In *IEEE Multi-Conference on Systems and Control*, pages 410–415, Buenos Aires, Argentina, 2016.

[39] Klaske van Heusden, Eyal Dassau, Howard C. Zisser, Dale E. Seborg, and Francis J. Doyle III. Control-relevant models for glucose control using *a priori* patient characteristics. *IEEE Trans. Biomed. Eng.*, 59(7):1839–1849, July 2012.

[40] J. P. Hespanha and A. S. Morse. Switching between stabilizing controllers. *Automatica*, 38(11):1905–1917, Nov. 2002.

[41] F. Garelli, R. Mantz, and H. De Battista. *Advanced Control for Constrained Processes and Systems*. IET Institution of Engineering and Technology, London, United Kingdom, 2011.

[42] A. Revert, F. Garelli, J. Picó, H. De Battista, P. Rossetti, J. Vehi, and J. Bondía. Safety auxiliary feedback element for the artificial pancreas in type 1 diabetes. *IEEE Trans. Biomed. Eng.*, 60(8):2113–2122, Aug. 2013.

[43] M. E. Willinska, L. J. Chassin, H. C. Schaller, L. Schaupp, T. R. Pieber, and R. Hovorka. Insulin kinetics in type 1 diabetes: Continuous and bolus delivery of rapid acting insulin. *IEEE Trans. Biomed. Eng.*, 52(1):3–12, Jan. 2005.

[44] J. Walsh and R. Roberts. *Pumping Insulin*. Torrey Pines Press, San Diego, CA, 4 edition, 2006.

[45] F. León-Vargas, F. Garelli, H. De Battista, and J. Vehi. Postprandial response improvement via safety layer in closed-loop blood glucose controllers. *Biomed. Signal Process Control*, 16:80–87, Feb. 2015.

[46] B. Kovatchev, G. Umpierrez, A. DiGenio, R. Zhou, and S. E. Inzucchi. Sensitivity of traditional and risk-based glycemic variability measures to the effect of glucose-lowering treatment in type 2 diabetes mellitus. *J. Diabetes Science and Technology*, 9(6):1227–1235, Nov. 2015.

[47] P. Keith-Hynes, B. Mize, A. Robert, and J. Place. The diabetes assistant: A smartphone-based system for real-time control of blood glucose. *Electronics*, 3(4):609–623, Nov. 2014.

Bios

Nicolás Rosales

Nicolás Rosales was born in Trelew, Argentina, in 1990. He obtained a B.S.E.E. degree at the National University of La Plata (UNLP), La Plata, Argentina, in 2015, where he is currently working towards his Ph.D. degree at the Laboratory of Industrial Electronics, Control and Instrumentation (LEICI). His main research interests are in artificial pancreas systems. He specializes in both open- and closed-loop glucose control strategies.

Patricio Colmegna

Patricio Colmegna obtained an Engineering degree at the University of Quilmes (UNQ), in 2010, and a doctoral degree in Engineering at Buenos Aires Institute of Technology (ITBA), in 2014. His doctoral research focused on applying optimal, robust and switched control algorithms to an artificial pancreas (AP) that aimed to not only mitigate glucose excursions, but also reduce patient burden. In 2017, he was named Research Assistant at the National Research Council (CONICET), and was part of the team that performed the first clinical AP trial in Latin America. Dr. Colmegna joined the Center For Diabetes Technology, University of Virginia, in early 2018, and is currently working on the development of a next-generation simulation facility for diabetes. This effort involves the design of new and more computationally efficient platforms for multi-model, multi-disease modeling and simulation.

Fabricio Garelli

Fabricio Garelli is currently Full Professor at the National University of La Plata (UNLP) and Official Member of the National Research Council (CONICET). He is the author of an awarded Ph.D. thesis, an IET book, and more than a hundred journal or conference papers. His research work focuses on constrained automatic control and estimation via sliding mode techniques, with application to industrial processes/bioprocesses, robotics and biomedical engineering (artificial pancreas).

Hernán De Battista

Hernán De Battista was born in La Plata, Argentina, in 1968. He obtained his M.Sc. in Engineering with highest honors in 1994, followed by a PhD in 2000, both at the National University of La Plata, Argentina. Currently, he is Full Professor at the School of Engineering, National University of La Plata, and Principal Researcher of the National Research Council (CONICET), Argentina. His main research interests are in non-linear control and its applications to renewable energies and biological systems. He has coauthored two books and 65 journal articles. He received the E. Galloni award from the Argentine Academy of Exact, Physical and Natural Sciences in 2002 and the S. Gershanik award from the Buenos Aires Academy of Engineering in 2006.

Demián García-Violini

Demián García-Violini obtained a B.Sc. degree in Automation and Control Engineering at the National University of Quilmes (UNQ), Buenos Aires, Argentina, in 2010, and a doctoral degree in Engineering at Buenos Aires Institute of Technology (ITBA), in 2015. He is currently a Postdoctoral Researcher at the Centre of Ocean Energy Research, National University of Ireland Maynooth, and he is also working as a Teaching Assistant in Control Systems courses at UNQ. His research interests include modeling, identification, and robust control for diverse problems, such as control of wave energy converters, type 1 diabetes mellitus, and synchronization between different cerebral structures.

Marcela Moscoso-Vázquez

Marcela Moscoso-Vázquez obtained a B.Sc. degree and a Master degree, both in Chemical Engineering, at the National University of Colombia, Medellín, in 2011 and 2014, respectively, supported by the Outstanding Graduate Student Scholarship. She also obtained a Doctoral degree in Engineering at Buenos Aires Institute of Technology (ITBA), Argentina, in 2019, supported by a CONICET doctoral scholarship.

She is currently a Postdoctoral Researcher at CONICET in Argentina, and is a Teaching Assistant at the Chemical Process Control course at ITBA. Her research interests include modeling and analysis of circadian rhythms, control-oriented modeling and identification for robust control of type 1 diabetes mellitus, and model-based control of chemical processes.

Emilia Fushimi

Emilia Fushimi was born in Buenos Aires, Argentina, in 1993. She obtained a B.S.E.E. degree at the National University of La Plata (UNLP), La Plata, Argentina, in 2016, where she is currently working towards her Ph.D. degree at the Laboratory of Industrial Electronics, Control and Instrumentation. She is also a Graduate Student Assistant at the Department of Electrical Engineering, UNLP. Her main research interests are focused on the artificial pancreas.

Ricardo S. Sánchez-Peña

Ricardo S. Sánchez-Peña has an EE degree from the University of Buenos Aires (UBA) and a M.S. and Ph.D. from the California Institute of Technology. Since 1977, he has worked at CITEFA, CNEA, CNIE and CONAE in Argentina. He has collaborated with NASA and the German and Brazilian space agencies. He has been a Professor at UBA and UPC (Spain) as an ICREA researcher. He has been visiting professor and researcher at various universities, as well as a consultant for companies in topics related to aerospace and energy applications in the USA and the EU. He has received awards from IEEE, NASA and ANCEFN. Presently he is Director of the Research & PhD Department, Buenos Aires Institute of Technology (ITBA), Investigador Superior of the National Research Council (CONICET), and he leads the Artificial Pancreas project in Argentina. Corresponding author. Email: rsanchez@itba.edu.ar.

Science Reviews
from the end of the world

Vol. 1, No. 1, December 2019 // pp. 54-73 /

Arsenic in Latin America

Marta I. Litter[1,2*], María A. Armienta[3], Ruth E. Villanueva-Estrada[4], Edda C. Villaamil Lepori[5] and Valentina Olmos[5]

[1] *Gerencia Química, Comisión Nacional de Energía Atómica-CONICET, Argentina*
[2] *Instituto de Investigación e Ingeniería Ambiental, Universidad Nacional de General San Martín, Argentina*
[3] *Universidad Nacional Autónoma de México, Instituto de Geofísica, Ciudad de México, México*
[4] *Universidad Nacional Autónoma de México, Instituto de Geofísica, Unidad Michoacán, México*
[5] *Cátedra de Toxicología y Química, Facultad de Farmacia y Bioquímica, Universidad de Buenos Aires, Argentina*
** Corresponding author. E-mail: marta.litter@gmail.com*

Abstract

An overview of arsenic (As) presence in waters in Latin America (LA) is presented. Aspects on As occurrence, effects of As on human health, regulations regarding the maximum allowable concentration of As in drinking water, analytical techniques for As determination, and conventional/emerging technologies for As removal developed in LA are mentioned. Arsenic presence has been identified in many LA countries in a range of concentrations, originated from various sources; however, its origin is mainly natural. Main analytical techniques available in LA laboratories are described. Pathologies derived from the chronic consumption of As, the metabolism of As in the human body and the effects of the different As chemical forms are detailed. A list of conventional and emerging technologies for As removal in LA waters for human consumption, for large, medium and small populations, rural and periurban, is reported. Conclusions and recommendations to face the problem are included.

Keywords:
Arsenic, occurrence, analytical methodologies, health effects, regulations, removal technologies

1. Introduction

Arsenic (As) is a metalloid abundantly present in the Earth's crust. Exposure in humans occurs through the consumption of contaminated water and food [1]. Pollution comes mainly from natural sources, i.e., from the release of As to soil and aquifers due to volcanic phenomena and disintegration of rocks. A few anthropic activities such as mining, industrial processes, smelting of metals, production of pesticides and wood preservatives [1] are sources of contamination. Although natural mineralization and microbial activities increase the mobilization of As in the environment, human activities exacerbate As contamination in soil and in water supplies [2]. Chronic exposure to As via drinking water has received more and more attention for its high prevalence in many parts of the world, and for the growing body of evidence of its impact on health [3]. Contamination of water by As is a worldwide problem with high impact in the poorest regions [4], with more than 226 million people exposed [5,6]. The most affected populations are those in low income countries. The higher concentrations and, consequently, the most significant health problems are localized in Argentina, Bangladesh, Nepal, Chile, China, Hungary, India, Mexico, Romania, Taiwan, Vietnam and the USA [7]. In Latin America (LA), the problem affects at least 14 countries (Argentina, Bolivia, Brazil, Chile, Colombia,

Cuba, Ecuador, El Salvador, Guatemala, Honduras, Mexico, Nicaragua, Peru and Uruguay), and the number of exposed people could be estimated in around 14 million. The most critical areas are in Argentina, Chile and México [8-9,10,11,12].

2. Distribution of arsenic in Latin America

Arsenic presence has been identified in many LA countries in a wide range of concentrations from various sources, mainly natural. Arsenate (As(V)) is the most abundant chemical form. A summary of As occurrence in each country is given below. Figure 1 shows the countries where natural As in water has been detected.

Figure 1. Distribution of arsenic in Latin America.

Argentina.- A compilation of studies conducted in Argentina related to the presence of As in water has been reported in various publications [7-12]; the Chaco-Pampean plain (about 1 million km^2) is the largest area affected by groundwater As contamination in LA. Arsenic release involves the influx from dissolution of volcanic glass, adsorption of As on Fe and Al mineral phases in relatively low pH zones, and high mobility of As in high pH zones [9]. In addition, mineralized, hydrothermal zones and hot springs are also major geogenic sources [9]. Co-existence of As and F in groundwater of the Chaco-Pampean plain has also been remarked [9]. Approximately 88% of 86 groundwater samples collected in 2007 exceeded the WHO guideline value (see section 5), posing a risk to the population since this water is used for human and livestock consumption. Hydrogeochemical studies have also been performed in the Salí river basin part of the Tucumano-Santiagueña hydrogeological province [9]. Arsenic concentrations ranged from 11.4 to 1,660 μg/L, with 100% of the samples above the WHO guideline value. Leaching from pyroclastic materials is favored by high pH and high bicarbonate waters. The presence of As in surface and groundwaters of the Argentine Altiplano (Puna) and Subandean valleys, which are consumed by 355,000 people, was also evaluated [9]. The concentrations measured in 61% of the 62 samples collected in an area of 30,000 km^2 exceeded the WHO limit. Arsenic occurrence was ascribed to geogenic sources [9].

Most of the studies in Argentina have focused on the sources and processes leading to arsenic enrichment in ground- and surface waters, finding that natural sources and geochemical conditions are the ones that affect arsenic occurrence and distribution the most.

Bolivia.- The presence of As was identified in various areas of Bolivia, mainly related to mining activities, ore deposits, geothermal manifestations, and leaching of volcanic rocks [9,10]. Many of the studies have focused on the Pilcomayo river basin and the Poopó lake basin [9]. Arsenic concentrations were above the WHO guideline value in 95% of the 41 sampled wells, with seven sites along four rivers reaching 623 μg/L. This was related to water contact with alluvial material in lower terrains, arsenopyrite oxidation, and dissolution from volcanic rocks. Groundwater average As concentration was 47 μg/L and ranged from below the detection limit to 200 μg/L in Kondo K, 245 μg/L in Santuario de Quillacas, 152 μg/L in the central region, and 187 μg/L in Pampa Aullagas. The Poopó river contained the highest As concentrations of the sampled surface waters, with 11,140 μg/L in the dry period. Geothermal processes are the main natural sources of As in the area; anthropogenic contamination is related to mine tailings [9]. The importance of mining in Bolivia is reflected in As occurrence; however, natural sources like geothermal processes are also an important source of As contamination in waters.

Brazil.- Mining has been an important source of As in the Iron Quadrangle at the Minas Gerais state [9,10]. Arsenic presence is related to the natural leaching of rocks and soils, as well as mining operations [10]. In the Ribeira valley (southeastern Brazil), Pb and As contaminated the Ribeira river as a result of Pb-Zn ore production and smelting. The Santana district in the Amazon region is also contaminated with As (up to 2.0 mg/L in some wells) produced from Mn ore benefit [9]. Environmental studies carried out in Brazil have shown that arsenic contamination in surface and groundwaters is mainly related to mineralization and ore exploitation.

Chile.- The area of Atacama Desert, northern Chile, is naturally rich in As; local people have been exposed to this metalloid for more than 4500 years [8]. In the Loa river, As concentrations of up to 2,000 μg/L were measured; these are the result of high evaporation at alkaline pH, and high salinity [9,10]. Arsenic-related health effects from As-rich drinking water pumped from this river were identified as early as 1962. Arsenic is mainly released from volcanic rocks and sulfide ore deposits at the Andean range and mobilized by snowmelts and rain to rivers and springs. At the Camarones valley, drinking water from waterfalls and from the Camarones river contains 48.7 μg/L and 1,252 μg/L of As, respectively [9]. In the Tarapacá region, As occurrence was ascribed to the presence of volcanic sediments, salt lakes, thermal areas, the predominance of closed basins, and anthropogenic sources [9]. However, As exposure has decreased, and As-related problems have been solved in most of the country [8,9]. The Atacama desert has been identified as one of the oldest places in the world where human exposure to arsenic has occurred undoubtedly due to natural As enrichment. In contrast with other countries where health effects have been caused mainly by groundwater consumption, as in Bangladesh and Argentina, superficial water is the main source of water affecting Chilean inhabitants.

Colombia.- Colombian geology indicates the presence of rocks containing As minerals; nonetheless, few studies have been developed to assess the actual concentrations in water [9]. A review of the occurrence and sources of As in Colombia was reported in 2014 [13]. Information showed that As concentrations in surface and groundwater, related mainly to mining and agriculture, exceeded national standards at some sites. The authors of this review highlight the importance of performing more research on the occurrence, origin and distribution of As in the country [13].

Cuba.- Arsenic has been detected at some sites in Cuba. At Isla de la Juventud, only one spring close to the Delita mine out of eight sampled points in the watershed was contaminated with up to 250 μg/L As [9,10,14]. The scarce presence of As in Cuba may be due to the geological characteristics of the island, with a predominance of limestones; however, it may reflect the need of additional studies covering the entire territory.

Ecuador.- In Papallacta lake, concentrations of As up to 369 μg/L at the surface and from 289 to 351 μg/L at depth were measured in water [9,10,15]. Discharges of geothermal waters to the Tambo river are the main source of As in the lake.

El Salvador.- Arsenic has been detected in the Olomega, Ilopango and Coatepeque lakes with the highest concentration (4,210 μg/L) measured at the Olomega lake. These waters are used by people living on the watersheds [9,10,16]. Arsenic in the Ilopango lake is linked to hydrothermal fluids. In the Ahuachapán and Berlin geothermal fields, As from geothermal origin was detected in springs and domestic wells. Arsenic was also found in Las Burras and Obrajuelo aquifers [9]. In the Bajo Lempa region, As presence is related to its occurrence in rocks and geothermal fluids, and probably to an anthropogenic source [17]. The studies developed in El Salvador indicate, thus, that geothermal processes are the main source of As in the country.

Guatemala.- At Mixco, in 2007, a concentration of 15 μg/L As, originated from leaching of volcanic rocks, was measured in the water of a well used for drinking water supply [9,18]. Later, in the area of the Marlin mine, up to 261 μg/L As were measured in wells downgradient from the tailings [9]. A relatively low As concentration was measured in the water from a well at Mixco; however, this concentration is still above WHO drinking water regulatory values and may pose a risk to the population.

Mexico.- Chronic As poisoning was first identified in 1958 at Comarca Lagunera, northern México [19]. Since then, As has been detected in many areas of the country. Its presence is mainly related to geogenic sources – mineralization, geothermal systems, sorption and release from minerals, salinization – but also to anthropogenic activities in some areas. An overview of As occurrence in groundwater and its possible sources was reported in 2008 [20]. In addition to this, areas with presence of As and F were described in 2013 [21], and another study [22] focused on the occurrence and mechanisms of As enrichment in geothermal zones.

Comarca Lagunera has been one of the most studied areas in Mexico, with groundwater As concentrations of up to 750 μg/L [10,23]. Although various sources have been proposed [24], it was concluded recently that the most probable one is related to extinct hydrothermal activity and sedimentary processes [23]. In addition, intensive groundwater exploitation and dam construction produced the advance of As rich water to the main granular aquifer [24]. Concentrations of As and F above the Mexican drinking water standards have also been measured at Chihuahua state in northern México [25,26]. Hydrogeological and geological interpretations indicated a geogenic source related to the recharge flow coming from mountains presenting arsenopyrite deposits [27]. In mining zones of México where As contamination has been identified, its presence in groundwater is related to natural and/or anthropogenic sources. At Zimapán, Hidalgo, water interaction with As-bearing minerals releases As to the deep fractured limestone aquifer, while the shallow aquifer was contaminated by tailings and infiltration of As-enriched water from smelter stacks [28,29]. In other non-mining areas like the Independencia basin, Guanajuato state, central México, weathering of rhyolites and oxidation of As-bearing minerals result in high As and F concentrations [30]. Hydrogeochemical and isotopic results indicated that As originates from the dissolution of silicates, while F is related to silicates, fluorite dissolution, thermal water, and a long residence time of groundwater. At Juventino Rosas municipality, also in Guanajuato state, hydrogeological and geothermal factors indicated that rhyolite units are the most probable source of As and F [31]. At Los Altos de Jalisco, western Mexico, mean As concentration in drinking water varied from 14.7 μg/L to 262.9 μg/L, reaching this value in the city of Mexticacán [32]. Figure 2 represents the oxidation of minerals with As in a Mexican mining zone.

High As concentrations have been detected mainly in Mexican aquifers, many of them corresponding to drinking water sources. However, As-enriched surface and groundwaters are also used for irrigation, and the element has been found in some crops. Arsenic is mainly related to natural sources, although, in mining areas, it is also originated from anthropic activities.

Figure 2. Oxidation of minerals with As in a Mexican mining zone.

Nicaragua.- Geogenic sources contaminated drinking water, from 10 to 122 μg/L As, in the southwestern part of the Sébaco valley. At El Zapote, arsenicosis was detected in people who had been consuming water from a polluted well (1,320 μg/L As) for two years; this well was closed in 1996. A study developed in 2004 showed that the northern zone of the country presented the highest As contents. At San Juan de Limay, presence of geogenic As was identified in 2005 [9,10,33,34]. The importance of As detection and analysis is shown by the closure of the polluted well at El Zapote, which stopped the exposure of the population to this highly contaminated water.

Peru.- The presence of As has been determined at several sites in Peru, mainly in the Andean region, released by weathering and mining operations. The Locumba river and its tributaries contain up to 1,680 μg/L. In the area of the Yucamane volcano, volcanic rocks and pyroclastic materials release As to the Collazas and Salado rivers. In the area of Puno, Andean highlands, As concentrations ranged from 140 to 230 μg/L in the river water. The Rimac river basin has been contaminated by mining activities, leaching of volcanic rocks and ore deposits with up to 1,630 μg/L As that were

measured in the year 2000 at Puente Santa Rosa [9]. In Peru, as observed in other countries, mineralization and mining activities are significant As sources.

Uruguay.- In the Raigón aquifer, in the southwestern part of the country, As concentrations ranged from 25 to 50 µg/L, and were related to continental sediments containing volcanic ash [9,10,35]. The importance of a multidisciplinary approach to determine As in health and in the environment of Uruguay was highlighted [36]. More studies are needed to have a complete overview of As occurrence, sources and possible health impact in Uruguay. However, the concentrations measured so far are lower than those determined in other countries like Argentina and Mexico.

3. Analytical methods for the analysis of arsenic in Latin America

The chemical behavior of As depends on environmental conditions such as acidity, oxidation-reduction state of the element, presence of iron, organic matter or other chemical species (e.g., sulfur), etc. Due to the low concentrations at which As may be present in an environment and the chemical behavior of As species, the selection of an adequate analytical technique for As determination will depend on the objectives of the study, the access to the appropriate analytical methodology, the cost of the analyses, and the water matrix. For these reasons, researchers seek analytical techniques with a high degree of precision and accuracy, as well as high sensitivity, which allow measuring concentrations up to the µg/L level.

A recent work compiles the information from 167 scientific manuscripts identified in the last 18 years, most of them focused on the work done in LA countries [10].

The most widely analytical technique used for As determination is atomic absorption spectrometry (AAS), specifically with the method of sample introduction through hydride generation (HG-AAS) [10]. The detection limit using HG-AAS is about 0.1 - 0.6 µg/L [11]. This technique presents important advantages, such as improved sensitivity and selectivity, and sample salinity does not affect analytical results [11]. Additionally, the HG-AAS technique is a simple methodology that requires relatively inexpensive and very versatile instrumentation, with excellent detection power for total and inorganic As [37]. From 167 identified papers in the last 18 years, 57% of them (95 papers) referred to the use of AAS as the most used analytical technique in LA for As determination. Another 40% of these documents are written by researchers from Mexico, 19% from Argentina and 16% from Brazil. Other countries that report scientific articles on the quantification of AAS by AAS are Cuba, Ecuador, Peru and Venezuela (the four countries represent 1%), Uruguay (2%) and Chile (4%).

The second most used analytical technique (i.e. 26% of the aforementioned 167 papers), is inductively coupled plasma spectrometry (ICP), mainly coupled with mass spectrometry ICP-MS [10]. From them, 30% of publications are from Mexico, 18% from Brazil and 16% from Argentina, while Chile and Bolivia report only 4%. The detection limit reached by this technique is 0.1 µg/L, and there is no need of sample preconcentration [11]. In general, ICP-MS and inductively coupled plasma optical emission spectrometry (ICP-OES) are robust and sensitive techniques, but they require very expensive equipment, special facilities and a long and complex training of analysts [37].

Electrochemical analytical techniques are the third most used methodology for As determination [10]. The anodic voltammetry technique has high analytical sensitivity and low cost, and it is easy to use within a concentration interval between 0.1 and 300 µg/L [37]. Argentina, Brazil, Chile, Ecuador and Venezuela reported the use of electrochemical techniques for the determination of As mainly in water and food samples [10].

The fourth most used technique for As determination is UV-VIS molecular spectrometry [10]. The methods based on this analytical technique are simple and economical; however, although sensitivity is high (10 to 50 µg/L), accuracy is low [11]. Mexico and Cuba are the main countries that reported the use of this technique for As determination in samples of water and mine tailings [10].

Figure 3 shows the schematic representation of the four main analytical techniques for As determination according to Gürkan et al. [38].

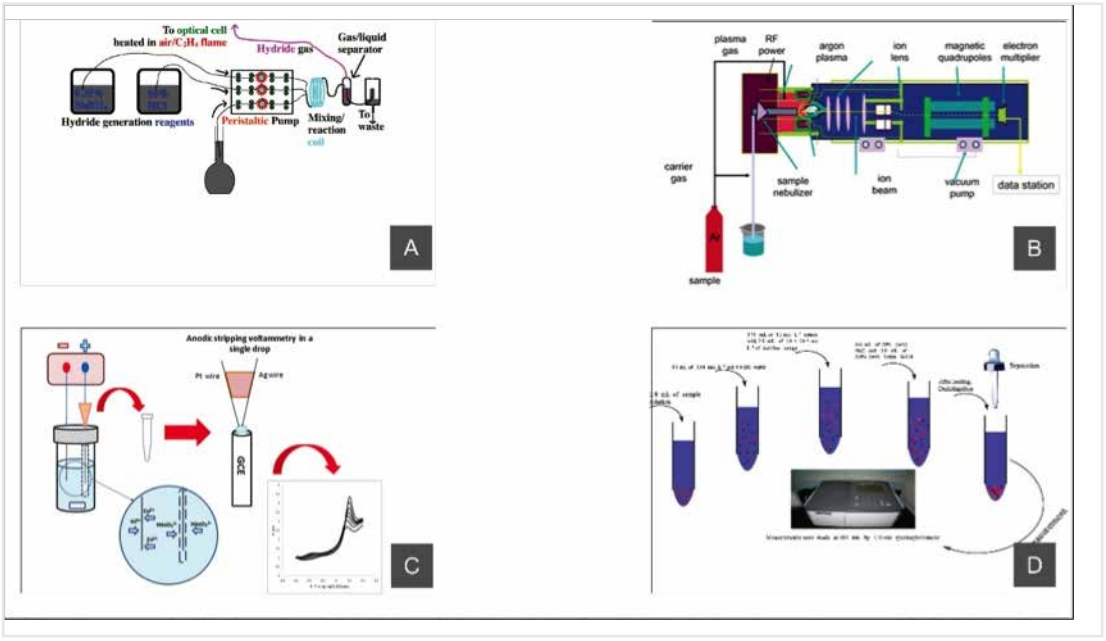

Figure 3. Schematic representation of the four main analytical techniques for As determination: A) HG-AAS, B) ICP-MS, C) Anodic voltammetry, D) UV-Vis spectrometry (Gürkan et al., 2015 [38], with permission).

The two most widely used techniques for As speciation are AAS and ICP combined with separation techniques (chromatography), and have been used together or coupled with other analytical techniques (hyphenated techniques) [10]. These coupled techniques are the best option for the determination of arsenical species because of their selectivity, adequate precision, high level of automation and relatively short response times [37]. X-ray fluorescence spectrometry is mainly used for the identification and determination of As in solid samples [10]. In quartziferous sands, the limit of detection reaches 40 mg/kg (without interferences). Portable equipment can detect up to 60 mg/kg [11]. The future of this technique, with reference to As determination in waters at the trace level, will be focused mainly through the development of preconcentration methodologies adaptable to laboratory equipment and to on-site determination [11].

Other techniques are neutron activation analysis (NAA) and Surface Plasmon Resonance Nanosensor (SPRN) [10]. NAA is an accurate and sensitive methodology; it has been used for the determination of total As in biological samples (nail, hair and other tissues) with a limit of detection of 0.001 μg/g [11]. SPRN is an autonomous sensor for mapping and monitoring As concentrations in water [39]. This system can be integrated to a portable suitcase, it is inexpensive, and can measure As concentrations below 5 μg/L [39]. However, there are still no results on the application of this method. The ARSOlux Biosensor has been tested in Argentina [40].

4. Effect of arsenic exposure on human health in Latin America

The consumption of water with high As concentrations for a prolonged period has been associated with a variety of health problems including issues related to skin, lungs, bladder, and kidneys, as well as neurological disease, cardiovascular disease, perinatal conditions and other benign diseases [10,41-46]. In Argentina, since the beginning of the 20th century, the set of symptoms and signs (clinical manifestations) associated with the consumption of water or food contaminated with As was denominated chronic endemic regional hydroarsenicism (HACRE, from the Spanish acronym, *Hidroarsenicismo Crónico Regional Endémico*), term that nowadays is being used by many local and regional authors [4,7,46-49].

Arsenic has been classified as a human carcinogen, and inorganic As (iAs) has been related to the development of skin, lung, liver, kidney, bladder and prostate cancer [50]. Prolonged As ingestion from water or food produces characteristic skin lesions such as melanosis, leukomelanosis, and keratosis. Other pathologies include diabetes mellitus, peripheral vascular disease, cardiovascular and respiratory diseases, and a wide variety of clinical manifestations including neurological effects, anemia, leukopenia, liver dysfunction, and high blood pressure.

To date, most research has examined cancer incidence after exposure to high As concentrations. However, numerous studies have reported various health effects caused by chronic exposure to low concentrations of As [11,46]. More systematic studies are needed to determine the link between As exposure and its related cancer and non-cancer end points [51].

It is known that human biotransformation of iAs generates metabolites of various levels of toxicity (Figure 4), and this is one of the factors that determines the nature and magnitude of its harmful effects. Trivalent species (arsenite (As(III)), monomethylarsonous acid (MMA(III)) and dimethylarsinious acid (DMA(III)) showed to be more toxic than pentavalent species (arsenate (As(V)), monomethylarsonic acid (MMA(V)) and dimethylarsinic acid (DMA(V)), due to their ability to bind to more than two hundred enzymes [52]. MMA(III) is, among all As metabolites, the most toxic metabolic intermediate, while DMA(V) is the least toxic species [53]. However, the quantification of As metabolic intermediates in human biological fluids, based on As oxidation state, is not feasible in many cases due to the lability of trivalent intermediates, which are rapidly oxidized to pentavalent forms. Therefore, the urinary metabolic profile of As is usually considered as the proportions of arsenite, arsenate, monomethylated arsenic (MMA(III) + MMA(V)) and dimethylated arsenic (DMA(III) + DMA(V)). Based on the toxicity of the metabolic intermediates, a protective metabolism of As is the one that shows elevated urinary DMA percentage, and low MMA, As(III) and As(V) percentages. On the contrary, an unfavorable metabolism will be the one that shows an elevated MMA percentage at the expense of a low DMA percentage. There is a wide variability in the relative proportions of urinary iAs metabolites between individuals. Percentages of the major three As species can vary from 5 to 25% for iAs (As(III) + As(V)), 10 to 30% for monomethylated metabolites (MMA(III) + MMA(V)), and 50 to 85% for dimethylated metabolites (DMA(III) + DMA(V)) [54,55]. Genetic factors (presence of polymorphism in genes linked to the metabolism of As) and non-genetic factors (age, gender, nutritional status, social habits, among others) have been studied in relation to their influence on As biotransformation processes and, consequently, on its toxicity [55]. Then, the analysis of the urinary metabolic profile will help predicting individual risk to develop As toxic effects.

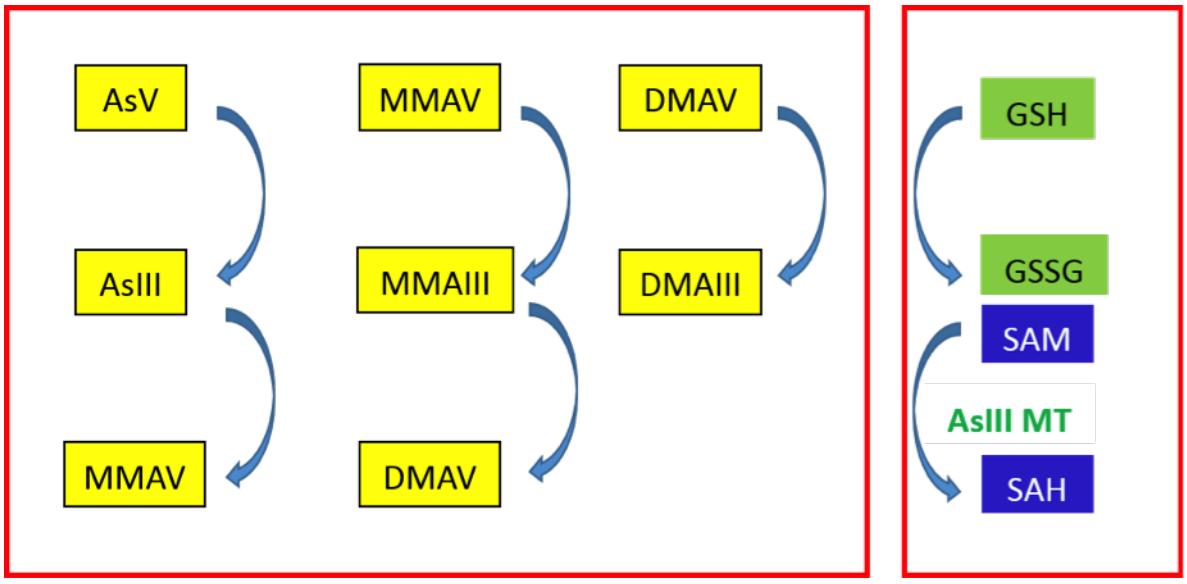

Figure 4. Simplified schematic representation of arsenic biotransformation (2). AsIII: arsenite; AsV: arsenate; AsIII MT: arsenite methyltransferase; DMAIII: dimethylarsinious acid; DMAV: dimethylarsinic acid; GSH: reduced glutathione; GSSG: oxidized glutathione; MMAIII: monomethylarsonous acid; MMAV: monomethylarsonic acid; SAH: S-adenosylhomocysteine; SAM: S-adenosylmethionine.

Even though the presence of As in drinking water has been described in practically all LA countries, studies relating As exposure to health effects are limited to a few ones. Chile, Mexico and Argentina are the countries where most studies on health effects originated from As exposure have been performed. Lung cancer is the most studied adverse effect of As exposure, followed by skin lesions, bladder cancer, effects of early exposure to As, skin cancer, immunotoxicity, kidney cancer, cardiovascular disease and other cancers (liver, prostate, larynx). Sufficient evidence of the association between As exposure and skin, lung and bladder cancers has been reported in Argentina, Chile and Mexico. Studies conducted in Argentina and Chile revealed a clear trend in lung cancer standardized mortality rates and odds ratios with increasing As concentration in drinking water ranging from less than 10 µg/L to a 65-year average concentration of 200-400 µg/L

[56,57]. Development of bladder cancer was related to As concentrations of more than 100 µg/L, and odds ratios increased significantly with the level of exposure [58,59].

The health effects resulting only from the early exposure to As are difficult to evaluate, since much of the population continues to be exposed until adult life, that is, they do not interrupt their exposure. In that way, the region of Antofagasta, in the north of Chile, has presented a unique pattern of human exposure to As through drinking water. Between 1958 and 1970, As concentration in water was above 800 µg/L. In 1970, with the installation of a treatment plant, As concentration in water decreased to values close to 10 µg/L. The population born in that area in the period between 1958 and 1970 presents the characteristics of having been early exposed to As. A steep increase in adult mortality due to lung, bladder cancer and kidney cancer was observed in the Chilean population, probably due to in utero and early life exposure to As [60,61].

Evidence of association between As exposure and kidney and liver cancer mortality rates was also reported in Chile and Argentina [46,56,62]. For other types of cancers (prostate, leukemia, brain, colon, breast, larynx, stomach, cervix and endometrium), the evidence in LA countries is scarce or absent [63-64,65]. While the carcinogenicity of As has been confirmed for specific cancers, the mechanisms behind the disease are still not well understood. Several mechanisms have been implicated in the development of As-associated cancers, including the generation of reactive oxygen species (ROS), the inhibition of DNA repair process, alterations in cellular signal transduction and alterations in DNA methylation. No single mechanism has emerged as a key event, and it is likely that iAs exerts carcinogenic effects through multiple mechanisms [61].

According to several studies, conducted mainly in Mexico, an association between As exposure and diabetes seems to occur. However, more studies are needed, specially focusing on the potential mechanisms of As-induced diabetes in humans. Metabolomic studies seem to be a way to discover the biochemical pathways that relate As exposure to diabetes [66]. The available information on the association of exposure to As and cardiovascular disease, liver dysfunction and chronic kidney disease covered a wide range of levels of exposure [67-68,69,70]. However, this information is scarce and inconclusive.

There is no curative treatment for arsenicosis and its clinical manifestations. However, national guidelines for the treatment have been published by the Ministries of Health of Argentina [71], Chile [72] and Peru [73]. In all cases, first-line actions should be focused on avoiding exposure by means of providing alternative sources of safe water. In Chile, the therapeutic decisions are based on urinary As levels [72] and the presence of symptoms. Indications include education, nutritional assessment, urinary As monitoring, antioxidant intake and referral to a specialist, if applicable. In Argentina, the national guidelines recommend avoiding exposure and symptomatic support treatment consisting of healthy protein foods diet [71]. In addition, the guideline indicates that specific symptoms should receive the corresponding treatment measures, as follows: stop smoking in case of chronic bronchitis, topical keratolytics for keratosis, and surgical exeresis for skin tumors [71].

Nevertheless, there are studies that investigate the influence of nutrients on As metabolism, which could, in turn, influence As toxicity. Studies conducted in Mexico and Uruguay investigated whether the differences in dietary intake of selected micronutrients and foods are associated with the metabolism of iAs. The daily intake of methionine, choline, folate, vitamin B12, vitamin C, Fe, Zn, Se and Na was significantly associated with the reduction of % iAs, and/or % DMA increase in one study conducted in Mexico [74]. Higher meat and folate consumption, a diet rich in green leafy and red-orange vegetables and eggs contributed to a higher methylation capacity according to the study conducted in Uruguayan children [75].

In conclusion, in LA, research focusing on curative options for chronic As exposure is beginning and it is aligned to the latest international research.

5. Regulations

The World Health Organization (WHO) and different environmental agencies such as the United States Environmental Protection Agency and the European Environment Agency, recommend a value of no more than 0.01 mg/L of As in drinking waters. This value has been adopted in most of the LA countries. In Table 1, the different regulations are displayed, with the concentration limits and the corresponding normative.

Country	Value (µg/L)	Normative	Reference
Argentina	10 (Still under discussion)	CAA (Argentine Food Code)	[76]
Bolivia	10	NB 512	[77]
Brazil	10	Regulation 2914	[78]
Chile	10 (a period of 10 years set to reach this value)	NCh409/1	[79]
Costa Rica	10	CAPRE normative, Min. Salud	[80,81]
Colombia	10	Resolución 2115	[82]
Ecuador	10	Instituto Ecuatoriano de Normalización	[83]
Guatemala	10	COGUANORNGO 29.001, CAPRE normative	[80,84]
Mexico	25	NOM-127-SSA1-1994 (modif. 2000)	[85]
Nicaragua	10	CAPRE normative, INAA 2001	[80,86]
Peru	10 (not established period to attain this maximum)	Min. Salud	[87]
Uruguay	20	Instituto Uruguayo de Normas Técnicas	[88]
Venezuela	20	Ministerio de sanidad y Asistencia Social	[89]

Table 1. Limits for As in drinking water in different LA countries

Honduras, El Salvador, Panama and Dominican Republic also follow the CAPRE normative [80]. Additionally, in LA, the As provisional guideline value established by the WHO (i.e., 10 µg/L) became law in Honduras (1995), El Salvador (1997) and Panama (1999) [9].

6. Arsenic removal technologies employed in Latin America

The most used processes for As removal employed in LA are adsorption, chemical precipitation, activated alumina, use of ion exchange resins, membrane technologies, distillation, and coagulation/filtration, which can be used alone or in combination. Use of geoadsorbents, natural materials, iron-based technologies, and solar applications can be also mentioned, especially at small scale or for households. Due to the amount of references on the subject and the multiple materials that can be used, only some references will be included here; the reader can consult references [9-10,11,21,46,90-111] and others therein.

For large and medium plants, coagulation/adsorption/filtration processes have been widely used in LA, with examples in Argentina (Santa Fe and Salta) since the 1990's. One of the most important ones is the patented ArCIS-UNR® process, developed at the *Centro de Ingeniería Sanitaria-Universidad Nacional de Rosario*, which uses polyaluminum chloride (PAC); it has been applied to real scale in populations up to 10,000 inhabitants. An optimized coagulation/filtration technology has also been developed by the *Instituto Nacional de Tecnología Industrial of Argentina* (INTI) and applied to groundwaters of Taco Pozo (Chaco) and Lobos (Buenos Aires) [10,11,46]. In northern Chile, a coagulation technology using $FeCl_3$ has been used since 1970 for plants in small and medium cities with centralized water supply [10,91]. In Guatemala, a full-scale treatment plant composed of a coagulation-filtration system with $FeCl_3$ was installed in Mixco (close to the capital city) in 2008 [10]. In 1999, the *Instituto Mexicano de Tecnología del Agua* (IMTA) adopted a coagulation-flocculation process using $Al_2(SO_4)_3$ as coagulant and other materials (zeolites, clays, bone carbon) as coadjuvants, which was tested in natural waters of Zimapán [10]. In Peru, a treatment plant in the city of Ilo was built in

1982; initially massive doses of 90% lime (CaO) were used, but the system was improved by the use of ferric chloride, ferric hydroxide plus sulfuric acid or $Mg(OH)_2$ together with commercial and natural flocculants [10]. In Brazil, a process with PAC and aluminum sulfate with a chlorine preoxidation step has been described [10].

The use of membranes (mainly reverse osmosis processes, RO) is another largely employed alternative for As treatment in large-medium plants [10,46,90,96,97]. Several RO plants have been installed in Argentina (Santa Fe, Cordoba, and La Pampa). The most important ones are those installed in the southern periphery of Buenos Aires City by state-owned company AySA (*Aguas y Saneamientos Argentinos*), benefiting more than 400,000 inhabitants [10,11,46,49].In northern Chile, desalinization of sea water is a valid option for coastal cities, and RO desalination plants have been installed in Antofagasta and Arica, especially for mining zones [10,46]. In Chihuahua, Mexico, more than 280 small RO plants have been implemented in rural communities; ultrafiltration membranes were also used [10,46]. In 2007, a desalination plant with a capacity of 21,000 m^3/day was installed in Los Cabos, Mexico [46].

On the other hand, in several places of LA, e.g. the Chaco-Pampean plain of Argentina, about 12% of the population is living in dispersed settlements consisting of less than 50 inhabitants, mostly the poorest members of the regional population. In these places, As is frequently found at high concentrations in water for human consumption. To solve the problem, a large number of commercial adsorbents or natural materials have been tested in different countries [10,11,46,90,96,97]. Most of them are materials containing iron or aluminum, but other constituents are also found in them. Aluminum hydrogels, Fe-rich laterites, commercial granular ferric oxide (GFO), granular ferric hydroxides/oxides (GFH/GFO), hematite, goethite (α-FeO(OH)), magnetic δ-FeOOH nanoparticles, hydrated Fe(III) oxide (HFO) nanoparticles supported on polymers, iron oxide coated sand, composite iron matrices, Fe(III)-coated silica sand, metallurgical slags, lime, aluminum sulfate, activated alumina, diatomites, natural clays, bentonites, zeolites, zerovalent iron (ZVI) in the form of μFe(0) microparticles, Fe fillings, iron wool, nails or packing wire, iron nanoparticles (nZVI)), Fe-Cu bimetallic nanomaterials, manganese greensand, sand-anthracite, manganese oxides, carbon activated with copper sulfate, pisolite, volcanic stones, steel wastes, basic oxygen furnace sludge, ArsenXnp (a commercial As sorbent), etc. can be mentioned, among others [10,11,46]. A mixture of an oxidant, activated clays and a coagulant (aluminum sulfate or ferric chloride), patented as ALUFLOC, was developed by CEPIS/SDE/OPS and evaluated at household scale in Puno (Peru), Salta and Tucumán (Argentina) [10,90,96,97,109].

Biomaterials and low-cost organic materials, such as natural hydroxyapatite obtained from charred cow bones, milled bones, bone char modified with nZVI, nacre, shells, chitosan, chitosan beads impregnated with nZVI, dead aquatic macrophytes, dried macroalgae, totora (*Schoenoplectus californicus*), paja brava (*Festuca orthophylla*), cellulose, sedges, sorghum biomass, waste biomass, iron-enriched activated carbon from lignite, maracuya shell (some modified with Fe(III)), a bioadsorbent taken from passion fruit, a bioadsorbent obtained from orange albedo coated with Fe(III), etc., were also tested [10]. Bacteria like *Pseudomonas aeruginosa*, *Microcystis novacekii* and sulfate reducing bacteria (SRB) were reported to be used for As removal. Phytoremediation with aquatic macrophytes such as water hyacinth (*Eichhornia crassipes*), lesser duckweed (*Lemna minor*) and valdivia duckweed (*Lemna valdiviana*) were also assayed [10,90].

Another cost-effective, environmental-friendly treatment technology for As removal is the use of horizontal subsurface flow constructed wetlands (SSFCW). In Chile, SSFCW constructed with zeolite, limestone and cocopeat; in Mexico, SSFCW containing an iron oxide substrate (tezontle) with two plant species (*Zantedeschia aethiopica* and *Anemopsis californica*) and without them were evaluated. Two Cyperaceae species, *Schonoeplectous americanus* and *Eleocharis macrostachya* were also studied in a SSFCW prototype system [10,90]. Other studies optimized As removal by capacitive deionization [93,96] and in-line electrochlorination to produce hypochlorous acid for oxidation and coprecipitation of As and Fe [112].

Mining effluents containing As have been especially considered in LA. In Brazil, several works reported As precipitation with trivalent iron salts and lime (CaO or $Ca(OH)_2$), and with Al-Fe (hydr)oxides, scorodite ($FeAsO_4 \cdot 2H_2O$) formation from industrial solutions, and $Mn_3(AsO_4)_2.4H_2O$ formation from nanosized birnessite (Mn(IV)). Coprecipitation by the use of selective coagulants/flocculants has been also studied to be applied in gold mining and other effluents [10,46,90]. In Chile, a plant for the treatment of mining effluents for dusts from copper smelters in the Chuquicamata and Ministro Hales minesand was constructed, stabilizing As as scorodite with ferric sulfate [46]. Byproducts of the iron mining industry, such as magnetite, hematite, iron hydroxides and/or foundry slag, have been also used to remove As [46]. Desalination plants applying RO processes have been used in Chile for the treatment of mining wastewaters [46].

Photochemical technologies were also important methods for As removal in LA. Photooxidation of As(III) with germicidal lamps (λ = 253.7 nm) and H_2O_2 addition, a combined technology employing UV/H_2O_2 and adsorption in columns filled with TiO_2 and GFH, and use of ZVI and nZVI plus solar irradiation have been tested [10,46,90]. The Solar Oxidation and Removal of As (SORAS) technology, a very simple process for poor, isolated populations, used with partial success in Bangladesh and India, was modified and tested in LA. This method consists in putting water in transparent

PET bottles and irradiating it with sunlight. This is done in the presence of small amounts of dissolved iron, causing the precipitation of iron(III) (hydr)oxides, As(III) oxidation and As(V) adsorption; clear water is obtained by further decantation or filtration (Figure 5). The addition of small amounts of citric acid – as drops of lemon juice – enhances the effectiveness of As removal due to the coupling of photo-Fenton processes. Because groundwaters in most regions of LA do not have enough iron to make the SORAS technology efficient, iron has to be externally added through some natural Fe-containing minerals or ZVI in different forms (iron wool, packing wire or nZVI). The method has been tested in laboratory waters and natural well waters of Argentina, Bolivia, Chile, Costa Rica, Mexico and Peru [10,46,90].

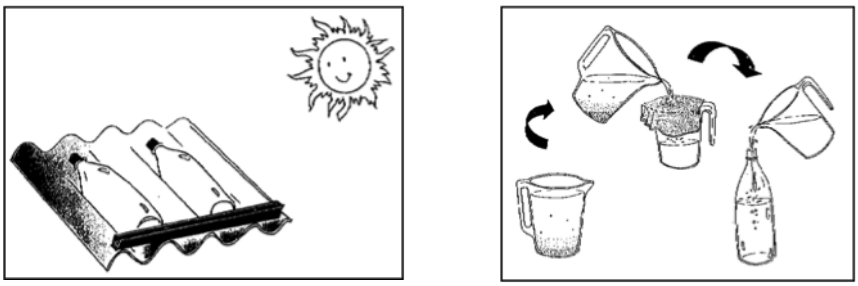

Figure 5. Schematic representation of the SORAS technology.

TiO_2 heterogeneous photocatalysis is also a promising emergent technology which allows the simultaneous oxidation of As(III) and removal of organic pollutants, toxic metals and microbiological contamination. An iron source should be added to retain As on a solid surface. PET plastic bottles have been impregnated with TiO_2 and used to remove As in Argentina and Brazil. Reduction of As(V) and As(III) over TiO_2 under UV light has been also attained in deoxygenated suspensions, with identification of As(0) and arsine (AsH_3) [10-1112,46,90,95,96,110].

A paper regarding toxicity of As(V) solutions has been also evaluated after treatment with nZVI with the AMPHITOX bioassay [113].

7. Conclusions

The contamination of surface and groundwaters with As in LA is a relevant problem for the region due to its dramatic consequences on health. Arsenic presence has been identified in many LA countries in a range of concentrations and originated from various sources, although in most of the locations it comes from natural sources. The Chaco-Pampean plain in Argentina is the largest area affected by groundwater As contamination. Research on the chemical and hydrogeological processes of As release and mobilization has been also developed in Mexico, Chile, Bolivia, Peru and Nicaragua. In most of the contaminated areas, As originates from geogenic sources, mainly volcanic rocks, hydrothermal fluids and As-bearing minerals. However, anthropogenic sources are also present in certain zones, most of them as a result of mining operations and, in some cases, related to agriculture. Mining is indeed the main As source in Brazil. It has been found that the element is in the As(V) form in most locations.

Regarding analytical methods on As determination, 167 papers in scientific journals have been identified in the last 18 years in LA. The most widely used analytical methodologies are AAS (57%), specifically HG-AAS, and ICP (27%), mainly coupled with MS. Electrochemical methods have been applied in Chile, Brazil and Argentina. UV-VIS spectrometry has been used mainly in Cuba and Mexico. XRF spectrometry, principally for solid samples, has been used in Mexico, Cuba, Brazil, Argentina, and Chile. Other methodologies are INAA, SPRN and the ARSOlux Biosensor. In LA, good scientific and infrastructure capacity for the analytical determination of As in various matrices is available.

Because the As problem has a great impact on health in LA, and its presence has also been reported in different matrices (food, hair, blood and bones), it is important to emphasize the quality assurance of the reported results. Therefore, it is suggested that a section dedicated to the interferences and the analytical quality control used for the quantification of this metalloid be added to the scientific publications, regardless of the analytical method used. This quality control could include some of the parameters established by ISO / IEC 17025: 2017 for analytical validation (uncertainty, repeatability and reproducibility, robustness), as well as the certified reference materials used.

Concerning effects on health, lung cancer is the most studied adverse effect of As exposure, followed by skin lesions, bladder cancer and the effects of early exposure to As. Chile is the country with the largest number of scientific publications related to the effects of As on health, followed by Mexico and Argentina, where studies on As exposure and cancer development are well described. Evidence of association between As exposure and kidney and liver cancer

mortality rates was also reported in Chile and Argentina. For other types of cancers (prostate, leukemia, brain, colon, breast, larynx, stomach, cervix and endometrium), the evidence is scarce or absent. While the carcinogenicity of As has been confirmed for several cancers, the mechanisms behind the disease are still not well understood, and, therefore, more well-designed studies are needed in that area. According to several studies, conducted mainly in Mexico, an association between As exposure and diabetes seems to occur; however, more studies should be conducted. In that way, metabolomic studies could help find some answers. The information available on the association of exposure to As and cardiovascular disease, liver dysfunction and chronic kidney disease covered a wide range of levels of exposure, but this information is still partial, scarce and inconclusive.

Investigations on As health effects are limited to Argentina, Chile and Mexico and, even in these countries, studies are scarce, scattered and consider different degrees of exposure, which hinders the comparison or integration into a meta-analysis. In Argentina, an epidemiological study of national scope started in 2019; it includes an analysis of morbidity and mortality due to cancers associated with the exposure to As through water ingestion. This study could be extended to other LA countries.

Arsenic removal from water can proceed through adequate treatments. Methods for large and medium plants have been implemented in several places using the most common technologies (coagulation-precipitation and RO). Other technologies use a very large number of adsorbing materials (natural geological materials, iron oxides and hydroxides, calcite, clays, etc.). Sorption agents coming from plants and animal residues have been tested especially for small communities, disperse settlements or individual households of low economical resources, where simple and economical equipment that can be easily handled and maintained by the population is required. Procedures using zerovalent iron from diverse materials are affordable and easy to operate and maintain, and sunlight may be used to improve their effectiveness. Phytoremediation and wetland construction are also promising technologies.

In addition, the LA experience gives valuable information that could be used to solve the As problem in other regions of the world, especially in countries of Asia where the first option is to find other water sources not contaminated with As. In all cases, water composition and socioeconomic features should be carefully considered for selecting the technology.

Although there are several sustainable solutions developed by local researchers, authorities, industries and international agencies have not practically developed any financial and technical cooperation action for mitigating the As problem in isolated rural and periurban LA populations, and As exposure has not been yet solved due to operation, social, and economic problems. In addition, there are zones still lacking As-free water options. Thus, much R&D work, together with political actions, should be undertaken in the region.

Acknowledgments

This work was supported by Agencia Nacional de Promoción Científica y Tecnológica (ANPCyT) from Argentina under PICT-2015-0208, and by BioCriticalMetals – ERAMIN 2015 grants. We appreciate the support of Olivia Cruz, Alejandra Aguayo, Nora E. Ceniceros Bombela and Blanca X. Felipe Martínez, from the Geophysics Institute at UNAM, who helped with the bibliographic search process.

References

[1] Argos, M., Ahsan, H., Graziano, J.H., 2012. Arsenic and human health: epidemiologic progress and public health implications. Rev Environ Health 27, 191-195.

[2] Lage, C.R., Nayak, A., Kim, C.H., 2006. Arsenic ecotoxicology and innate immunity. Integr Comp Biol 46, 1040-1054.

[3] US Environmental Protection Agency, 2012.Arsenic in Drinking Water.US Environmental Protection Agency, United States.

[4] Litter, M.I., 2010. La problemática del arsénico en la Argentina: el HACRE. Rev Soc Argent Endocrinol Ginecol Reprod (SAEGRE) 17, 5-10.

[5] Murcott, S., 2012. Arsenic Contamination in the World — an International Sourceboo.IWA Publishing, London, UK.

[6] McCarty, K.M., Hanh, H.T., Kim, K.W., 2011.Arsenic geochemistry and human health in South East Asia. Rev Environ Health 26 (1), 71-78.

[7] Bundschuh A, Pérez Carrera M, Litter MI (Eds.), 2008. Distribución del arsénico en la región Ibérica e Iberoamericana. CYTED, ISBN 978-84-96023-61-1.

[8] Figueiredo, B.R., Litter, M.I., Silva, C.R., Mañay, N., Londono, S.C., Rojas, A.M., Garzón, C., Tosiani, T., Di Giulio, G.M., De Capitani, E.M., dos Anjos, J.Â.S.A., Angélica, R.S., Morita, M.C., Paolielo, M.M.B., Cunha, F.G., Sakuma, A.M., Licht, O.A., 2010. Medical geology: a regional synthesis. In: Selinus, O., Finkelman RB, Centeno JA (eds) Medical Geology: A Regional Synthesis. Medical geology studies in South America. Book Series International Year of Planet Earth, Springer Netherlands, pp. 79-106.

[9] Bundschuh, J., Litter, M.I., Parvez, F., Román-Ross, G., Nicolli, H.B., Jean, J.-S., Liu,C.-W., López, D., Armienta, M.A., Gómez Cuevas, A., Cornejo, L., Cumbal, L., Guilherme, L.R.G., Toujaguez, R., 2012. One century of arsenic exposure in Latin America: A review of history and occurrence from 14 countries, Sci. Total Environ. 429, 2-35.

[10] Litter M.I., Armienta M.A., Villanueva Estrada R.E., Villaamil Lepori E., Olmos V., Arsenic in Latin America, Part I, In: Arsenic in Drinking Water and Food, S. Srivastava (Ed.). Springer, pp. 71-112.

[11] Litter, M.I., Botto, L., Difeo, G., Farfán Torres, E.M., Frangie, S., Herkovits, J., Ingallinella, A.M., Olmos, V., Savio, M., Schalamuk, I., Taylor, S., Berardozzi, E., García Einschlag, F.S., Arsénico en agua.Informe final. 2018. Grupo ad hoc arsénico en agua, Red de Seguridad Alimentaria, Consejo Nacional de Investigaciones Científicas y Técnicas. ISSN 2618-2785. DOI: 10.13140/RG.2.2.29582.20800. rsa.conicet.gov.ar/wp-content/uploads/2018/08/Informe-Arsenico-en-agua-RSA.pdf. (Accessed November 2018).

[12] Litter, M.I., Ingallinella, A.M., Olmos, V., Savio, M., Difeo, G., Botto, L., Farfán Torres, E.M., Taylor, S., Frangie, S., Herkovits, J., Schalamuk, I., González, M.J., Berardozzi, E., García Einschlag, F.S., Bhattacharya, P., Ahmad, A., Arsenic in Argentina: technologies for arsenic removal from groundwater sources, investment costs and waste management practices, Sci. Total Environ., 690 (2019), pp. 778–789.

[13] Alonso, D.L., Latorre, S., Castillo, E., Brandão, P.F.B. 2014. Environmental occurrence of arsenic in Colombia: A review, Environ. Pollut. 186:272–281.

[14] Toujague, R., Leonarte, T., Reyes Verdecia, A., Miravet, B.L., Leal, R.M. 2003. Arsénico y metales pesados en aguas del área Delita, Isla de la Juventud, Cuba, Ciencias de la Tierra y el Espacio 4:27–33.

[15] Cumbal, L.H., Bundschuh, J., Aguirre, V., Murgueitio, E., Tipán, I., Chávez, C. 2009. The origin of arsenic in sediments from Papallacta lake area in Ecuador. In: Bundschuh, J., Armienta, M.A., Birkle, P., Bhattacharya, P., Matschullat, J., Mukherjee, A.B. (eds) Natural arsenic in groundwaters of Latin America, CRC Press, London, pp. 81–90.

[16] López, D.L., Bundschuh, J., Birkle, P., Armienta, M.A., Cumbal, L., Sracek, O., Cornejo, L., Ormachea, M. 2012. Arsenic in volcanic geothermal fluids of Latin America, Sci. Total Environ. 429:57–75.

[17] López, D.L., Ribó, A., Quinteros, E., Mejía, R., López, A., Orantes, C. 2014. Arsenic in soils, sediments, and water in area with high prevalence of chronic kidney disease of unknown etiology. In: Litter, M.I., Nicolli, H.B., Meichtry, J.M., Quici, N., Bundschuh, J., Bhattacharya, P., Naidu, R. (eds) One Century of the Discovery of Arsenicosis in Latin America (1914-2014), CRC Press, London, pp. 251–254.

[18] Garrido Hoyos, S.E., Avilés Flores, M., Rivera Huerta, M.L., Nájera Flores, M.C. 2007. Diagnóstico de la presencia de arsénico en agua de pozo, Mixco, Guatemala. Final report TC-0711.3. Jiutepec, Mexico: Instituto Mexicano de Tecnología del Agua.

[19] Cebrián, M.E., Albores, A., García-Vergas, G., Del Razo, L.M. 1994. Chronic arsenic poisoning in humans: The case of Mexico. In: Nriagu, J.O. (ed.) Arsenic in the environment Part II Wiley, New York, pp. 93–107.

[20] Armienta, M.A., Segovia, N. 2008. Arsenic and fluoride in the groundwater of Mexico, Environ.Geochem. Health 30:345-353.

[21] Alarcón-Herrera, M.T., Bundschuh, J., Nath, B., Nicolli, H.B., Gutierrez, M., Reyes-Gomez, V.M., Nunez, D., Martín-Dominguez, I.R., Sracek, O., 2013. Co-occurrence of arsenic and fluoride in groundwater of semi-arid regions in Latin America: Genesis, mobility and remediation, J. Hazard. Mater. 262:960–969.

[22] Birkle, P., Bundschuh, J., Sracek, O. 2010, Mechanisms of arsenic enrichment in geothermal and petroleum reservoirs fluids in Mexico, Water Res. 44:5605–5617.

[23] Boochs, P.W., Billib, M., Gutiérrez, C., Aparicio, J. 2014, Groundwater contamination with arsenic, RegiónLagunera, México. In: Litter, M.I., Nicolli ,H.B., Meichtry, J.M., Quici, N., Bundschuh, J., Bhattacharya, P., Naidu, R. (eds) One Century of the Discovery of Arsenicosis in Latin America (1914-2014), CRC Press, London, pp. 132–134.

[24] Ortega-Guerrero, A. 2017. Evaporative concentration of arsenic in groundwater: health and environmental implications, La Laguna Region, Mexico, Environ. Geochem. Health 39:987-1003.

[25] Espino-Valdés, M.S., Barrera-Prieto, Y., Herrera-Peraza, E. 2009. Arsenic presence in North section of Meoqui–Delicias aquifer of State of Chihuahua, Mexico, Tecnociencia Chihuahua 3: 8–17.

[26] Reyes-Gómez, V., Alarcón, M., Gutiérrez, M., Nuñez, D. 2013. Fluoride and Arsenic in an Alluvial Aquifer System in Chihuahua, Mexico: Contaminant Levels, Potential Sources, and Co-occurrence, Water Air Soil Pollut. 224:1433–1448.

[27] Mar Camacho, M. L., Gutierrez, M., Alarcon-Herrera, M.T., Villalba, M.L., Deng, S. 2011. Occurrence and treatment of arsenic in groundwater and soil in northern Mexico and southwestern USA, Chemosphere 83:2011–225.

[28] Armienta, M.A., Villaseñor, G., Rodriguez, R., Ongley, L.K., Mango, H. 2001. The role of arsenic-bearing rocks in groundwater pollution at Zimapán Valley, México, Environ.Geol. 40:571–581.

[29] Sracek, O., Armienta, M.A., Rodríguez, R., Villaseñor, G. 2010. Discrimination between diffuse and point sources of arsenic at Zimapán, Hidalgo state, Mexico, J. Environ. Monit. 12:329–337.

[30] Ortega-Guerrero, A., 2009. Presencia, distribución, hidrogeoquímica y origen de arsénico, fluoruro y otros elementos traza disueltos en agua subterránea, a escala de cuenca hidrológica tributaria de Lerma-Chapala, México, Rev. Mex. Cienc. Geol. 26:143–161.

[31] Morales-Arredondo, I., Rodríguez, R., Armienta, M.A., Villanueva-Estrada, R.E. 2016. The origin of groundwater arsenic and fluorine in a volcanic sedimentary basin in central Mexico: a hydrochemistry hypothesis, Hydrogeol. J. 24:1029–1044.

[32] Hurtado-Jiménez, R., Gardea-Torresdey, J.L. 2006. Contamination of drinking water supply with geothermal arsenic in Los Altos de Jalisco, Mexico, pp. 179–190. In: Bundschuh, J., Armienta, M.A., Birkle, P., Bhattacharya, P., Matschullat, J., Mukherjee, A.B. (eds) Natural arsenic in groundwaters of Latin America, CRC Press, London, pp. 179–190.

[33] Altamirano Espinoza, M., Bundschuh, J. 2009. Natural arsenic groundwater contamination of the sedimentary aquifers of southwestern Sébaco valley, Nicaragua, Bundschuh, J., Armienta, M.A., Birkle, P., Bhattacharya, P., Matschullat, J., Mukherjee, A.B. (eds) Natural arsenic in groundwaters of Latin America, CRC Press, London, pp. 109–122.

[34] Armienta, M.A., Rodríguez, R., Segovia, N., Monteil, M. 2010. Medical Geology in Mexico, Central America and the Caribbean. In: Selinus, O., Finkelman, R.B., Centeno, J.A. (eds) Medical geology a Regional Synthesis, Springer, N.Y. pp. 59–78.

[35] Guérèquiz, R., Mañay, N., Goso-Aguilar, C., Fernández-Turiel, J.L., García-Valles, M. 2009. Environmental risk assessment of arsenic in the Raigon aquifer. Uruguay. Biologist (Lima) 7. Special issue. C0130.

[36] Mañay, N., Pistón, M., Goso, C. 2014. Arsenic environmental and health issues in Uruguay: A multidisciplinary approach. In: Litter, M.I., Nicolli, H.B., Meichtry, J.M., Quici, N., Bundschuh, J., Bhattacharya, P., Naidu, R. (eds) One Century of the Discovery of Arsenicosis in Latin America (1914-2014), CRC Press, London, pp. 485–487.

[37] Litter, M.I.; Armienta, M.A.; Farías, S.S. (Ed.). 2009. Iberoarsen. Metodologías analíticas para la determinación y especiación de arsénico en aguas y suelos, Editorial Programa Iberoamericano de Ciencia y Tecnología para el Desarrollo, CYTED.

[38] Gürkan, R., Kir, U., Altunay, N. 2015. Development of a simple, sensitive and inexpensive ion-pairing cloud point extraction approach for the determination of trace inorganic arsenic species in spring water, beverage and rice samples by UV-Vis Spectrophotometry. Food Chemistry. 180: 32-41.

[39] Salinas, S., Mosquera, N., Yate, L., Coy, E., Yamhure, G., González, E., 2014. Surface plasmon resonance nanosensor for the detection of arsenic in water. Sensors and Transducers. 183 (12): 97-102.

[40] K. Siegfried, S. Hahn-Tomer, A. Koelsch, E. Osterwalder, J. Mattusch, H.-J. Staerk, J.M. Meichtry, G.E. De Seta, F.D. Reina, C. Panigatti, M.I. Litter, H. Harms, Introducing Simple Detection of Bioavailable Arsenic by Using the ARSOlux Biosensor in Rafaela, Santa Fe Province in Argentina, Int. J. Environ. Res. Public Health 12 (2015) 5465–5482. doi:10.3390/ijerph120x0000x, http://www.mdpi.com/1660-4601/12/5/5465.

[41] Brouwer, O.F., Onkenhout, W., Edelbroek, P.M., de Kom, J.F., de Wolff, F.A., Peters, A.C., 1992.Increased neurotoxicity of arsenic in methylenetetrahydrofolate reductase deficiency. Clin. Neurol.Neurosurg. 94, 307-310.

[42] Chen, C.J., Chen, C.W., Wu, M.M., Kuo, T.L. 1992.Cancer potential in liver, lung, bladder and kidney due to ingested inorganic arsenic in drinking water. Br. J. Cancer 66, 888-892.

[43] Hopenhayn-Rich, C., Biggs, M.L., Fuchs, A., Bergoglio, R., Tello, E.E., Nicolli, H., Smith, A.H., 1996. Bladder cancer mortality associated with arsenic in drinking water in Argentina. Epidemiology 7, 117-124.

[44] Rahman, M., Tondel, M., Ahmad, S.A., Chowdhury, I.A., Faruquee, M.H., Axelson, O., 1999. Hypertension and arsenic exposure in Bangladesh. Hypertension 33, 74-78.

[45] Smith, A.H., Goycolea, M., Haque, R., Biggs, M.L.., 1998. Marked increase in bladder and lung cancer mortality in a region of Northern Chile due to arsenic in drinking water. Am J Epidemiol 147, 660-669.

[46] Litter M.I., Armienta M.A., Villanueva Estrada R.E., Villaamil Lepori E., Olmos V., Arsenic in Latin America, Part I, In: Arsenic in Drinking Water and Food, S. Srivastava (Ed.). Springer, pp. 113-181.

[47] Ayerza, A. Arsenicismo regional endémico (keratodermia y melanodermia combinadas) (continuación). Bol. Acad. Medicina 1917; 2-3:41-55.

[48] Gerstenfeld, S., Jordán, A., Calli, R., Farías, P., Malica, J., Gómez Peña, M.. L., Aguirre, L., Salvatierra, M., Leguizamón, E., Coronel, C., Flores Ivaldi, E., 2012. Determinación de zonas de riesgo al agua arsenical y prevalencia de HACRE en Villa Belgrano, Tucumán, Argentina. Rev. Argent. Salud Pública, 24-29.

[49] Bardach, A.E., Ciapponi, A., Soto, N., Chaparro, M.R., Calderon, M., Briatore, A., Cadoppi, N., Tassara, R., Litter, M.I. 2015.Epidemiology of chronic disease related to arsenic in Argentina: A systematic review. Sci. Total Environ. 538:802–816.

[50] International Agency for Research on Cancer (IARC).2012. Arsenic, metals, fibres, and dusts. Vol 100 C. A review of human carcinogens. IARC Monographs on the Evaluation of Carcinogenic Risks to Humans, World Health Organization. Lyon (France). http://publications.iarc.fr/Book-And-Report-Series/Iarc-Monographs-On-The-Evaluation-Of-Carcinogenic-Risks-To-Humans/Arsenic-Metals-Fibres-And-Dusts-2012. (Accessed April 2018).

[51] Agency for Toxic Substances and Disease Registry (ATSDR). 2013. Course: Arsenic Toxicity. Environmental Health and Medicine Education. https://www.atsdr.cdc.gov/ csem/csem.asp?csem=1&po=1.1. (Accessed October 2018).

[52] Khairul, I., Wang, Q.Q., Jiang, Y.H., Wang, C., Naranmandura, H. 2017.Metabolism, toxicity and anticancer activities of arsenic compounds.Oncotarget. 4;8(14):23905–23926.

[53] Styblo, M., Del Razo, L.M., Vega, L., Germolec, D.R., LeCluyse, E.L., Hamilton, G.A., Reed, W., Wang, C., Cullen, W.R., Thomas, D.J. 2000. Comparative toxicity of trivalent and pentavalent inorganic and methylated arsenicals in rat and human cells. Arch. Toxicol., 74: 289–299.

[54] Bailey, K.A., Wu, M.C., Ward, W.O., Smeester, L., Rager, J.E., García-Vargas, G., Del Razo, L.M., Drobná, Z., Stýblo, M., Fry, R.C. 2013. Arsenic and the epigenome: interindividual differences in arsenic metabolism related to distinct patterns of DNA methylation. J Biochem. Mol. Toxicol. 27:106–115.

[55] Olmos, V., Navoni, J.A., Calcagno, M.L., Sassone, A.H., VillaamilLepori, E.C. 2015. Influence of the level of arsenic exposure on its metabolic profile, in a population from an endemic area of Argentina. Association with the presence of the T860C polymorphism in arsenic 3-Methyl Transferase Gene. Hum. Exp. Toxicol. 34: 170–178.

[56] Hopenhayn-Rich, C., Biggs, M.L., Smith, A.H. 1998.Lung and kidney cancer mortality associated with arsenic in drinking water in Córdoba, Argentina. Int. J. Epidemiol. 27:561–9.

[57] Ferreccio, C., González, C., Milosavjlevic, V., Marshall, G., Sancha, A.M., Smith, A.H. 2000. Lung cancer and arsenic concentrations in drinking water in Chile. Epidemiology 11:673–679.

[58] Smith, A.H., Goycolea, M., Haque, R., Biggs, M.L. 1998.Marked increase in bladder and lung cancer mortality in a region of Northern Chile due to arsenic in drinking water. Am. J. Epidemiol. 147:660–9.

[59] Ferreccio, C., Yuan, Y., Calle, J., Benitez, H., Parra, R.L., Acevedo, J., Smith, A.H., Liaw, J., Steinmaus, C. 2013. Arsenic, Tobacco Smoke, and Occupation Associations of Multiple Agents with Lung and Bladder Cancer. Epidemiology 24:898–905.

[60] Steinmaus, C., Ferreccio, C., Acevedo, J., Yuan, Y., Liaw, J., Durán, V., Cuevas, S., García, J., Meza, R., Valdés, R., Valdés, G., Benítez, H., VanderLinde, V., Villagra, V., Cantor, K.P., Moore, L.E., Perez, S.G., Steinmaus, S., Smith, A.H. 2014. Increased lung and bladder cancer incidence in adults after in utero and early-life arsenic exposure.Cancer Epidemiol. Biomarkers Prev. 23:1529–1538.

[61] Bailey, K.A., Smith, A.H., Tokar, E. J., Graziano, J.H., Kim, K.W., Navasumrit, P., Ruchirawat, M., Thiantanawat, A., Suk, W.A., Fry, R.C. 2016.Mechanisms Underlying Latent Disease Risk Associated with Early-Life Arsenic Exposure: Current Research Trends and Scientific Gaps. Environ. Health.Persp. 124:170–175.

[62] Ferreccio, C., Smith, A.H., Durán, V., Barlaro, T., Benítez, H., Valdés, R., Aguirre, J.J., Moore, L.E., Acevedo, J, Vásquez, M.I., Pérez, L., Yuan, Y., Liaw, J., Cantor, K.P., Steinmaus, C. 2013b. Case-control study of arsenic in drinking water and kidney cancer in uniquely exposed Northern Chile. Am. J. Epidemiol., 178(5):813-8.doi: 10.1093/aje/kwt059.

[63] Liaw, J., Marshall, G., Yuan, Y., Ferreccio, C., Steinmaus, C., Smith. A.H. 2008. Increased childhood liver cancer mortality and arsenic in drinking water in northern Chile. Cancer Epidemiol. Biomarkers Prev. 17:1982–1987.

[64] Molina, R., Schulz, C., Bernardos, J., Dalmaso, M. 2014. Association between arsenic in groundwater and malignant tumors in La Pampa, Argentina. In: Litter, M.I., Nicolli, H.B., Meichtry, J.M., Quici, N., Bundschuh, J., Bhattacharya, P., Naidu, R. (eds) One Century of the Discovery of Arsenicosis in Latin America (1914-2014), CRC Press, London, pp. 644–645.

[65] Aballay, L.R., Díaz, M. del P., Francisca, F.M., Muñoz, S.E. 2012. Cancer incidence and pattern of arsenic concentration in drinking water wells in Córdoba, Argentina. Int. J. Environ. Health Res. 22:220–231.

[66] Martin, E., González-Horta, C., Rager, J., Bailey, K.A., Sánchez-Ramírez, B., Ballinas-Casarrubias, L., Ishida, M.C., Gutiérrez-Torres, D.S., Hernández Cerón. R., Viniegra Morales, D., BaezaTerrazas, F.A., Saunders, R.J., Drobná, Z., Mendez, M.A., Buse, J.B., Loomis, D., Jia, W., García-Vargas, G.G., Del Razo, L.M., Stýblo, M., Fry, R. 2015. Metabolomic characteristics of arsenic-associated diabetes in a prospective cohort in Chihuahua, Mexico. Toxicol. Sci. 144:338–346.

[67] Yuan, Y., Marshall, G., Ferreccio, C., Steinmaus, C., Selvin, S., Liaw, J., Bates, M.N., Smith, A.H. 2007. Acute myocardial infarction mortality in comparison with lung and bladder cancer mortality in arsenic-exposed region II of Chile from 1950 to 2000. Am. J. Epidemiol. 166: 1381–1391.

[68] Osorio-Yáñez, C., Ayllon-Vergara, J.C., Aguilar-Madrid, G., Arreola-Mendoza, L., Hernández-Castellanos, E., Barrera-Hernández, A., De Vizcaya-Ruiz, A., Del Razo, L.M. 2013. Carotid intima-media thickness and plasma asymmetric dimethylarginine in Mexican children exposed to inorganic arsenic. Environ. Health Perspect. 121:1090–6.

[69] Zaldivar, R. 1980. A morbid condition involving cardio- vascular, bronco pulmonary, digestive and neural lesions in children and young infants after dietary arsenic exposure. Zbl. Bakt. I Abt. Orig. B. 170: 44–56.

[70] Robles-Osorio, M.L., Pérez-Maldonado, I.V., del Campo, D.M., Montero-Perea, D., Avilés-Romo, I., Sabath-Silva, E., Sabath, E. 2012. Urinary arsenic levels and risk of renal injury in a cross-sectional study in open population. Rev. Invest. Clin. 64:609–614.

[71] Ministerio de Salud (MSAL). 2011. Hidroarsenicismo crónico regional endémico (HACRE). Módulo de capacitación para atención primaria. Programa Nacional para la Prevención y Control de las Intoxicaciones (PRECOTOX). Ministerio de Salud. http://www.msal.gob.ar/images/stories/bes/graficos/0000000332cnt-03-Capacit_hidroarsenicismo. pdf. (Accessed November 2018).

[72] Ministerio de Salud (MINSAL). Guía Clínica: Vigilancia Biológica de la Población Expuesta a Arsénico, beneficiarios de la ley 20.590. Santiago: MINSAL, 2014. https://www.minsal.cl/sites/default/files/files/Guia_Clinica_Vigilancia_Arsenico_final.pdf. (Accessed November 2018).

[73] Ministerio de Salud (MINSA). 2012. Guía de practica clínica para el diagnóstico y tratamiento de la intoxicación por arsénico, 2012 Perú. http://bvs.minsa.gob.pe/local/MINSA/2109.pdf. (Accessed November 2018).

[74] López-Carrillo, L., Gamboa-Loira, B., Becerra, W., Hernández-Alcaraz, C., Hernández-Ramírez, R.U., Gandolfi, A.J., Franco-Marina, F., Cebrián, M.E. 2016. Dietary micronutrient intake and its relationship with arsenic metabolism in Mexican women. Environ. Res. 151:445–450.

[75] Kordas, K., Queirolo, E.I., Mañay, N., Peregalli, F., Hsiao, P.Y., Lu, Y., Vahter, M. 2016. Low-level arsenic exposure: Nutritional and dietary predictors in first-grade Uruguayan children. Environ Res. 147:16–23.

[76] Código Alimentario Argentino. 2012. Bebidas hídricas, aguas y aguas gasificadas. Capítulo XII. http://www.anmat.gov.ar/alimentos/codigoa/CAPITULO_XII.pdf. (Accessed January 2018).

[77] Instituto Boliviano de Normalización y Calidad A Norma Boliviana NB 512-2010, Agua potable – Requisitos.

[78] Health Brazil. 2011. Standards and drinkability standard of water intended for human consumption. Administrative Rule 2914, Brasília.

[79] NCh 409/1 Instituto nacional de Normalización, INN-Chile. 2005. Drinking Water- Part 1- Requirements.

[80] CAPRE. 1994. Normas de Calidad del Agua para Consumo Humano. Regional committee coordinator of potable water supply institutions and sanitation of Central America, Panamá, and Dominican Republic, San José.

[81] Ministerio de Salud, Costa Rica. 2005. Reglamento para la Calidad del Agua Potable. Pub. L. No. 32327-S.

[82] Ministerio de la Protección Social y Ministerio de Ambiente, Vivienda y Desarrollo Territorial. Resolución 2115. 2007. República de Colombia, Bogotá.

[83] INEN (Instituto Ecuatoriano de Normalización). 2006. Norma 1108: Sobre requisitos del agua potable. Registro Oficial Nº 231, Quito, Ecuador.

[84] Guatemala, Ministerio de Salud Pública y Asistencia Social, Unidad Ejecutora del Programa de Acueductos Rurales. 2001. Norma guatemalteca obligatoria, agua potable (especificaciones), CONGUANOR, NGO, 29.001. Guatemala: UNEPAR.

[85] Modificación a la Norma Oficial Mexicana NOM-127-SSA1-1994. 2000. Salud Ambiental. Agua para uso y consumo humano. Límites permisibles de calidad y tratamientos a los que debe someterse el agua para su potabilización. Diario Oficial de la Federación, 22 noviembre de 2000, Mexico City, Mexico.

[86] INAA. 2001. Normas Técnicas para el diseño de abastecimiento y potabilización de agua. Normas NTON 09003-99.

[87] Ministerio de Salud. Reglamento de la calidad del agua para consumo humano. Lima: Dirección General de Salud Ambiental. 2011. http://www.digesa.minsa.gob.pe/publicaciones/descargas/Reglamento_Calidad_Agua.pdf. (Accessed November 2018).

[88] UNIT 2010, Instituto Uruguayo de Normas Técnicas (UNIT-BID/Fomin) Referencia 833:2008. Agua Potable: Requisitos. http://www.ose.com.uy/descargas/Clientes/Reglamentos/unit_833_2008_.pdf (Accessed January 2014).

[89] Gaceta Oficial de la República de Venezuela Año CXXV – Mes V Caracas, 13 de febrero de 1.998, Número 36.395, Ministerio de Sanidad y Asistencia Social Número S.G.-018-98 11 De 02 De 1.998 187° Y 138.

[90] Litter, M.I., Morgada, M.E., Bundschuh, J. 2010. Possible treatments for arsenic removal in Latin American waters for human consumption. Environ. Pollut. 158:1105–1118.

[91] Sancha, A.M., Castro, M. L. 2001. Arsenic in Latin America: Occurrence, Exposure, Health Effects and Remediation. In: Chappell, W.R., Abernathy, C.O., Calderon, R.L. Arsenic Exposure and Health Effects IV, Elsevier B.V., Amsterdam, pp. 88-96.

[92] Höll., W., Litter, M.I. 2010. Ocurrencia y química del arsénico en aguas. Sumario de tecnologías de remoción de arsénico de aguas. In: Litter, M.I., Sancha, A.M., Ingallinella, A.M. (eds) Tecnologías económicas para el abatimiento de arsénico en aguas, Editorial Programa Iberoamericano de Ciencia y Tecnología para el Desarrollo, Buenos Aires, pp. 17–31.

[93] Litter, M., Fernández, R., Cáceres, R., Grande Cobián, D., Cicerone, D., Fernández Cirelli, A. 2008. Tecnologías de bajo costo para el tratamiento de arsénico a pequeña y mediana escala. Revista Ingeniería Sanitaria y Ambiental 100:41–50.

[94] Cortina, J.L., Litter, M.I., Gibert, O., Valderrama, C., Sancha, A.M., Garrido, S., Ciminelli, V.S.T. 2016. Latin American experiences in arsenic removal from drinking water and mining effluents. In: Innovative Materials and Methods for Water Treatment-Separation of Cr and As, N. Kabay, M. Bryjak (eds), CRC-Taylor & Francis, pp. 391–416.

[95] Litter, M.I., Bundschuh, J. 2012. Emerging options for solving the arsenic problems of rural and periurban areas in Latin America. In: Ng, J.C., Noller, B.N., Naidu, R., Bundschuh, J., Bhattacharya P. (eds.) Understanding the Geological and Medical Interface of Arsenic. Taylor and Francis Group, London, pp. 267–270.

[96] Litter, M.I., Alarcón-Herrera, M.T., Arenas, M.J., Armienta, M.A., Avilés, M., Cáceres, R.E., Cipriani, H.N., Cornejo, L., Dias, L.E., FernándezCirelli, A., Farfán, E.M., Garrido, S., Lorenzo, L., Morgada, M.E., Olmos-Márquez, M.A., Pérez-Carrera, A. 2012. Small-scale and household methods to remove arsenic from water for drinking purposes in Latin America.Sci. Total Environ. 429:107–122.

[97] Hering, J.G., Chen, P.Y., Wilkie, J.A., Elimelech, M. 1997. Arsenic removal from drinking water during coagulation. J. Environ Eng ASCE 123:800–807.

[98] Bundschuh, J., García, M.E., Birkle, P., Cumbal, L.H., Bhattacharya, P., Matschullat. J. 2009. Occurrence, health effects and remediation of arsenic in groundwaters of Latin America. In: Bundschuh, J., Armienta, M.A., Birkle, P., Bhattacharya, P., Matschullat, J., Mukherjee, A.B. (eds) Natural arsenic in groundwater of Latin America. CRC Press/ Balkema Publisher, Leiden, pp. 3–15.

[99] Sancha, A.M. 2010. Remoción de arsénico por coagulación y precipitación. In: Litter, M.I., Sancha, A.M., Ingallinella, A.M. (eds) Tecnologías económicas para el abatimiento de arsénico en aguas, Editorial Programa Iberoamericano de Ciencia y Tecnología para el Desarrollo, Buenos Aires, pp. 33–41.

[100] Sancha, A.M. 2010. Importancia de la matriz de agua a tratar en la selección de las tecnologías de abatimiento de arsénico. In: Litter, M.I., Sancha, A.M., Ingallinella, A.M. (eds) Tecnologías económicas para el abatimiento de arsénico en aguas, Editorial Programa Iberoamericano de Ciencia y Tecnología para el Desarrollo, Buenos Aires, pp. 145–153.

[101] Sancha, A.M. 2010. Experiencia chilena en la remoción de arsénico a escala de planta de Tratamiento. In: Litter, M.I., Sancha, A.M., Ingallinella, A.M. (eds) Tecnologías económicas para el abatimiento de arsénico en aguas, Editorial Programa Iberoamericano de Ciencia y Tecnología para el Desarrollo, Buenos Aires, pp. 169–178.

[102] Bundschuh, J., Litter, M., Ciminelli, V., Morgada, M.E., Cornejo, L., Garrido Hoyos, S., Hoinkis, J., Alarcón-Herrera, M.T., Armienta, M.A., Bhattacharya, P. 2010. Emerging mitigation needs and sustainable options for solving the arsenic problems of rural and isolated urban areas in Iberoamerica - A critical analysis. Water Res. 44:5828–5845.

[103] Ingallinella, A.M., Fernández, R.G. 2010. Experiencia argentina en la remoción de arsénico por diversas tecnologías. In: Litter, M.I., Sancha, A.M., Ingallinella, A.M. (eds), Tecnologías económicas para el abatimiento de arsénico en aguas, Editorial Programa Iberoamericano de Ciencia y Tecnología para el Desarrollo, Buenos Aires, pp. 155–167.

[104] Hering, J.G., Katsoyiannis, I.A., Ahumada Theoduloz, G., Berg, M., Hug, S.J. 2017. Arsenic Removal from Drinking Water: Experiences with Technologies and Constraints in Practice. J. Environ. Eng. 143:1-1.

[105] Cardoso, S., Grajeda, C., Argueta, S., Garrido, S. 2010. Experiencia satisfactoria para la remoción de arsénico en Mixco, Guatemala. In: Litter, M.I., Sancha, A.M., Ingallinella, A.M. (eds), Tecnologías económicas para el abatimiento de arsénico en aguas, Editorial Programa Iberoamericano de Ciencia y Tecnología para el Desarrollo, Buenos Aires, pp. 179–189.

[106] Alarcón-Herrera, M.T., Martín-Domínguez, I.R., Benavides Montoya, A. 2007. Wetlands for arsenic removal. In: WETPOL 2007 2nd International Symposium on Wetland Pollutant Dynamics and Control, Tartu, Estonia.

[107] Litter, M.I., Pereyra, S., LópezPasquali, C.E., Iriel, A., Senn, A.M., García, F.E., Blanco Esmoris, M.F., Rondano, K., Pabón, D.C., Dicelio, L.E., Lagorio, M.G., Noel, G.D. 2015. Remoción de arsénico en localidades de la provincia de Santiago del Estero, Argentina. Evaluación del acceso, uso y calidad de agua en poblaciones rurales con problemas de arsénico, Rev. Ing. Sanit. Amb. 125:13–25.

[108] Cumbal Flores, L., Zúñiga Salazar, M. 2010. Quitosano impregnado con partículas de óxido de hierro: un biosorbente que remueve selectivamente arsénico de aguas. In: Litter, M.I., Sancha, A.M., Ingallinella, A.M. (eds). Tecnologías económicas para el abatimiento de arsénico en aguas, Editorial Programa Iberoamericano de Ciencia y Tecnología para el Desarrollo, Buenos Aires, pp. 269–289.

[109] Castro de Esparza, M.L. 2010. Remoción de arsénico del agua de pozos de zonas rurales de Puno, Perú empleando ALUFLOC. In: Litter, M.I., Sancha, A.M., Ingallinella, A.M. (eds), Tecnologías económicas para el abatimiento de arsénico en aguas, Editorial Programa Iberoamericano de Ciencia y Tecnología para el Desarrollo, Buenos Aires, pp. 243–255.

[110] Morgada, M.E., Litter, M.I. 2010. Tecnologías fotoquímicas y solares para la remoción de arsénico de soluciones acuosas. Estado del arte. In: Litter, M.I., Sancha, A.M., Ingallinella A.M. (eds) Tecnologías económicas para el abatimiento de arsénico en aguas, Editorial Programa Iberoamericano de Ciencia y Tecnología para el Desarrollo, Buenos Aires, pp. 73–89.

[111] Morgada, M.E., Levy, I.K., Salomone, V., Farías, S.S., López, G., Litter, M.I. 2009. Arsenic(V) removal with nanoparticulate zerovalent iron: effect of UV light and humic acids. Catal. Today 143:261–268.

[112] Kunz, S., Romero, L.G., Otter, P., Feller, J. 2017. Treatment of arsenic-contaminated water using in-line electrolysis, co-precipitation and filtration in Costa Rica, Water Sci. Technol. Water Supply 18(1):ws2017089 DOI: 10.2166/ws.2017.089.

[113] Pérez Coll, C.S., Pabón-Reyes, C., Meichtry, J.M., Litter, M.I. 2018.Monitoring of toxicity of As(V) solutions by AMPHITOX test without and with treatment with zerovalent iron nanoparticles. Environ. Toxicol. Pharmacol. 60:138–145.

Bios

Marta I. Litter

Prof. Dr. Marta Litter has a PhD in Chemistry (Buenos Aires University, Argentina), with postdoctoral studies at the University of Arizona, USA. She is Senior Researcher of the National Research Council (CONICET), Full Professor at the National University of General San Martín (UNSAM) and has been Head of the Division of Environmental Chemistry Remediation (National Atomic Energy Commission), all of this in Argentina. She has more than 200 scientific publications in international journals, books and book chapters. She was the International Coordinator of the Iberoarsen CYTED network. She received the Mercosur Prize in Science and Technology (2006 and 2011) and was President of the International Congress on Arsenic in the Environment (2014). She is an active member of the 'Arsenic in water' ad-hoc group of experts of the Food Safety Network of the National Scientific and Technical Research Council (Red de Seguridad Alimentaria, CONICET). She is considered a pioneer in photocatalysis in Argentina (2016) and has been accepted as a Member of TWAS (2018). Corresponding author. Email: marta.litter@gmail.com.

María Aurora Armienta Hernández

Dr. María Aurora Armienta Hernández is a Research Professor at Geophysics Institute, Autonomous National University of Mexico (UNAM), Mexico. She has a Bachelor in Chemical Engineering, a M.Sc. in Analytical Chemistry, and a PhD in Hydrology. Her research is focused on environmental geochemistry, hydrogeochemistry, medical geology and geochemical processes related to volcanic activity. She has identified contamination processes and sources of metals and metalloids in groundwater, rivers and soils in various regions in Mexico, and developed solutions to the pollution problem. She has published 118 international peer reviewed articles, 47 extended abstracts, and 30 book chapters. Dr. Armienta has supervised 12 PhD, 19 M.Sc., and 30 Bachelor theses. She has been awarded a Level III National Researcher (the highest level) by the National Science Council of Mexico. She was the Mexican coordinator of the Iberoarsen international network. In March 2013, she received the "Juana Ramírez de Asbaje" award in recognition of her academic achievements at the University of Mexico. In 2012, 2013 and 2014 she was one

of the ten most cited UNAM researchers in Earth sciences. In 2015, Dr. Armienta received the Academic and Research career recognition by the Mexican Geohydrological Society, and in 2018 she was named Teacher of the Year in Earth Sciences by the Mexican Geophysical Union.

Ruth Esther Villlanueva-Estrada

Dr. Ruth Esther Villanueva-Estrada graduated as Chemist at the School of Chemistry, at the Autonomous National University of México (UNAM) (1996), where she later on obtained a Master's degree in Chemical Oceanography (2001) and a Doctorate in Geochemistry (2007). She is a staff member of the Geophysics Institute, Group of Dangers and Risks by Natural Phenomena (UNAM). She has published 23 articles in high-impact indexed journals, 3 book chapters, 10 extensive abstracts with arbitration and 7 technical reports. Currently, she is Head of Laboratory at the Geothermal Fluids Geochemistry, Geophysics Institute (UNAM-Michoacán Unit). Her research focuses on studies on A) renewable energy resources geochemistry, B) aqueous environmental geochemistry, and C) geochemical modeling of water-rock interaction.

Edda C. Villaamil Lepori

Prof. Dr. Villaamil Lepori has obtained a doctorate at the University of Buenos Aires, Toxicology Area (2000). She is Consulting Professor at the University of Buenos Aires, and Honorary Active Partner and Member of the Scientific Advisory Board of the International Life Sciences Institute (ILSI) in Argentina. She is the author of 71 articles published in specialized journals, 6 book chapters, and 314 papers presented at scientific meetings. On 77 occasions, she was a speaker at national and international meetings, and she has received 18 awards and distinctions. She is an experienced human resources trainer – she has directed research groups, doctoral and postdoctoral students, residents, researchers from CONICET and UBA, and interns from national and foreign universities. Considering national subsidized research projects (FONCyT, FONTAR, CONICET, UBACyT, SECyT-MINCyT) she has directed 13 projects, co-directed 7 projects, participated as a researcher in 17 projects, and has coordinated 3 international projects in the region (AECI) related to the topic of Arsenic. She acts in the area of Toxicology, with emphasis on Toxicology of Persistent Pollutants, Environmental Toxicology and Occupational Toxicology. In her professional activities she has interacted with 129 collaborators in co-authorships of scientific works.

Valentina Olmos

Dr. Valentina Olmos has obtained a Doctorate in Pharmacy and Biochemistry at the University of Buenos Aires (2016). She is Researcher and Professor Teaching Assistant at the School of Pharmacy and Biochemistry, University of Buenos Aires. Her research is focused on arsenic exposure assessment and arsenic health risk assessment. She is an Emeritus member of the Argentine Society of Toxicology (Asociación Toxicológica Argentina) and a full member of the Society of Toxicology (SOT, USA). She is review editor at Acta Toxicológica Argentina Journal since 2006. She is an active member of the 'Arsenic in water' ad-hoc group of experts of the Food Safety Network of the National Scientific and Technical Research Council (Red de Seguridad Alimentaria, CONICET). She authored 33 scientific publications in national and international scientific journals. She authored more than 50 presentations to national and international scientific meetings.

INSTRUCTIONS FOR AUTHORS

GUIDELINES

1. Length

Research reviews should not be less than 7000 words or more than 10,000 words (plus up to 15 figures and up to 50 references).

2. Structure

Whenever possible articles should adjust to the standard structure comprising:
(a) Graphical abstract,
(b) Abstract,
(c) Introduction describing the focus of the review,
(d) Article main body including assessment and discussion of available information (may be further subdivided),
(e) Conclusions,
(f) Bibliography.

3. Format

Authors must submit their articles in a Microsoft Word archive. Figures must be embedded in the article and also submitted in a separate .zip or .rar file.

4. References

References must be numbered in the text ([1] [2] [3]) and identified with the same numbers in the *References* section. Up to 50 references are allowed. The following are examples to take into account in each case.

BOOKS:
- *Single author*
Chung, R. *General Chemistry: Fundamental Knowledge,* 2nd ed.; McGuffin-Hill: Kansas City, 2003.
- *More than one author*
Chung, R.; Williamson, M. *General Chemistry: Fundamental Knowledge*, 2nd ed.; McGuffin-Hill: Kansas City, 2003.
- *Edited Book*
Kurti, F. Photodissociation and Reactive Scattering. In *The Rise of Chemical Physics*; White, AD, Ed.; Wilson: New Jersey, 2007; Vol. 128; p. 257.
- *Book in Series*
Goth, V. Polymer Chemistry. In *The Foundational Course in Organic Chemistry*; ACDC Symposium Series 1151; American Chemical Fraternity: Seattle, 2014; pp 123-149.
- *Article from a reference book*
Powder and Metallurgy. *Dictionary of Chemical Technology*, 3rd ed.; Wilson: New Jersey, 1971; Vol. 12, pp 68-82.

ARTICLES:
- *Article in a scientific journal*
Evans, A.; Stitch, M.; Smithers, ET; Nope, JJ Complex Aldol Reactions to the Total Synthesis of Phorboxazole B. *J. Am. Chem*. Soc. 2012, 122, 10033-10046.
- *Article in a popular/non-scientific magazine*
Tatum, CJ Super Organics. *Wireless* , June 2001, pp 76-93.
- *Article from an online journal*
Turkey-Lopez, E. Inexact Solutions of the Quantum Double Square-Well Potential. *Chem. Ed.* [Online] 2007, 11, pp. 838-847. http://chemeducator.org/bibs/0011006/11060380lb.htm (accessed Aug 5, 2019).

PUBLICATION ETHICS

The journal considers that the primary objective of all submissions must be a contribution of relevant and appropriate content, and that all review processes must be structured based on that general criterion. Therefore, there is an emphasis on the concern to maintain the highest quality and ethics standards in the reception, evaluation and publication of articles. These standards include the three participants of the process: author, reviewer and editor.

1. Author's responsibilities

- Submitted manuscripts should maintain rigorous scientific criteria for data validation and conclusions.
- All data (Figures, Tables, etc.) reproduced from previous published articles must give the appropriate recognition to the source. Plagiarism is cause enough to reject the submission.
- Authorship must include all individuals who have contributed in a substantial way to the composition, prior investigation, and execution of the paper. Minor contributions must be acknowledged, but these contributors should not be listed as authors. The main author or authors of the article will make sure that all participants of the paper have approved the final version of the document submitted.
- All authors must reveal in their final manuscript any financial or other type of conflict of interests that might interfere with the results and interpretations in their research. All funding received to carry out the project must be acknowledged.
- After the article is published, in the event an author notices a crucial fault or inaccuracy, he or she should immediately report that fault or inaccuracy, so that an Erratum can be issued as soon as possible.

2. Reviewer's responsibilities

Reviewing is a time-consuming process that is carried out *ad honorem* by *bona fide* scientists conversant with the subject of the reviewed paper. The quality and the ethical standards of the journal depend critically on the quality of the reviewing process, and the following guidelines are established:

- All documents sent to the journal for review will be considered confidential documents and will not be discussed with external third parties.
- When invited, a potential reviewer should decline if: (a) the subject of the article is not within his/her area of expertise; (b) there is any kind of conflict of interest; (c) if the review cannot be finished within the period established by the journal.
- Any criticism or objections to the paper should be done in a neutral tone and based on reasonable grounds, not limited to simple opinions or purely subjective expressions.

3. Editor's responsibilities

- The editors are responsible for selecting the papers that will be published in the journal. The Editorial Management must comply with the ethical standards of the journal, as well as with all legal guidelines, including the prohibition of plagiarism and any other form of copyright infringement.
- The editors will evaluate and make decisions on the articles sent to the journal regardless of the gender, sexual orientation, religious beliefs, ethnic origin, nationality or political ideology of the authors.
- Revealing information identifying reviewers is forbidden.
- The final version of all materials can be published only with the prior approval of their author.
- The editors will refrain from publishing manuscripts that imply a conflict of interests because of any possible connection with other institutions, companies and authors.
- Before deciding to send an article to a peer review, the editors are committed to thoroughly read all texts received and determine their appropriateness to the thematic universe of the journal.
- If a misbehavior or unethical action by an author or reviewer is identified, the editors must request the informer of such conduct or action to provide the evidence that may justify a possible investigation. All accusations will be handled seriously until reliable results are obtained regarding its truthfulness or falseness. If an investigation takes place, the editors are responsible for choosing the appropriate way in which it will be carried out. They can also request the advice and assistance from the Editorial Board, as well as from reviewers and authors.
- In the event a serious non-malicious mistake or a dishonest conduct by an author or a reviewer is proved, the editors shall act according to the nature and seriousness of the case. The actions the editors may take include, but are not limited to: notifying the author or reviewer of the existence of a serious mistake or misapplication of the ethical standards of the journal; writing a strong statement that reports and warns about a bad practice or unethical behavior; publishing that statement; unilaterally withdrawing the reported paper from the review or publication process; revoking the paper if it has already been published; communicating the journal's decision and the reasons behind it to the general public; and banning paper submissions by the people involved for a certain period of time.

PRIVACY STATEMENT

The names and email addresses entered in this journal site will be used exclusively for the stated purposes of this journal and will not be made available for any other purpose or to any other party.

NEXT ISSUE

Vol. 1, No. 2

TO BE PUBLISHED ON MARCH 15, 2020

GUEST EDITOR: FABIO DOCTOROVICH

ARTICLES

ISSN 2683-9288

Science Reviews
from the end of the world

Centro de Estudios sobre Ciencia, Desarrollo y
Educación Superior
538 Pueyrredón Av. - 2° C – Second building
Buenos Aires, Argentina - C1032ABS
(54 11) 4963-7878/8811
sciencereviews@centroredes.org.ar
www.scirevfew.net